Acta Biomaterialia 193 (2025) 20–48

Contents lists available at ScienceDirect

Acta Biomaterialia

journal homepage: www.elsevier.com/locate/actbio

Review article

3D bioprinting approaches for enhancing stem cell-based neural tissue regeneration

Cemile Kilic Bektas, Jeffrey Luo, Brian Conley, Kim-Phuong N. Le, Ki-Bum Lee [1,*]

Department of Chemistry and Chemical Biology, Rutgers, The State University of New Jersey, 123 Bevier Road, Piscataway, NJ 08854, USA

ARTICLE INFO

Keywords:
3D bioprinting
Stem cells
Neural tissue regeneration
Tissue engineering
Neurogenesis

ABSTRACT

Three-dimensional (3D) bioprinting holds immense promise for advancing stem cell research and developing novel therapeutic strategies in the field of neural tissue engineering and disease modeling. This paper critically analyzes recent breakthroughs in 3D bioprinting, specifically focusing on its application in these areas. We comprehensively explore the advantages and limitations of various 3D printing methods, the selection and formulation of bioink materials tailored for neural stem cells, and the incorporation of nanomaterials with dual functionality, enhancing the bioprinting process and promoting neurogenesis pathways. Furthermore, the paper reviews the diverse range of stem cells employed in neural bioprinting research, discussing their potential applications and associated challenges. We also introduce the emerging field of 4D bioprinting, highlighting current efforts to develop time-responsive constructs that improve the integration and functionality of bioprinted neural tissues.

In short, this manuscript aims to provide a comprehensive understanding of this rapidly evolving field. It underscores the transformative potential of 3D and 4D bioprinting technologies in revolutionizing stem cell research and paving the way for novel therapeutic solutions for neurological disorders and injuries, ultimately contributing significantly to the advancement of regenerative medicine.

Statement of significance: This comprehensive review critically examines the current bioprinting research landscape, highlighting efforts to overcome key limitations in printing technologies—improving cell viability post-printing, enhancing resolution, and optimizing cross-linking efficiencies. The continuous refinement of material compositions aims to control the spatiotemporal delivery of therapeutic agents, ensuring better integration of transplanted cells with host tissues.

Specifically, the review focuses on groundbreaking advancements in neural tissue engineering. The development of next-generation bioinks, hydrogels, and scaffolds specifically designed for neural regeneration complexities holds the potential to revolutionize treatments for debilitating neural conditions, especially when nanotechnologies are being incorporated. This review offers the readers both a comprehensive analysis of current breakthroughs and an insightful perspective on the future trajectory of neural tissue engineering.

1. Introduction

The anatomical basis of life has always been a curiosity and interest of people for ages, and the first simplified studies on anatomy appeared as early as 19th century [1]. Following these studies, several tissue types, including connective tissue, epithelium, muscle, and blood vessels, could be characterized using compound microscopes [2]. The discovery of 2D culture techniques enabled scientists to grow mammalian cells on thin surface-coated Petri dishes, bringing about a new age of examining and manipulating mammalian cells to comprehend their molecular biology better. 2D culture assays have been utilized effectively and remain popular due to their low cost, simplicity, and robustness across cell types [3,4]. While 2D cell cultures have been instrumental in advancing our understanding of cellular processes, they possess inherent limitations in recapitulating the intricate complexities of cell-to-cell interactions observed *in vivo*. This stems from the fundamental difference in the cellular microenvironment compared to the natural 3D tissue architecture. When confined to flat, artificial surfaces,

* Corresponding author.
E-mail address: kblee@rutgers.edu (K.-B. Lee).
[1] https://kblee.rutgers.edu/

https://doi.org/10.1016/j.actbio.2025.01.006
Received 16 August 2024; Received in revised form 12 December 2024; Accepted 7 January 2025
Available online 8 January 2025

cells undergo significant morphological alterations, adopting a flattened and spread-out morphology. This dramatic change in cell shape extends beyond the cytoskeleton and impacts the nucleus, leading to alterations in its shape and size. These nuclear morphological changes have been demonstrated to profoundly affect various cellular processes, including gene expression and protein synthesis [5]. Therefore, relying exclusively on 2D cultures to study cell-cell interactions and their downstream effects can introduce inconsistencies that may compromise the accurate translation of findings to *in vivo* conditions [5,6].

Although *in vivo* models are the gold standard for many studies, the method is expensive, subjects to tense regulations, requires continued use of animals for daily observation, and may cause serious distress and pain to the animal [7]. To this end, three-dimensional (3D) cell culture methods offer significant advantages over 2D cultures. They promote optimal cell growth, function, and differentiation by better mimicking the complexity of the *in vivo* environment. By providing a more natural 3D architecture, these cultures maintain normal cell shape and foster critical cell-extracellular matrix interactions. This reduces artificial stress often associated with cell flattening in 2D systems [8], thereby improving cell longevity and creating a more informative cellular microenvironment. As a result, 3D culture systems have gained prominence as they provide a more robust, physiologically relevant, and functionally representative platform for studying cellular behavior than traditional 2D models [9].

Over the years, numerous applications of scaffold-free (such as spheroids and organoids) and scaffold-based 3D models have been used to construct neural-tissue-like structures. These models have successfully combined biomaterials, small chemicals, and a wide range of cell types. Although scaffold-free models mimic the early developmental stages well, they lack organization and key features of the neural tissue, including mechanical stability, structural support, and porosity to maintain cell viability. Scaffold-based systems overcome the limitations of scaffold-free systems, especially by providing porosity, mechanical and structural support, and better organizational control [3]. However, traditional tissue engineering approaches consisting of scaffolds, cells, and growth factors have limitations in producing complex and patient-specific 3D tissue constructs that make them logistically and economically unfeasible for clinical applications. To this end, 3D bioprinting has developed as a potential new technology in which the printed substance, bioink, comprises biomaterials, active biomolecules, and cells. Advantages of 3D bioprinting over other traditional approaches include accurate control of cell distribution and deposition, cost-effectiveness, and scalability. The versatility of 3D bioprinting in producing tissue constructs for specific injuries has led to new avenues of discovery, increasing the likelihood of full recovery [10,11].

The detrimental effects of nerve injuries on a patient's quality of life include the loss of muscular function, reduced sensation, and the experience of extreme pain. The 'gold standard' for tissue restoration involves transferring healthy nerves from an uninjured body region to the damaged site. However, this approach often leads to additional complications, including donor site morbidity and the potential immune rejection [12]. Developing engineered constructs through tissue engineering and regenerative medicine is a promising and viable alternative for nerve repair. Stem cells, which can differentiate into many cell types, including neurons, have been shown to be highly effective in regenerative medicine. Today, the use of bioprinting and the discovery of stem cells have created a brighter future for nerve regeneration. For this purpose, many studies have been conducted on combining 3D bioprinting techniques and stem cells in nerve repair applications. Recent studies have revealed that 3D bioprinting may generate accurate structures for nerve bundles and tailored neural scaffolds to bridge and stabilize the defect gap while also delivering cells and bioactive molecules [13–19].

2. Advances in stem cell-based 3D bioprinting for nerve regeneration

2.1. Current literature gap

3D bioprinting technology and the regenerative medicine field have significantly advanced since the first U.S. patent for 3D bioprinting was awarded in 2006 [20]. Since then, 3D bioprinting has become one of the most promising technologies toward a possible solution for organ shortage. This technology was especially compelling to researchers for its reliability, efficiency, and quick production of scaffolds for a wide range of applications. At the same time, stem cells offer tremendous promise in tissue engineering by representing an unlimited cell source for modeling healthy or diseased tissues and substituting damaged tissues and organs. 3D bioprinting has been successfully performed with many stem cell types by offering precision control over the material it is being fabricated. The importance of controlling material fabrication is heightened when investigating system development, diseases, and regeneration processes, particularly in intricate systems such as the human nervous system. Therefore, 3D bioprinting has been well adapted to the field of tissue engineering, and the number of publications on bioprinting has been continuously increasing over the past two decades. 3D bioprinting, bioinks, bioprinting methods, bioprinting with stem cells, opportunities, and challenges have been extensively discussed in many review papers [10,21–25]. In contrast to existing reviews on 3D bioprinting applications in neural tissue regeneration [26,27], this paper emphasizes the integration of advanced nanomaterials with dual functionality into 3D bioprinting processes, specifically targeting neurogenesis pathways to enhance neural tissue regeneration. Additionally, we introduce the emerging field of 4D bioprinting, focusing on the development of time-responsive constructs that improve the integration and functionality of bioprinted neural tissues, which sets our work apart in addressing future directions for neural tissue engineering.

2.2. 3D bioprinting techniques targeted for stem cell encapsulation

The conventional classifications for three-dimensional (3D) bioprinting technologies based strictly on the working principles of 3D bioprinters, such as ink-jet printing, extrusion-based printing, and laser-assisted printing, have been used routinely in the literature. In this review, we aim to provide a more cyto-centric highlight of the available 3D printing technologies by organizing them into two major categories: droplet-based printing (DBP) and continuous filament printing (CFP).

2.2.1. Droplet-based printing (DBP)

Droplet-based printing (DBP) is regarded as a non-contact printing technique in which the printing nozzle or the donor does not "contact" the printing plate or the receiver since the ink, typically liquid of very low viscosity, is formed and deposited as droplets. By utilizing these technologies, researchers can accurately place droplets containing known types and amounts of cells onto their chosen substrate. The ability to "print" cells directly in droplets of media without needing a printable viscous support gel is especially attractive from a cyto-centric perspective since it allows for higher cell viability (95 %) [28]. These printing methods also enable researchers to arrange droplets carrying different cell types into pre-designed patterns, thereby engineering the microarchitecture and cell composition toward the target tissue. While the droplet volume, cell density loaded in the droplet, and capacity to accurately put the droplet onto the substrate differ amongst DBP technologies, DBP generally delivers superior printing resolution than CFP [29].

From a cell-printing perspective, DBP can be further categorized into nozzle DBP and nozzle-free DBP technologies. When a nozzle is required as part of the apparatus, as in inkjet printing, the issue of nozzle clogging must be addressed. Therefore, the cell density used with the nozzle DBP needs to be much lower than that in nozzle-free DBP. Cells also

experience high shear stress as they travel through the nozzle and orifice. Droplet volume using nozzle DPB is typically larger and results in slightly lower printing resolution compared to nozzle-free DBP.

Nozzle-free DBP technologies such as laser-induced forward transfer (LIFT) [30] and acoustic droplet ejection (ADE) [31] currently offer one of the highest bioprinting resolution, down to the single-cell level or approximately 10 to 30 micrometers, as defined by the smallest features or the droplet volume (picoliter level).

From sterility and cost perspectives, printing time has been one of the main concerns related to DBP. Biosafety cabinets or air-filter enclosures have been added into the printing area of several commercially available DBP printers to address sterility issues caused by extended printing times [32]. For premium systems with DBP and extrusion modalities, researchers must also consider the time needed to switch between modalities.

2.2.2. Continuous filament printing (CFP)

CFP requires a printable polymeric bioink whose viscosity needs to be in a range appropriate to be extruded through a nozzle so a filament can be formed [33,34]. For cell-laden bioinks, meticulous optimization of both the material composition and the printing process is crucial. This ensures minimal detrimental impact on the embedded cells, encompassing both chemical and mechanical considerations. Extrusion-based 3D printing typically has low resolution, as the smallest printed feature is defined by the diameter of the printed filament and not by the ability of the printers to precisely control the x-y coordination. Extrusion-based 3D printing inherently necessitates the use of a nozzle, introducing potential concerns analogous to those encountered with nozzle-based DBP. Careful consideration and optimization of nozzle design and printing parameters are crucial to mitigate these challenges and ensure consistent printability and cell viability. The higher viscosities of the printed materials required in these technologies also create additional mechanical stress on the ink and, subsequently, the embedded cells. In many cases, post-printing processing such as crosslinking is required to ensure printing fidelity – the ability for the printed structure to stay as close as possible to the computer-aided design (CAD) - and structural integrity. Newer technologies, such as freeform reversible embedding of suspended hydrogels (FRESH), facilitate the fabrication of complex 3D tissues and organs by printing them within a gel support bath [35]. Another example is microfluidic 3D printing, which enable researchers to crosslink the material in the printhead before extruding it through the nozzle and employ a "buffering" flow to reduce shear stress on cells [36,37]. In general, these technologies do offer a stronger or better stand-alone printed structure.

2.2.3. Others

While certain 3D printing technologies may not be suitable for direct cell incorporation, they can still contribute to neural tissue engineering through a stepwise approach. This involves printing an acellular scaffold followed by subsequent seeding or placement of cells or organoids, enabling the creation of complex neural tissue. The two main advantages of such an approach are the larger material selection and the better printing resolution. Technologies such as stereolithography (SLA) offer resolution in the 30-micron range, where two-photon lithography (two-photon polymerization, TPP) can bring the resolution down to the nanoscale [38]. While higher resolution almost always results in the trade-off of relatively longer printing time, it is generally acceptable for a acellular construct from the sterility standpoint. From a scale-up and cost-effective standpoint, the time-to-resolution ratio is one critical metric that commercial 3D printer manufacturers constantly aim to improve [39–41].

2.3. Established stem cell sources for the novel neural bioprinting applications

2.3.1. Neural stem cells

Neural stem cells (NSCs) arise from the ectoderm germ layer and can differentiate into neuronal and glial cell lineages. Neurons have a poor regenerative capacity, but it has been reported that neurogenesis occurs throughout adulthood in the human brain. Initially met with skepticism, this process is now widely recognized in most mammalian species, including rodents, monkeys, and humans. In adults, neurogenesis is limited to certain neurogenic regions, where neuroblasts are consistently generated, migrate to their target circuits, and differentiate into neurons, becoming part of the neural network [42,43]. Therefore, an abundant source of patient-derived neural stem cells is still lacking; however, human induced pluripotent stem cells (hiPSCs), derived from reprogrammed adult somatic cells, can be primed towards a neuronal lineage generating hiPSCs-NSCs. Primary human neural progenitor and stem cells can be isolated from brain regions post-mortem. NSCs can help repair neural tissue in the central nervous system (CNS) and peripheral nervous system (PNS) by replacing lost neurons and glial cells caused by traumas such as traumatic brain damage, spinal cord injury, stroke, or peripheral nerve injury [44] (Fig. 1). Neuronal differentiation is initiated by the expression of early neuronal markers (i.e., Beta-III tubulin (TUBB3)) followed by the expression of mature neuronal markers (i.e., MAP2, NeuN, etc.) and active voltage-gated ion channels with spontaneous action potentials. Notably, the CNS has significantly less regenerative capacity compared to the PNS. However, transplantation of NSCs often results in poor cell viability and integration into host tissue. As a result, biomaterials have widely been used to improve NSC transplantation to CNS microenvironments, given their capability to promote cell-cell interaction, protect cargo from harmful proteases, and release anti-inflammatory biomolecules. A previous report utilizing a self-assembled peptide-based hydrogel, a hydrogel that spontaneously organizes into a functional structure, facilitated NSC transplantation and enhanced cellular survival while mitigating glial scarring in a traumatic brain injury model [45]. The authors functionalized a self-assembling peptide, RADA16, with IKVAV, a sub-unit of extracellular matrix protein (ECM) laminin, to establish a favorable ECM environment for cellular transplantation [45]. Furthermore, three-dimensional (3D)-bioprinting of ECM-comprising components can aid in developing scaffolds to facilitate cellular transplantation and improve functional outcomes. For example, a recent report detailed the use of a 3D-printed collagen/silk fibroin scaffold seeded with NSCs, which could promote nerve regeneration after spinal cord injury [46]. Another publication, 3D-printed polyurethane hydrogel, and embedded NSCs to potentially treat traumatic brain injury [15]. Bioprinting can also be combined with materials to release therapeutic molecules for synergistic therapeutic effect [47]. Briefly, the authors describe a fibrin-based bioink to print hiPSC neural progenitor cells and deliver guggulsterone, a steroid and anti-cancer drug, to differentiating cells. This approach differentiated hiPSC neural progenitor cells into dopaminergic neurons using a three-dimensional culture [47]. Moreover, NSCs are known to respond to biophysical and topographical cues of underlying biomaterials. This causes variations in mechanotransduction pathways, which can regulate NSC migration and differentiation. To this end, a recent report demonstrated the use of 3D-printed hydrogels with aligned microchannels to guide neural stem cell migration [48]. In their study, they provided evidence to support the idea that 3D printing has the ability to match the dimension of hydrogels precisely with the lesion site of potential brain injuries, thus showcasing its potential usefulness. In another study 3D bio-printed iPSC-derived spinal neural progenitor cells along with oligodendrocyte progenitor cells, which are responsible for myelinating axons in the spinal cord, embedded in Matrigel along with a blend of alginate and methylcellulose [49].

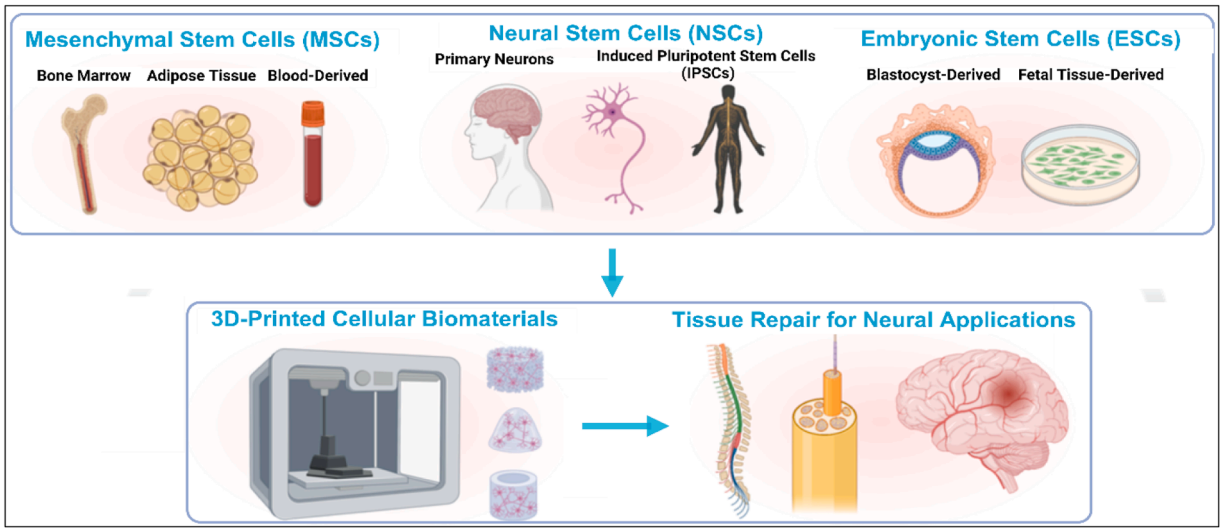

Fig. 1. Sources of stem cells used in 3D bioprinting for neural tissue engineering. Mesenchymal stem cells (MSCs), neural stem cells (NSCs), induced pluripotent NSCs (iPSCs-NSCs), and embryonic stem cells (ESCs) have been used in 3D printing to provide anti-inflammatory and neuroprotective effects to neural injuries as well as to regenerate neural tissue. Cell-seeded scaffolds or hydrogels as well as biomaterials with embedded cells can promote the repair of injuries such as spinal cord, peripheral nerve, or traumatic brain injuries.

2.3.2. *Mesenchymal stem cells*

Mesenchymal stem cells (MSCs) are promising for neural tissue repair, despite their origin from the mesoderm germ layer, which is different from the ectodermal origin of neural tissue. They have unique properties such as immunomodulatory capabilities, the ability to differentiate into supportive cell types, and the secretion of growth factors that aid tissue regeneration [37,50–56]. While an abundant source of viable NSCs can prove challenging and is one of the main reasons iPSCs have gained popularity, MSCs can be efficiently sourced from various tissues, most often including adipose tissue, bone marrow, and umbilical cord blood (Fig. 1). They can be differentiated into a wide range of tissue types, including myocytes, chondrocytes, endothelial cells, and more. For purposes of this review, we will focus only on neural-related applications of MSCs, which can be utilized to either replace lost neural tissue through transdifferentiation or stimulate endogenous mechanisms to promote neurogenesis through anti-inflammatory mechanisms. In the context of MSC transdifferentiation, it has been reported that the utilization of 3D-printing techniques has shown great potential in facilitating the transdifferentiation process specifically for applications in neural tissue engineering. One study used 3D printing to fabricate gelatin and graphene-based nerve conduits with microstructure channels to adhere to MSCs. Then, by combining topographical, mechanical, and electrical stimuli provided by the conductivity and incorporation of graphene, MSCs were found to differentiate into a Schwann cell (SC)-like phenotype. The authors found that transdifferentiated SCs exhibited SC-related markers and elevated nerve growth factor (NGF) expression, a common growth factor known to stimulate neurogenesis and cellular proliferation [52,53]. Similarly, another study demonstrated that 3D bio-printed and scaffold-free nerve constructs seeded with human gingiva-derived MSCs improved nerve regeneration. Briefly, the authors generated MSC spheroids and 3D-printed the spheroids to generate an array that fused into a 3D conduit-like structure. This conduit structure improved functional recovery in a rat facial nerve injury model, improved histological outcomes such as enhanced neuronal markers (i.e., TUBB3), and promoted axonal alignment [56]. MSCs possess remarkable anti-inflammatory abilities, which can have a positive impact on the nervous system by releasing anti-inflammatory cytokines/chemokines and pro-regenerative trophic factors. Mesenchymal stem cells have been extensively employed to treat CNS-related diseases and injuries ranging from stroke, traumatic brain injury, and spinal cord injury [57,58].

MSCs have the ability to undergo transdifferentiation into neurons, which can contribute to their therapeutic effects. Recently, MSCs were 3D-bioprinted in a fibrin-based bioink to yield tyrosine hydroxylase (TH) and TUBB3 -positive neurons after 12 days of culture with a range of small molecules and growth factors [37]. The authors also demonstrate the release of dopamine and characterize the electrophysiology of the MSC-derived neurons.

2.3.3. *Embryonic stem cells*

Embryonic stem cells (ESCs) are isolated from embryos and are multipotent cells from which neurons can be derived and utilized for neural tissue engineering [59–61]. The human embryonic stem cells that originate from the neural crest region can be referred to as hESC—NSCs, as shown in Fig. 1. Recently, hESC—NSCs were employed for nerve repair using a 3D-printed polycaprolactone/polypyrrole (PCL/PPy) conductive scaffold. From this material, the authors generated a nerve guidance conduit using an electrohydrodynamic jet 3D printing process and seeded hESC—NSCs to ultimately generate peripheral neurons positive for neurofilament heavy chain (NF-H) for potential nerve repair [62]. Moreover, embryoid bodies (EBs), which are three-dimensional spheroids of embryonic stem cells, can also be used to generate neural progenitor cells. One report demonstrated the fabrication of a 3D-printed PCL/gelatin methacrylate (GelMA) tubular structure with tunable porosity for spinal cord repair [63]. They demonstrated that PCL/GelMA scaffolds seeded with EBs, along with the addition of retinoic acid, a common neurogenic drug used to drive embryonic neuronal differentiation, efficiently generated neurons with regiospecific neuronal markers such as an anterior brain marker, orthodenticle homeobox 1 (OTX1), and posterior spinal cord marker, homeobox c4 (HOXC4). Therefore, a potential advantage of using ESC-derived NSCs as well as EBs may be their differentiation potential to generate regiospecific neurons for therapeutic applications. However, clinically sourcing ESCs and effectively controlling neuronal differentiation and sub-type differentiation remain critical hurdles when using ESCs for neural tissue engineering. The most commonly used cell types in neural tissue engineering, along with the hydrogel/matrix selections, the inclusion of nano/micro materials or stimuli, associated printing methods, *in vivo* testing status, and key findings are listed in Table 1.

Table 1
Overview of 3D bio-printed neural tissue scaffolds and disease models.

Cell Type	Hydrogel/ Matrix	Nano/micro material /stimuli	Printing Method	*In vivo*	Key Findings/ Application	References
BMSCs + RSCs (1×10^6 cell/ml, mixed in ink)	GelMA (10 %)	None	CFP, Extrusion, 23 G needle	Adult female SD rat, transection, T10-T11	Spinal cord injury (SCI), axon regeneration, motor function recovery	[50]
MSCs	Gelatin/ Graphene PLA (Black Magic 3D),	Electrical (10 mV, 50 Hz, 2–10 min/ day, 10 days)	CFP, melt extrusion (graphene PLA only)	None	Electrical stimuli applied within the 3D gelatin matrix enables enhanced differentiation of MSC to SC	[53]
canine AdMSCs, (1×10^6 cell/ml, post-print loading)	PCL	None	CFP, melt extrusion	Female Wistar rat, sciatic	Peripheral nerve injury (PNI)	[54]
MSCs	Acrylamide/Methylene bis-acrylamide	Ca^{2+}	CFP, gel extrusion (0.31-mm ID SS needle)	Male SD Rat, Cranial defect (5 mm, bilateral)	Traumatic Brain injury: cranioplasty – Repair defects and safely degrade after 8 weeks	[45]
MSCs (2×10^6 cells/ml, mixed in ink)	Fibrinogen 20 mg ml^{-1}, sodium alginate (0.5% w/v), genipin (0.3 mg ml^{-1})		CFP, microfluidic (LOP™) print head	None	Personalized disease-models and drug-screening; high cell viability; expression of neural markers	[37]
PC-12	PCL	Reduced graphene oxide (r-GO)	CFP, Electro-hydrodynamic (EHD) jet	None	PNI: supported neural differentiation of PC12 cells	[62]
EBs (from mESC)	PCL-Alginate PCL-GelMA	None	CFP, melt extrusion (PCL) + gel extrusion (G20 needle, Alginate, GelMA)	None	SCI: complex heterogeneous tubular scaffold with tunable porosity; potential *in-vitro* model	[63]
NSCs	Collagen / silk fibroin	None	CFP, gel extrusion, 210-μm nozzle)	SD rats – T10 transection	SCI: promoted injury repair; reduced glial scarring, regenerated axons	[46]
hIPSCs	Fibrinogen / Alginate	None	CFP, microfluidic (LOP™) print head	None	Enhanced cell survival and differentiation	[36]
NSCs (seeded post-printing	GelMA-DA	None	SLA printing - 355 nm UV laser	None	Promoted neural differentiation	[64]
primary cortical neuron	RGD-gellan gum	None	CFP, hand-held (manual) gel extrusion	None	Created brain-like structures	[65]
Schwann cells (1×10^6 cells/ml)	RGD-alginate, hyaluronic acid, fibrin	None	CFP, gel extrusion	None	PNI: low-viscosity hydrogel bioprinting	[66]
U87MG / MM6 monocyte /macrophages	Alginate	None	CFP, gel extrusion, multi-nozzle (up to 6)	None	Disease model / drug screening: spatially controllable tumor construct	[67]
Glioblastoma cells (GL261), macrophages (RAW264.7)	GelMA	None	CFP, gel extrusion	None	Disease model: 3D-printed mini-brains actively recruited microphages	[68]
mESCs	Alginate	None	Laser-direct writing (193 nm ArF laser)	None	Disease model / drug screening: customizable *in-vitro* cancer models	[69]
human glioma stem cells (GSC23) human glioma cells (U118)	Alginate	None	CFP, coaxial (gel) extrusion, 21 G/16 G needles	None	Disease model: mimicked glioblastoma microenvironment	[70]
None	Alginate; collagen, fibrin	Gelatin supporting bath	CFP, FRESH, 150-micron SS needle	None	Enabled printing of low viscosity inks; achieved 200-micron resolution	[35]

Abbreviations: GelMA: Gelatin methacrylate, BMSCs: Bone mesenchymal stem cells, RSCs: Rat Schwann cells, SD Rat: Sprague-Dawley rat, CFP: continuous filament printing, PLA: polylactic acid, MSCs: Mesenchymal stem cells, SC: Schwan cells, PCL: polycaprolactone, AdMSCs: Adipose-tissue-derived multipotent mesenchymal stromal cells, Ca^{2+}: Calcium ion, ID: Inner diameter, PC-12: Cell line derived from rat pheochromocytoma, EBs: Embryoid body, mESCs: mouse embryonic stem cells, G20 needle: gauge 20 needle, PNI: Peripheral nerve injury, SCI: Spinal cord injury, NSCs: Neural stem cells, hIPSCs: Human induced pluripotent stem cells, GelMA-DA: Dopamine grafted gelatin methacrylate, SLA: stereolithography, RGD: Arginine–glycine–aspartic acid, FRESH: Freeform reversible embedding of suspended hydrogels.

2.4. Engineering hydrogel matrices for stem cell culture and bioprinting

Bioprinting technology is an innovative engineering method that aims to combine cell-laden biomaterials, referred to as bioinks, with advanced additive manufacturing techniques in tissue engineering and regenerative medicine to create functional tissues. Spatially complex scaffolds to meet the biological complexity of 3D cell culture for tissue regeneration or replacement, and the disease modeling can be fabricated using various bioprinting techniques as covered in Section 1 (Fig. 2). As the predetermined structural architecture is created through layer-by-layer deposition of cell-laden bioinks, this technique employs bioinks, live cells, and small molecules to fabricate precisely controlled complex structures to mimic native organs and tissues. The bioprinted scaffold offers key advantages over other scaffold fabrication methods, such as defined porosity for optimal diffusion of nutrients and water, and appropriate mechanochemistry of the bioinks to promote cell migration and cell-cell adhesions necessary for the development of a functional tissue while enabling personalized printing. The selection of the bioinks, thus, is one of the most critical points in 3D bioprinting approaches, and it is as important as the selection of the 3D bioprinting technique. Table 1 summarizes the common bioinks used in neural tissue engineering applications.

Bioink provides physical and biochemical cues necessary for cell attachment, growth, development, and proliferation, where it can specifically be formulated according to the needs of the tissue to be engineered, as well as for neural tissues to increase the likelihood of recovery after neurological diseases or injuries [71].

The ECM composition of the nervous system is unique; where normally the most abundant ECM components are collagen, laminin, and fibronectin in other tissues and organs, they are found in lower amounts

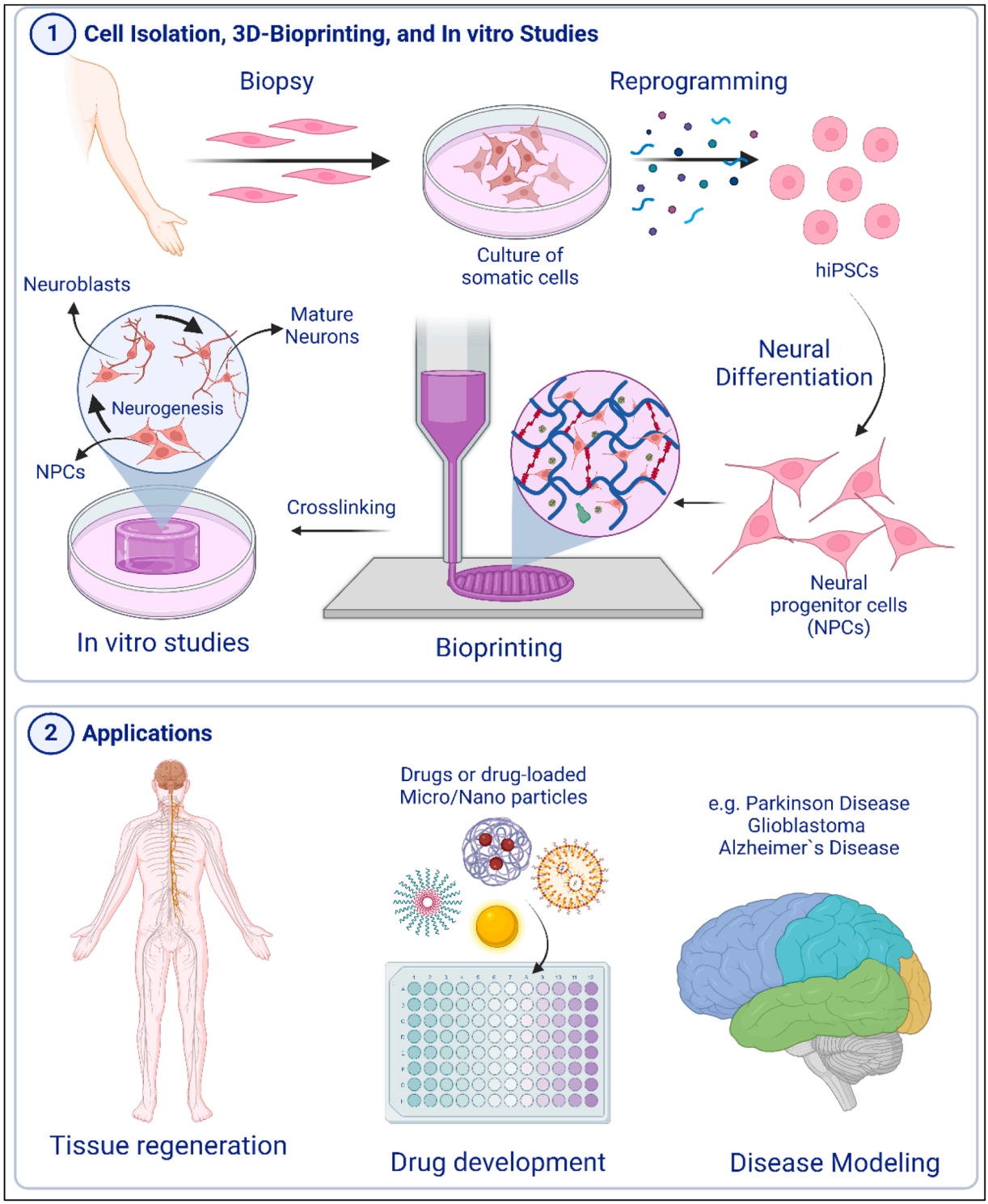

Fig. 2. Overview of 3D bioprinting for neural tissue engineering applications using induced pluripotent stem cell (iPSC) approach. Somatic cells are derived from the patient and reprogrammed to stem cells which have potential to differentiate into other cell types including neural cells. Human iPSC- neural progenitor cells (NPCs) are used in the bioink formulation which may contain biomaterials, cells, bioactive molecules, nano and micro particles, and drugs. Bioprinted scaffolds are used in many applications including neural tissue regeneration, drug development and screening, and *in vitro* disease modeling. Created with BioRender.com.

in the neural system. On the other hand, the proteoglycans of the hyaluronan, tenascins, and lecticans are plentiful [72]. In addition to the ECM, soluble small molecules like cytokines, chemokines, and growth factors are present, and their function is influenced by their concentration [73]. As a cell source for neural regeneration applications, stem cells offer tremendous advantages due to their ability to proliferate in the undifferentiated multipotent state (renewable source) and hold the capability to become a variety of tissue-specific cell types [74]. An ideal bioink, thus, should promote the growth and differentiation of the stem cells by providing a proper micro-environment. Hydrogels are gold-standard materials for the bioinks as they can form 3D hydrophilic networks, provide printability, biodegradation, and mechanical properties (by transducing the mechanical cues to the neural cells), and mimic the natural extracellular matrix (ECM) of the tissues in which

cells remain viable and functional. Natural biopolymers (e.g. gelatin, alginate, and collagen) are the most widely used sources for the bioinks as they better create a biomimetic environment and are advantageous over synthetic polymers due to their self-assembling ability, biodegradation, biocompatibility and biomimicking of ECM and composition [75]. In contrast, synthetic polymers, such as polyethylene glycol (PEG) and pluronic acid (also known as poloxamer), present a unique set of benefits that make them highly suitable for various applications. These advantages encompass enhanced mechanical stability, which ensures the durability and integrity of the polymers under different conditions. Additionally, these synthetic polymers are characterized by their ease of modification, allowing for the introduction of functional groups or other molecules to tailor their properties for specific purposes. Furthermore, they exhibit compatibility with a wide array of scaffold fabrication techniques. This includes electrospinning, a method that produces fine fibers for creating complex structures; 3D printing, which enables the construction of custom-designed shapes and geometries; and freeze-drying, a technique used to create porous scaffolds by removing water under low temperatures and pressure. These attributes make synthetic polymers like PEG and pluronic acid versatile materials for engineering applications, particularly in the development of scaffolds for tissue engineering and regenerative medicine [10,33]. Despite synthetic polymers being tailorable, most of them have inherent problems, including not having natural cell binding sites that can attract the cells to attach and develop. However, it is possible to modify synthetic polymers using different functionalization strategies, such as RGD conjugation, to tether bioactive cues into them, which can lead to control over the attachment, morphogenesis, and proliferation of the cells and the degradation of the scaffold [76].

Aside from those with self-assembling capabilities, hydrogels need to crosslink after printing. This can be achieved through either chemical crosslinking or non-covalent interactions, ensuring the stability of the printed scaffold (Fig. 3). The chemically crosslinked hydrogel network has nonreversible covalent bonds between polymeric chains, resulting in a stable and strong hydrogel with proper shape fidelity after printing. Chemical crosslinking is achieved in numerous ways, including chemical crosslinking such as azide-alkyne cycloaddition [77] and enzymatic crosslinking [78], or photocrosslinking via visible [79], near-infrared [80], and ultraviolet light [81]. On the other hand, physical crosslinking methods do not involve nonreversible bond formation but instead rely on the formation of noncovalent bonds such as ionic crosslinking [82], electrostatic interactions [83], and hydrophobic interactions [84]. Noncovalent interactions usually result in weaker hydrogels compared to chemically crosslinked ones, but they provide a milder and more cell-friendly environment to the cells [85]. The crosslinking strategy is an important parameter for 3D bioprinting as the gelation kinetics, mechanical properties, post-printing shape fidelity, and the viability of the encapsulated cells are all dependent on it [76]. Combining two different crosslinking strategies is a widely used approach to capitalize on the benefits of both methods, resulting in the development of advanced bioinks that excel in cell viability and printability [86–88].

Either natural or synthetic, covalently or non-covalently crosslinked, bioinks should satisfy certain criteria to fabricate functional living structures with suitable mechanical and biological features. Ideal bioinks should include: 1) biocompatibility: it should support the adhesion, proliferation, and differentiation of the cells with sufficient viability; 2) printability: the bioink should be flowable and deformable to form a stable 3D construct; 3) mechanical stability: the bioink should retain its 3D shape post-printing; 4) biomimicry: the 3D printed construct should mimic the target tissue structurally and compositionally; and 5) biodegradability: the bioink's degradation rate should be tailored to match the target tissue, considering the tissue-specific degradation mechanisms, such as enzymatic, oxidative, hydrolytic, or cell-mediated processes [89].

2.4.1. *Biocompatibility*

Biocompatibility is one of the most imperative parameters in fabricating 3D bioprinted structures that are required to have minimal inflammation, no cytotoxic side effects, compatible with cellular

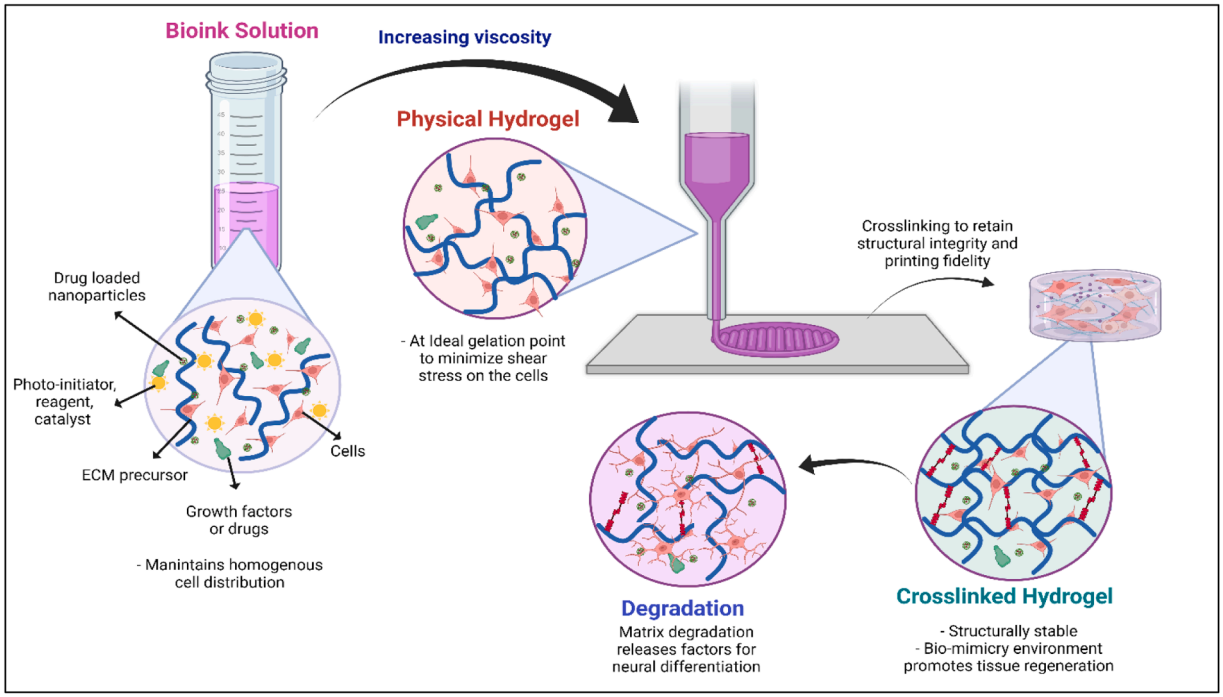

Fig. 3. Schematic representation of 3D bioprinting stages for extrusion based bioprinting method. Bioink solution may contain extracellular matrix (ECM) precursor, cells, growth factors or drugs, nano/micro particles, photoinitiator, and catalyst distributed homogenously throughout the ink. Bioprinting is achieved at ideal physical gelation point of the bioink and bioprinted scaffold is crosslinked to ensure stability under culture conditions. The scaffold undergoes biodegradation which enables releasing factors for neural differentiation and regeneration of the damaged tissue. Created with BioRender.com.

functions such as cell attachment, viability, proliferation, and migration. Biocompatibility can be further enhanced by incorporating both biochemical and biophysical cues. This includes adding soluble factors like growth factors or their mimics and tailoring the scaffold's morphology at the micro and nanoscale. These strategies promote optimal cell-scaffold interaction, ultimately leading to improved *in-vivo* outcomes [10,90]. Biocompatibility becomes especially important for neural cells, considering their less robustness against environmental stresses compared to other cell types such as fibroblasts [91]. While many biocompatible synthetic and natural polymers have been utilized as bioink sources, synthetic hydrogels usually limit cell functions, including their proliferation and adhesion. Natural biomaterials with inherent cell binding sites and bioactivity are the ideal bioink sources to promote cell functions [92]. The biodegradable, biocompatible, and versatile properties of collagen make it the preferred choice for researchers studying neural regeneration, thus making it the most widely used natural hydrogel. Collagen hydrogels are also among the first hydrogels used in clinical trials for treating peripheral nerve damage, such as NeuroGen [93] and Neuromaix [94]. Jiang et al. (2020) have successfully used 3D bioprinted neural stem cells (NSCs)-laden collagen/silk fibroin (CS) scaffolds for the repairment of the spinal cord injury model in Sprague-Dawley rats [46]. Their magnetic resonance and diffusion tensor imaging results showed that the 3D bioprinted CS + NSCs group had the best spinal cord continuity, reduced glial scarring, and abundant regenerative axons compared with other groups in the study.

Others have used gelatin, a denatured form of collagen, for neural tissue engineering applications due to its low cost, biocompatibility, and inherent cell binding sites that allow enhanced cell attachment and proliferation [95]. For 3D bioprinting applications, gelatin is usually utilized after functionalization with methacrylic anhydride to yield a well-known photocrosslinkable semi-synthetic material known as methacrylated gelatin (GelMA). The arginine-glycine-aspartic acids (RGD) and matrix metalloproteinase sequences of the gelatin are unaffected upon functionalization; thereby, GelMA retains the cell adhesion and degradation properties even after photocured under UV light [81].

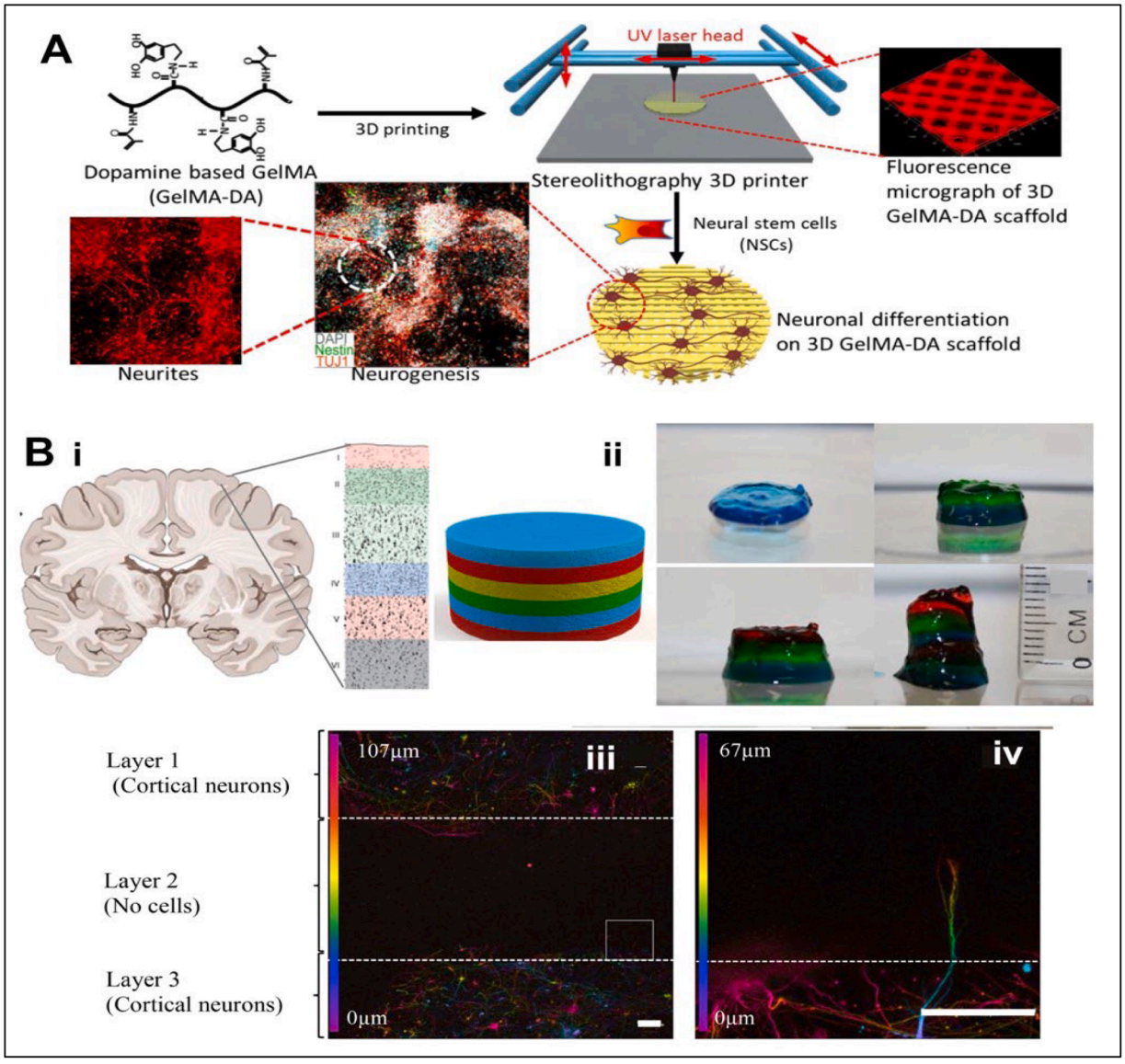

Fig. 4. Functionalization of bioinks for promoted neurite outgrowth. A) Dopamine functionalized gelatin methacrylate (GelMA) bioinks for enhanced neural differentiation (reproduced with permission from Ref. [64]). B) Arginine-glycine-aspartic acids (RGD) modified gellan gum bioinks to form artificial brain-like structures. i) A representation of the 6 layers of the brain in the human cortex, ii) bioprinted brain-like structures, iii) confocal images of neurons at different layers of the bioprinted construct, and iv) zoom-in image of area from B (iii) pointing axon penetration to acellular layer. Scale bars are 100 μm (reproduced with permission from Ref. [65]).

Hamid et al. (2021) have fabricated a multi-material tubular composite using PCL, embryonic body (obtained from mouse embryonic stem cells (mESCs)-laden GelMA hydrogels that were bioprinted within the scaffold, and retinoic acid to induce differentiation [63]. The scaffolds were shown to support EBs neuronal differentiation, as evidenced by βIII-tubulin positive neurons displaying axonal extensions, cell migration, and neuronal patterning that occur during neural tube development. Cytotoxicity is one of the main concerns with photocrosslinking-based bioprinting due to the use of photoinitiator, light irradiation (usually UV), and generation of free radicals during crosslinking. Xu et al. (2020) studied the effect of UV intensity and UV exposure time, and their studies showed that cell viability decreased significantly upon increased UV intensity and duration [96]. However, it is possible to overcome these limitations by using less cytotoxic photoinitiators or photoinitiators that are activated at visible light [97], optimizing the extent of irradiation [96], and washing bioprinted scaffolds following the printing to remove the excess photoinitiator [98].

Fibrin is also often used for neuronal regeneration owing to its excellent plasticity, flexibility, biocompatibility, and ability to be equipped with cells, proteins, and growth factors. By combining fibrinogen and thrombin, it is possible to obtain fibrin hydrogels. This combination leads to the aggregation of protofibrils, which then assemble into a branched 3D network gel structure [99]. Abelseth et al. (2019) have developed a fibrin-based bioink, bioprinted human induced pluripotent stem cell (hIPSCs) aggregates and reported enhanced cell survival and differentiation into mature neural phenotypes [36].

Bioinks without inherent cell binding sites can be functionalized to promote cell adhesion, proliferation, and migration. For example, Zhou et al. (2018) have functionalized GelMA with dopamine (DA) to enhance neurite outgrowth [64] (Fig. 4A). The results showed that GelMA-DA scaffolds have highly porous and interconnected 3D environment which enable enhanced neural stem cell (NSC) growth and differentiation with elevated TUJ1 and MAP2 gene expressions. Lozano et al. (2015) modified the gellan gum with RGD, a common sequence of collagen, laminin, and fibronectin. The modified gellan gum was then combined with primary cortical neurons to construct 3D bioprinted brain-like structures and examined the axonal growth [65] (Fig. 4B). They reported enhanced cell viability, attachment, and development of neuronal networks. YIGSR RNIAEIIKDI, IKVAV, and RYVVLRP are other peptide sequences found on laminin and known to promote neural cell adhesion [100,101].

2.4.2. Printability

Stem cells are highly sensitive to their culture and printing conditions, with their viability, proliferation capacity, and differentiation potential influenced by various chemical and physical factors. This sensitivity underscores the critical role of the environment in maintaining and manipulating stem cells. Factors such as culture medium composition, presence of specific growth factors, temperature, and mechanical forces all significantly influence stem cell behavior. Moreover, techniques for handling and printing these cells, including adjusting bioink viscosity and precision of deposition in 3D bioprinting, require careful optimization to maintain the integrity and desired outcomes of stem cell cultures. Thus, understanding and controlling these variables is crucial for advancing stem cell research and for successful application in tissue engineering and regenerative medicine. Due to their sensitivity, stem cells require specialized bioinks and mild procedures to satisfy their essential biological requirements, proper differentiation, and survival [102]. The printability of the bioink, thus, is a critical point for stem cell bioprinting and it is defined as the ability of a bioink to form and maintain reproducible complex 3D structures with an appropriate temporal, spatial, and volumetric control in adequate resolution [89]. Printability plays a direct role in influencing both the mechanical strength and the cell functions. This is because the structure that is printed can have a significant impact on the fate of the cells after the printing process [103]. Bioink should be studied considering three main stages of the printing: 1) status of bioink before bioprinting (liquid/sol state), 2) during bioprinting (solidification timing), and 3) post-printing (sol/gel state) [104].

Viscosity is the first stage in printability which defines the flowability and deformability of the bioink for well-defined filaments/jets/droplets to be deposited with a proper volumetric, spatial, and temporal control [89]. A common challenge of the bioprinting process is that the bioink should ensure both the printing fidelity and the viability of the cells. Viscous materials usually yield good printing fidelity, but the shear stress imposed during printing more likely harm cells which limits the printable bioinks [102]. When it comes to applications related to nerve tissue engineering, it is highly desirable to utilize low viscosity bioinks. These bioinks possess the unique capability of forming stable 3D structures, thereby creating a soft environment that facilitates the migration of embedded cells. However, printing of the low viscosity bioinks is extremely challenging in terms of the stability of the printed scaffold due to poor mechanical features of the deposited material [66]. A detailed study on the effect of bioink viscosity in 3D printing has been reported by Tirella et al. (2009) on 3D printed microstructures using a pressure-assisted microsyringe (PAM) system, a type of rapid prototyping technique [105]. Each 3D printing approach requires different solution viscosity such as 1–20 mPa.s for inkjet-based printers [106], 30 - 6 $\times$ 10^7 mPa.s for extrusion-based printers [107], and 1 - 300 mPa.s for laser-aided printers [75,108].

Rapid solidification is the second important parameter of bioprinting. The crosslinking should be done under mild conditions to cause minimal cell damage and death. Crosslinking can be achieved physically (ionic reactions, hydrogen-bonding, etc.), chemically (covalent reactions), and enzymatically (by using proteases) [21]. Physical crosslinking is an ideal pathway to be used during extrusion of the bioink, which usually yields mechanically weak bioinks but creates more cell friendly environment than other crosslinking methods [109].

Crosslinking density is also an important parameter during printing since low crosslinking density may lead to faster flow, unstable deposition, and poor print fidelity of the bioink on substrate and high crosslinking density may cause printer nozzle blockage. The printability and the crosslinking degree should be in balance for adequate printing fidelity [85].

The final stage of the printability is the shape fidelity and maintenance of it during culturing. If the physical crosslinking methods are employed during crosslinking, other crosslinking pathways should be introduced to the system, ideally following printing on the substrate to ensure the stability of the printed scaffold under culture conditions. The deposited layers can also be crosslinked at each layer to improve the print fidelity and to provide structural support to the following layers [21,66].

Overall, characterization of the bioink before introducing the cells into the system is necessary to understand shrinking/swelling properties, elasticity, viscosity, and gelation kinetics as all may affect the overall size, resolution, and integrity of the scaffold upon culturing [21, 110].

2.4.3. Mechanical compatibility

The ECM`s interaction with stem cells is influenced by both its protein composition and its physical properties. Specifically, surface topography and bulk stiffness of the ECM are essential parameters that are shown to have a significant impact on stem cell behavior in terms of neurogenesis, neuronal cell migration, nerve repair, and axonal growth. For example, Saha et al. (2008) reported an optimal differentiation of NSCs on intermediate stiffness substrates (500 Pa) where astrocytic differentiation was favored on hard surfaces [111]. It has also been demonstrated that stem cells have mechanical memory of their previous environments and the signals coming from topology that influence their cell fate in the future. Chan et al. (2013) reported an increased neuronal yield from hiPSCs when topographical cues, especially 2 μm gratings, are incorporated into the differentiation protocol [112]. Remarkably,

hiPSCs showed enhanced differentiation when first exposed to topography and then moved to unpatterned control compared to the cells seeded directly on the unpatterned surface.

Stem cell behavior is also affected by the modulus of their 3D environment. Neural tissues have unique biophysical properties with low elastic modulus (90–230 kPa for spinal cord and <1 kPa for adult brain slices) and are softer than bone, heart, and cartilage [113]. Therefore, the bioink must mimic the stiffness of the target tissue for adequate cellular responses. Studies showed that increased hydrogel modulus decreased the NSCs proliferation, and NSCs within the softest hydrogels showed the greatest neuronal marker, b-tubulin III, expression [114]. Similarly, MSCs were reported to adopt neuronal phenotype in type I collagen and hyaluronic acid 3D substrates at 1 kPa elastic modulus, but they differentiated into glial cells in the same substrate at 10 kPa [115]. If the selected bioink, thus, is stiffer, stem cells may differentiate into other lineages than expected. Shear stress should also be optimized during printing to maintain viability and ensure proper cell differentiation. Shear stress exhibited on the embedded cells is influenced by viscosity, printing nozzle diameter, and printing pressure [116]. High shear stress may cause cell death by damaging cell membrane integrity and was reported to decrease rat adrenal medulla endothelial RAMEC cell viability by almost 40 % when constructs are printed at high pressure (40 psi) compared to those printed at low pressure (5 psi) [117]. High-resolution prints are commonly obtained by using a small nozzle diameter and high viscosity. Blaeser et al. (2016) has used a straightforward fluid-dynamics model to minimize the shear stress at possible highest viscosity that allows optimal printing resolution and cell viability [118]. They have used alginate as model hydrogel and mixed with hMSCs for drop-on-demand 3D bioprinting. Their studies showed that even a short-time exposure to high levels of shear stress affects the cells and alters their long-term proliferation, but below a specific shear stress threshold (around 5 kPa) no side effects were observed. Thus, it is critical to prevent excessive shear forces during printing for maximal cell viability.

3. Stem cell-based 3D bioprinting to enhance neural therapies

3.1. Improving disease models' accuracy using 3D bioprinting

Conventionally, pathogenic mechanisms of neurological disorders are modeled using 2D monolayer cell cultures or animals. On the other hand, it is important to note that 2D cultures are excessively simplistic in nature, lacking the ability to accurately depict the intricate and multifaceted nature of human reactions. In animals, cancer is induced by developing genetically engineered animals or through surgical implantation to understand the progress of the disease, but they frequently cannot capture human physiology and behaviors [119]. A 3D culture model can be a better representation of cancer studies as it can mimic migration of cells, cell-to-cell interactions (e.g. communication between stromal cells and tumor), and dynamic diffusion of molecules such as growth factors, cytokines, oxygen, and nutrients along the model [120]. 3D culture models, therefore, are being explored to build a robust model to understand the disease pathology and progression, carry out related analysis, and screen drug candidates. For example, up to now, spheroid cultures [121], organoids [122], cancer-on-a-chip devices [123], and polymeric scaffolds [124] have been developed and served as powerful tools for *in vitro* cancer modeling. However, the main drawback of these models is their lack of spatial organization in terms of shape, size, and control over the positioning of multiple cell types precisely. In this sense, 3D bioprinting has a significant advantage over above mentioned 3D culture models as it allows layer-by-layer assembly of different types of cells and molecules in a high throughput manner [120]. Therefore, the 3D bioprinting system provides a valuable method for developing biomimetic and reliable *in vitro* disease models to effectively develop, test, and screen therapeutics and drugs.

3.1.1. Bioprinting brain cancer models

Glioblastoma, the most common malignant adult brain cancer type, is amongst the cancer types that have the worst outcomes, with only a 1 % survival rate in 10 years [67]. This tumor can invade normal brain tissue aggressively and diffusively because of its infiltration ability, which makes glioblastoma reoccur easily within different parts of the brain [125]. To understand the progress and infiltrative nature of the tumor, it is vital to work on an *in vitro* disease model that mimics the native tumor microenvironment (TME) for the cells to represent their invasive behavior. Two-dimensional (2D) tumor models, cultured on tissue culture polystyrene (TCPS) dishes, do not fully replicate the complex conditions found in living organisms. These models lack the three-dimensional (3D) architecture, cell-cell interactions, and environmental cues found *in vivo*, leading to differences in cell behavior and treatment responses. While animal models offer a more complex system, including these factors, they often fail to accurately reproduce the exact physiological and behavioral outcomes seen in humans due to interspecies differences. This highlights the limitations of current modeling approaches in capturing the complexities of human tumor biology and emphasizes the need for more sophisticated, representative models to bridge the gap between *in vitro* studies and clinical realities. 3D *in vitro* glioblastoma models, therefore, offer a simple and realistic way to understand tumor characteristics. In their study, Ma et al. (2018) reported a comparative study of genome analysis of glioblastoma cells cultured in 2D and 3D conditions [126]. They showed that 2D and 3D cultured cells not only significantly differed in cell morphology but also in the gene expressions where 8117 and 3060 genes were upregulated and downregulated, respectively. KEGG pathway analysis demonstrated that upregulated genes were related to PPAR and PI3K-Akt signaling pathways, and downregulated genes were associated with metabolism, TGF-beta, and ECM-related pathways. Therefore, their study showed the power of a 3D culture system, which provided more realistic results than 2D cultures.

With its automated fabrication process, 3D bioprinting has emerged as a technology that can satisfactorily capture the complexity of the tumor microenvironment. This is made possible by using multiple cell types and biomaterials, allowing for high resolution and reproducibility in the creation of scaffolds. Heinrich et al. (2019) reported a bioprinted glioblastoma cells and glioblastoma-associated macrophages (GAMs) to fabricate a mini-brain model to study the crosstalk between these cell types and to test the therapeutics [68] (Fig. 5A). Their studies demonstrated that in the mini-brains macrophages were actively recruited and polarized to GAM-specific phenotypes by glioblastoma cells which overlaps with the patient survival and transcriptomic data. Furthermore, therapeutics were shown to be effective in inhibiting the interaction between glioblastoma cells and GAMs, which in turn resulted in more response to chemotherapy and reduced tumor growth. In another study, Kingsley et al. (2019) bioprinted embryonic stem cell-encapsulating microbeads using laser direct-write (LDW) that enables precise controlling of the size and pattern [69]. The beads, which were loaded with cells, exhibited the ability to simultaneously generate self-assembled multicellular tumor spheroids and embryonic bodies. Transferrin, a common ligand for receptor-mediated drug delivery, was used to study the effect of bead size on the ligand internalization and the results showed that larger beads exhibit more heterogeneity in uptake of the ligands. They concluded that LDW is a promising approach to fabricate 3D *in vitro* cancer models at controlled size, shape, and pattern to test the effect of drugs. In a different study Wang et al. (2018) created shell-core alginate hydrogel microfibers embedded with human glioma stem cells (GSC23) (formed shell) and human glioma cells (U118) (formed core) to study drug resistance of glioma cells [70] (Fig. 5B). Hydrogel fibers were bioprinted using custom-made coaxial extrusion bioprinting device and crosslinked simultaneously as deposited into the crosslinking solution. Western blot analysis of the cells encapsulated into G/U fibers (shell-GSC23 and core-U118) showed enhanced expression of matrix metalloproteinase-2 (MMP2) and O6-methylguanine-DNA

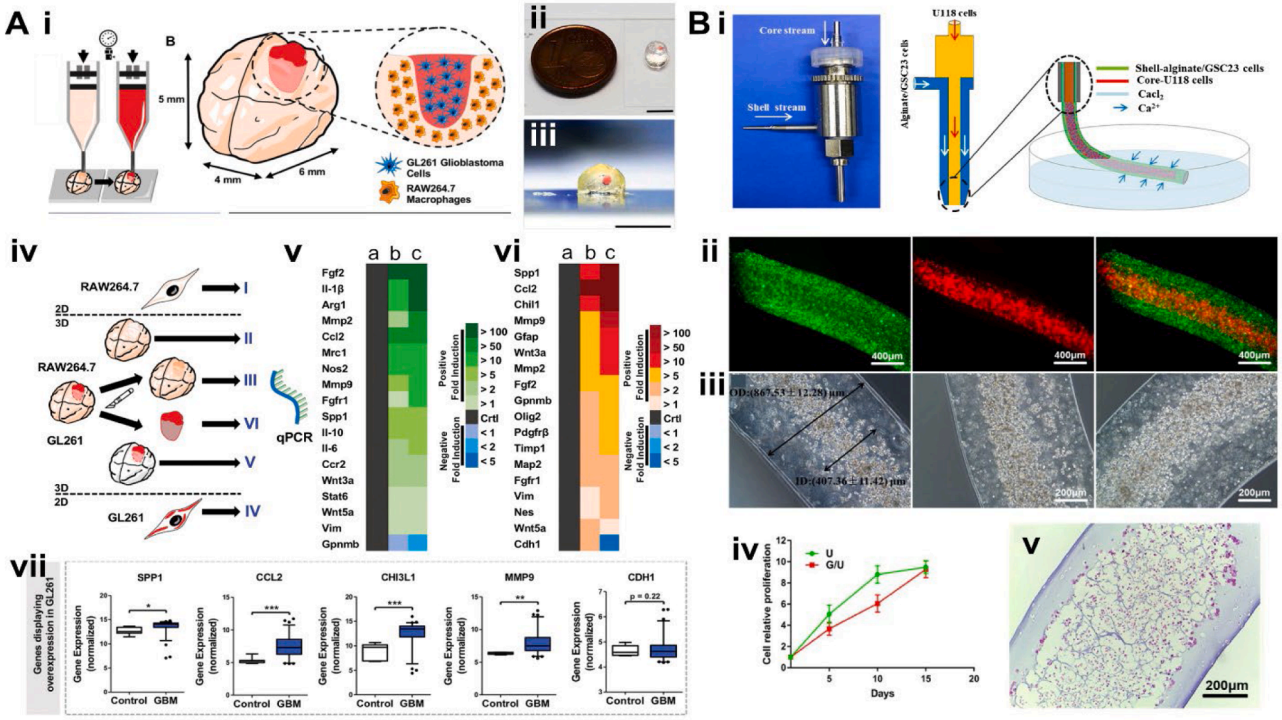

Fig. 5. 3D bioprinting to mimic the brain tumor (glioblastoma) microenvironment. A) A mini-brain model to study crosstalk between glioblastoma cells (GL261) and glioblastoma-associated macrophages (GAMs) (RAW264.7). i) schematics of the bioprinting process of mini-brains. ii-iii) Bioprinted mini-brains highlighting the glioblastoma area in red. Scale bar = 5 mm. iv) Schematics of experimental setup for RAW264.7/GL261 co-culture model. v) Heat map of expressed genes of macrophages (RAW264.7) for I) 2D culture, II) 3D culture, III) 3D co-culture model. vi) Heat map of expressed genes in glioblastoma cells (GL261) for I) 2D culture, II) 3D culture, and co-culture model. vii) Comparative transcriptomic analysis in human glioblastoma patients from public database GEO (GSE16011) for genes reported to be upregulated in the 3D bioprinted mini-brains for macrophages (reproduced with permission from Ref. [68]). B) Shell-core coaxial bioprinted alginate hydrogels embedded with human glioma stem cells (GSC23) (shell) and human glioma cells (U118) (core) for drug resistance studies of glioma cells. i) Schematic representation of coaxial bioprinting and crosslinking. ii) Cell-laden alginate shell-core hydrogels. Shell cells (GSC23) were labeled with green (PKH 67 dye) and core cells (U118) were labeled with red (PKH 26 dye). iii) Inner and outer diameter of fibers (left image). Shell-core hydrogel microfibers were cultured for 5 (middle image) and 10 (right image) days. iv) Proliferation of cells co-cultured in shell-core (GSC23/U118) and cultured in only core (U118) hydrogel microfibers. v) Hematoxylin and eosin (H&E) staining of longitudinal section of shell-core hydrogel microfibers (reproduced with permission from Ref. [70]).

methyltransferase (MGMT) compared to U fibers (core-U118). mRNA expression of the drug resistance and tumor invasion genes, namely MGMT, matrix metalloproteinase-9 (MMP9), and vascular endothelial growth factor receptor-2 (VEGFR2), were also upregulated in G/U fibers when compared to U fibers indicating dependence of U core cells to G shells for proper biological functions. In addition, the study revealed that the drug resistance of U118 cells cultured in G/U fibers was significantly greater than that of cells cultured in U fibers. Moreover, the drug had a more pronounced effect on the cell viability of the G/U cultured cells, resulting in higher survival rates. The findings of this study suggest that the coaxial extrusion approach can effectively imitate the glioblastoma microenvironment. This has important implications for the field of drug development and screening, offering promising opportunities for future research.

To summarize, the implementation of 3D bioprinting offers a robust means of generating unique tumor models, enabling comprehensive investigations into disease progression and providing a platform for testing drugs and therapeutics, as highlighted in the aforementioned studies. In addition to their ability to replicate tumors *in vitro*, 3D bioprinted tumor models have the potential to revolutionize personalized therapies and individualized tests for drug susceptibility and resistance [13].

3.1.2. Bioprinting neurodegenerative disease models

Neurodegenerative diseases present a significant challenge to human health, especially with the increasing elderly population in recent years. These age-dependent diseases such as Alzheimer`s disease, Huntington`s disease, Parkinson`s disease, frontotemporal dementia, spinocerebellar ataxia, and amyotrophic lateral sclerosis show diverse pathophysiology with some effects on movement of the patient, some cause cognitive and memory disorders, and others affect a person`s capacity to breath and speak [127]. Despite the huge work and dedication to understanding the disease mechanisms and developing therapeutics, there is currently no cure, and there is an urgent need for novel and effective treatment methods. Animals are valuable experimental models for creating a disease model system for studying the underlying mechanisms of these diseases. However, they often fail to fully replicate the diseases and predict human clinical trial results since the clinical or neuropathological phenotypes observed in humans do not readily overlap with the animal models [128]. With the discovery of hiPSCs, stem cells reprogrammed from adult somatic cells, it is now possible to create patient-specific cell lines [129,130] which opens new avenues for personalized medicine studies as iPSCs can represent the genetic phenotypes and also the pathology of the diseases when differentiated into specific cell types such as neurons [131]. As mentioned above, 3D bioprinting is a powerful tool for developing 3D structures that mimic the native and heterogeneous features of neural tissues with the aid of a wide variety of bio-inks and high-resolution scaffold fabrication. Most of the 3D bioprinting research, however, focused on the formation of neural tissues using healthy stem cell lines rather than patient-specific cell lines. Gu et al. (2016) reported the use of direct-write printing of neural stem cells for the first time, where they encapsulated the cells in a

bioink composed of alginate, carboxymethyl-chitosan, and agarose [132]. The encapsulated cells were sufficiently viable and able to differentiate into GABAergic neurons and glial cells by forming networks and synaptic contacts. Abdelrahman et al. (2022) developed functional 3D models of dopaminergic neurons ultrashort self-assembling tetrapeptide scaffolds, demonstrating biocompatibility with both primary mouse and human embryonic stem cell-derived dopaminergic neurons [133]. The study highlighted the ability to record spontaneous neural activity for over a month and enhanced neurite outgrowth through vascularization in co-cultured models, showing the potential of these 3D models for advancing research on neurodegenerative disorders. In another study, Lozano et al. (2015) fabricated brain-like structures using RGD-modified gellan gum bioinks and cortical neurons [65]. The encapsulated cortical neurons exhibited 80 % viability and could successfully differentiate into glia and neurons. They also demonstrated the outgrowth of the neurites from cortical neurons between the layers by printing 3 layers composed of the middle acellular layer sandwiched between cortical neuron encapsulated layers. The neurites could penetrate up to 100 μm into the acellular layer in 5 days. Hinton et al. (2015) developed a novel 3D printing technique termed freeform reversible embedding of suspended hydrogels (FRESH) to fabricate complex 3D tissues/organs that are printed in a gel support bath [35] (Fig. 6A, B).

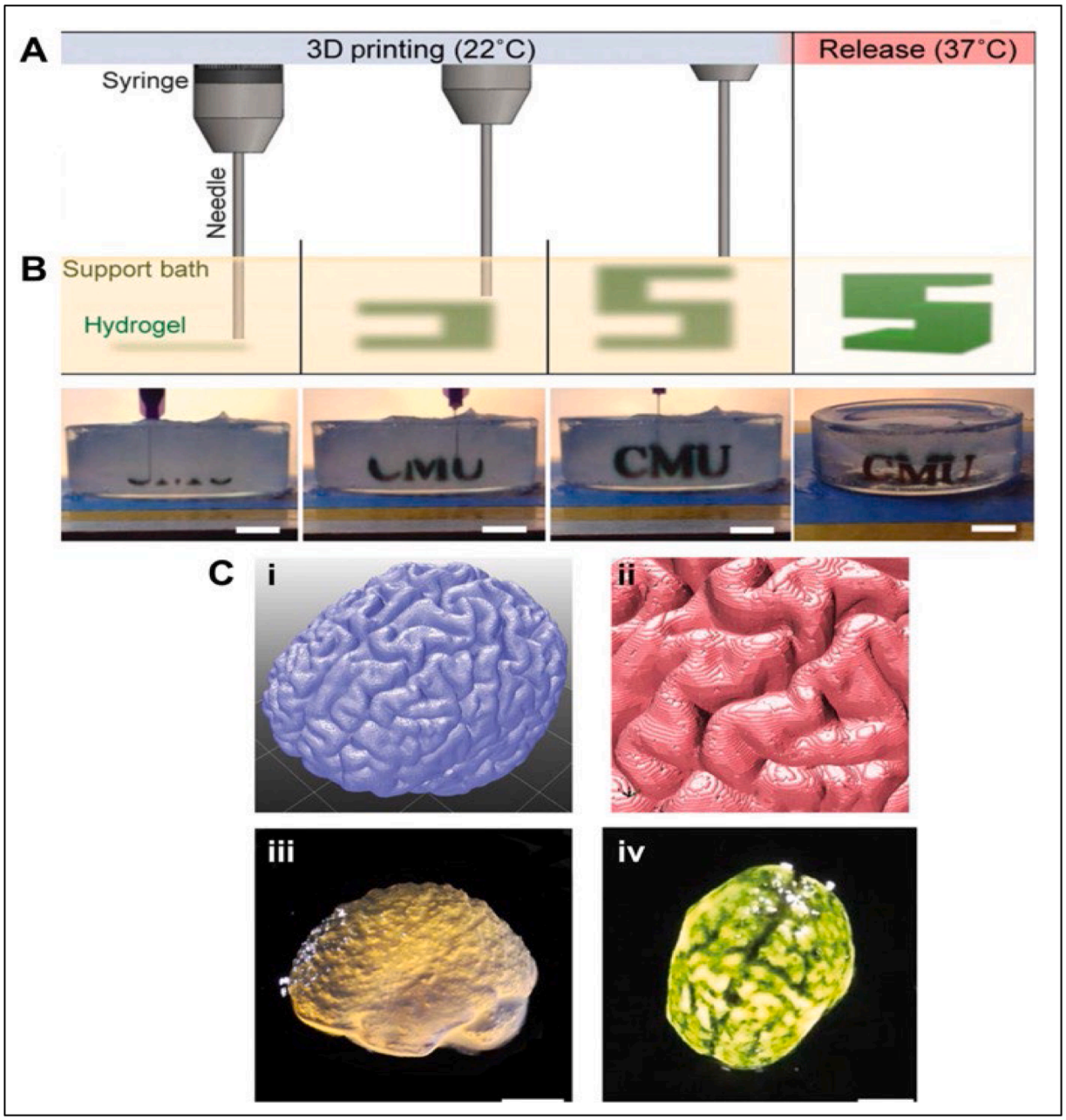

Fig. 6. Freeform reversible embedding of suspended hydrogels (FRESH) bioprinting to fabricate complex 3D tissues/organs. A) A schematic representation of FRESH bioprinting approach showing the deposition and crosslinking of hydrogel (green) in a supporting bath (gelatin slurry). Scale bar= 1 mm. B) Images of `CMU` was FRESH bioprinted in black and released by melting the gelatin support (gray material in the petri dish) at 37 °C. C) FRESH bioprinting of complex structures based on data from whole brain imaging. i) 3D image of human brain rendered from MRI data to be used for FRESH bioprinting. ii) A zoomed image of brain model showing the complexity of the outer structure. iii) Lateral view of 3D bioprinted structure mimicking the anatomical features such as cortex and cerebellum. iv) A top-down view of brain model dripped with a black dye to visualize white matter folds. Scale bar = 1 cm (reproduced with permission from Ref. [35]).

With this technique, they replicated the complex external surface of the human brain using an alginate-based bioink at a 200 μm resolution (Fig. 6C). This study emerged as a proof-of-concept study showing the possibility of printing complex brain anatomy with cerebellum and cortex structures. Although it lacks internal organization, with the development of 3D printing technology, it will be possible to print subtypes of brain tissue with vascularization, signaling molecules, and cells in the near future. In another study, 3D-core-shell model of Alzheimer`s disease was developed by bioprinting with human neural progenitor cells using a coaxial bioprinter, incorporating Matrigel as the core bioink and alginate as the shell bioink [134]. These constructs demonstrated self-clustering, long-term cell viability, and enhanced differentiation, while also exhibiting amyloid-β aggregation and increased expression of AD-related genes, providing a promising platform for advancing neurodegeneration research. Such platforms have a great potential to be used for drug development and screening, studying neurodegenerative diseases, and developing tissue-engineered constructs for CNS and PNS tissue replacement.

3.2. Expanding the utility of 3D bioprinting via nanomaterials

Numerous nanomaterials have been incorporated into 3D bioprinting techniques for a variety of purposes. Table 2 above summarizes the target application and key findings of publications that incorporate neuronal cells or show considerable potential for neuronal applications. Additional discussion about key bioink properties, results, and implications for future studies are found in Sections 3.2 and 3.3. Abbreviations: GO- graphene oxide, HA – hydroxyapatite, PEG- poly(ethylene glycol), PEO- poly(ethylene oxide), PCL- poly(ε-caprolactone), PEDOT:LS- poly(3,4-ethylenedioxythiophene): sulfonated lignin PEDOT:PSS-poly(3,4-ethylenedioxythiophene) polystyrene sulfonate, PETE-S- poly (sodium 4-(2-(2,5-bis(2,3-dihydrothieno[3,4-b][1,4]dioxin-5-yl)thiophen-3-yl)ethoxy)butane-1-sulfonate), PS- polystyrene, PLGA- poly-lactic-*co*-glycolic acid, t-ZnO- tetrapodal zinc oxide.

3.2.1. Incorporating nanomaterials to enhance scaffold properties and printing fidelity

3.2.1.1. Enabling new bioprinting modalities. Due to the relative infancy of 3D bioprinting, technical constraints still limit the scale and feasibility of printed designs. For example, commercially available stereolithography photoinitiators require UV light to achieve reasonable reaction kinetics, thus limiting the viability of encapsulated cells. Here, nanomaterials with unique physicochemical properties can bridge the gap between design constraints imposed by 3D printers and biological conditions conducive to cell growth and regeneration.

Most stereolithography photoinitiators for 3D bioprinting are active in the UV region, which is detrimental to cell viability. While visible light photoinitiators are available, most are (1) hydrophobic and incompatible with most water-based bioprinting inks or (2) have limited absorption in the relevant wavelengths. In an effort to tackle this restriction, Pawar et al. devised a strategy involving the utilization of a nanoparticle system for enclosing a hydrophobic photoinitiator (TPO) known for its remarkable visible light activity. This approach facilitated the bioprinting of aqueous solutions [155]. The photoinitiator encapsulation involved two major steps: an oil-in-water microemulsion followed by spray-drying to yield a nanoparticle powder. The encapsulated TPO was found to have greater photoinitiator activity than Irgacure 2959 (commercially available water soluble photoinitiator) when exposed to 395 nm (purple) light. Moreover, the TPO nanoparticle could be suspended in an aqueous, PEGDA-based printing solution to form stereolithography hydrogels at non-UV wavelengths. This system can be further employed to encapsulate other hydrophobic, high efficiency photoinitiators in cell-based aqueous 3D bioprinting solutions to enable more work with visible light stereolithography.

Sacrificial support bath printing has been adopted to temporarily hold overhanging structures when printing softer materials. Current biocompatible support baths ' technical limitations (e.g., ionic sensitivity and thermal stability) led Afghah et al. to develop a more robust nanoclay-hydrogel support bath [151]. Commercially available Pluronic F127 (gel at physiological temperatures, liquifies at 10 °C; PF) and Laponite RDS (mechanical support and thixotropic behavior; RDS) nanoparticles were chosen to form the final PF-RDS support bath with calcium ions included as a crosslinker for alginate-based bioprinting. Inclusion of RDS was found to not significantly affect PF gelation kinetics. Interestingly, there was an optimal concentration of PF to RDS (10 % to 3 %) when looking to increase storage modulus. The authors speculate that after a certain concentration, RDS nanoparticle interactions with PF become saturated. Hence, the overall hydrogel storage modulus reverts to the softer PF. This increase in storage modulus was accompanied by a decrease in flow index and an increase in yield stress. Self-recovery time (i.e., recovery of storage modulus after deformation) was found to be shorter for composites with higher concentrations of PF. Various shapes, including stars (sharp angles) and nostrils (overhangs), were printed with good printing fidelity and without damage when the support bath was cold-melted (Fig. 7A). NIH-3T3 cells were included in the alginate bioprinting ink and found to retain high viability even when printed in the PF-RDS support bath. This support bath can serve as a more stable alternative to conventional support baths, such as Carbopol (disrupted by ions) and gelatin (melts at physiological temperatures).

While most support baths are quickly removed from 3D bioprinted structures shortly after crosslinking, long-term culture may be required in specific applications, such as prolonged *in vitro* tissue maturation. Bakht et al. detail the development of a cellulose nanocrystal (CNC) support bath that is robust enough to withstand at least 4 weeks of static culture and 2 weeks of microfluidic perfusion culture [137]. Various 3D bioprinting inks (gelatin, alginate, gelatin methacrylate, platelet lysate) were readily printed within the CNC support bath with high printing fidelity. Once the desired structure is printed within the CNC suspension, the support bath is "locked" and converted into a fibrillar matrix via a calcium chloride solution. This printing process was found to be compatible with various cells, including adipose-derived mesenchymal stem cells (ADSC) directly mixed within the bioprinting ink for deposition within the CNC suspension. Since cellulose is not degradable by mammalian enzymes (e.g., matrix metalloproteases), the CNC support structure can be used until exogenous cellulase is added. The enzymatic release is non-destructive to (cell-embedded) bioinks and compatible with cell culture conditions. Key demonstrations include bioprinting ADSC embedded within a miniaturized femur model and a dynamic organ-on-a-chip model. Embedded ADSCs were found to maintain high proliferation and viability over 14 days of static culture and subsequent cellulase release from the CNC support matrix. These results indicate that the CNC support matrix is porous enough to allow adequate nutrient exchange for cell growth. For the organ-on-a-chip demonstration, endothelial cells and breast cancer cells were printed in concentric circles and monitored during perfusion culture. The endothelial cells developed an inner lumen, while the cancer cells self-assembled into microaggregates. Even though the CNC fibrillar matrix was shared, the cells remained within their designated areas. The researchers took advantage of the inherent inertness and impermissiveness of cellulose to create a strong support bath/matrix for 3D bioprinting.

In addition to modulating the properties of various bioinks to facilitate printing, nanomaterials can be employed to help stabilize and retain printing fidelity after the product hydrogel is formed. Zhang et al. included GO in an alginate/gelatin 3D bioprinting ink and noted significantly better printing fidelity [145]. When lattice hydrogels were formed without embedded cells, GO-supplemented samples displayed better retention of the initial printing structure compared to hydrogels lacking GO (Fig. 7B). Lattice holes were consistent throughout regardless of GO inclusion, while lattice lines underwent noticeable diameter

Table 2
Nanomaterials previously used to supplement 3D bioprinting inks.

Nanomaterial	Morphology	Application	Key Finding	Refs.
Carbon	Nanofiber	Modulate light penetration and crosslinking efficiency	Developed different curvatures due to differing internal forces. Increased neurogenesis (cell seeding)	[135]
Cationic silica	Nanoparticle	Improve long-term printing fidelity	Reduced changes to printed structure during crosslinking and culture	[136]
Cellulose	Nanocrystal	Sacrificial printing bath	Improved printing fidelity including sharp angles and overhangs. Stable until exogenous cellulase	[137]
Cellulose	Nanofiber	Biophysical cues and modulate mechanical properties	Improved printing fidelity and increased mechanical strength	[138]
Cellulose and graphene	Nanosheet	Light-based conversion of cellulose to graphene	Conversion of cellulose to graphene at micron-scale resolution occurs with femtosecond pulses at ambient conditions. Increased electrical properties after "printing" graphene	[139]
$NaHPO_3$ and NaCl	Microparticle	Sacrificial porogen	Increased porosity, lowered mechanical properties, increased drug loading, and reduced burst release	[140]
NaCl	Microparticle	Sacrificial porogen	Increased porosity and primary rat dorsal root ganglia infiltration	[141]
Fe_2O_3	Nanoparticle	Modulate light penetration and crosslinking efficiency	Developed different curvatures due to differing internal forces. Increased neurogenesis (cell seeding)	[135]
Gelatin	Nanoparticle	Improve thixotropic recovery	Printed overhanging structures without support baths	[142]
Au-tipped CdS	Nanoparticle (rod)	High efficiency photoinitiator at visible/NIR wavelengths	Enabled high resolution two-photon voxel photopolymerization	[143]
Graphene	Nanosheet	Photothermal activation of shape memory polymer	Deformed scaffolds reverted to original shape via NIR light. Increased neurogenesis (cell seeding)	[144]
GO	Nanosheet	Improve long-term printing fidelity	Reduced changes to printed structure during culture	[145]
GO	Nanosheet	Modulate light penetration and crosslinking efficiency	Developed different curvatures due to differing internal forces. Increased neurogenesis (cell seeding)	[135]
GO	Nanosheet	Modulate electrical properties	Incorporated GO into printing ink before reduction (rGO) to restore electrical conductivity and reduce impedance	[146]
GO and Pluronic P123-coated Graphene	Nanosheet	Modulate mechanical properties	Disrupted structure of polyurethane-nanoparticle ink, resulting in softer scaffold. Increased neurogenesis and astrogenesis (cell encapsulation)	[147]
GO-SiO_2-PS	Nanoparticle (disc)	Modulate electrical and drug release properties	Increased drug loading, magnetic field-accelerated drug release, and magnetic field-induced electrical stimulation. Increased neurogenesis (cell seeding and *in vivo*)	[148]
GO, PCL, and PEO	Nanofiber	Biophysical cues, sacrificial porogen, and drug carrier	Nanofibers used to form 3D structures via electrohydrodynamic jet printing. Decreased mechanical strength with increasing graphene content	[149]
HA	Nanoparticle	Modulate light penetration and crosslinking efficiency	Developed different curvatures due to differing internal forces. Increased neurogenesis (cell seeding)	[135]
HA and Laponite	Nanoparticle	Drug carrier	Reduced burst release/enabled sustained release. Different nanoparticles found to have different release profiles	[150]
Laponite RDS + Pluronic F127	Nanoparticle (disc)	Sacrificial printing bath	Improved printing fidelity including sharp angles and overhangs	[151]
Monomethoxy PEG-PCL	Nanoparticle	Drug carrier	Reduced burst release/enabled sustained release. Increased neurogenesis and myelin secretion (cell seeding and *in vivo*)	[152]
$NaYF_4$:Yb,Tm	Microparticle	High efficiency photoinitiator at visible/NIR wavelengths	Enabled NIR-based direct writing with overhands	[153]
$NaYF_4$:Yb,Tm/$NaYF_4$	Nanoparticle	High efficiency photoinitiator at visible/NIR wavelengths	Enabled high resolution multi-photon voxel photopolymerization	[154]
n-butyl acetate, sodium dodecyl sulfate, and polyvinylpyrrolidone	Nanoparticle	Solubilize hydrophobic, high efficiency photoinitiator (TPO)	Higher crosslinking efficiency than free TPO or water soluble photoinitiator	[155]
PEDOT:LS	Nanoparticle	Modulate electrical properties	Enhanced neuronal differentiation and functional/histological recovery after SCI	[156]
PEDOT:PSS	Nanoparticle	Temporary ionic crosslinking and modulate electrical properties	Improved printing fidelity and increase electrical conductivity	[157]
PEDOT:PSS	Nanoparticle (lyophilized)	Modulate electrical properties	Increased electrical conductivity and caused cells to respond to electrical stimulation. Increased neurogenesis (cell encapsulation)	[158]
PEO	Microparticle	Sacrificial porogen	Increased porosity, greater cell spreading and proliferation, altered printability	[159]
PEO	Nanofiber	Biophysical cues and drug carrier	Nanofibers used to form 3D structures via electrohydrodynamic jet printing. Can include silver and PEDOT:PSS nanoparticles	[160]
PETE-S	Monomer	Modulate electrical and mechanical properties	*In situ* crosslinked PETE-S "nanoscale network" increases electrical conductivity and cell proliferation at optimized concentrations	[161]
PCL and Gelatin	Nanofiber	Biophysical cues	Increased mechanical strength and promoted longer neurites. Increased neurogenesis (cell seeding)	[162]
PCL diol-poly(lactide) diol	Nanoparticle	Water stable dispersion of hydrophobic polymer	Printed hydrophobic polymer in water-containing bioink. Increased neurogenesis (cell encapsulation and *in vivo*)	[15]
PLGA	Nanoparticle	Drug carrier	Reduced burst release/enabled sustained release and increased mechanical properties. Increased neurogenesis (cell seeding)	[163]
$Ti_3C_2T_x$	Nanosheets	Modulate electrical and wettability properties, impart photothermal activity	Surface coating increased scaffold electrical conductivity, hydrophilicity, cell adhesion, and neurogenesis. Can induce neural electrical activity via light (640 nm)	[164]
Ti_3C_2	Nanosheets	Modulate electrical and mechanical properties	Increased mechanical strength and electrical conductivity (concentration dependent)	[165]
t-ZnO	Microparticle (tetrapodal)	Cell activity sensor	Enabled noninvasive monitoring of dopaminergic neuron differentiation	[166]

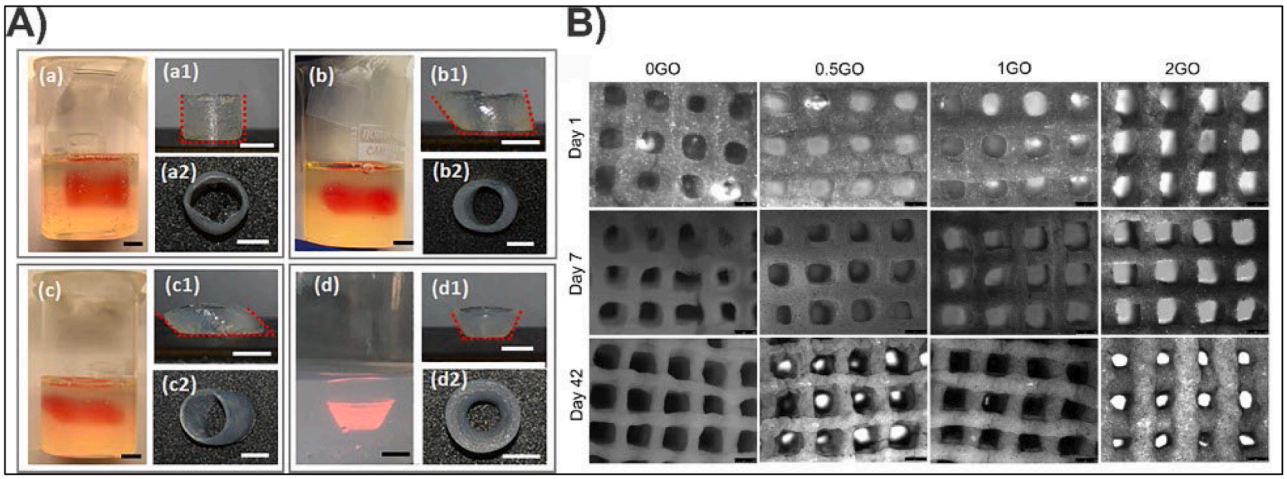

Fig. 7. Nanomaterials support high-fidelity 3D bioprinting. (A) Laponite nanodiscs were added to Pluronic F127 and $CaCl_2$ to form a support bath for 3D bioprinting (reproduced with permission from Ref. [151]). The resulting support bath is shear thinning, meaning the bioprinting needle can readily deform the support bath for freeform printing and ink deposition. After the needle and shear stress is removed, the bath increases in stiffness to support the deposited structure (including overhanging structures). This support bath was compatible with cell-laden alginate inks. (B) Graphene oxide (GO) was used to supplement an alginate/gelatin bioink to improve printing fidelity after prolonged incubation in cell culture media (reproduced with permission from Ref. [145]). While excessively high GO concentration led to eventual scaffold shrinkage when cells were encapsulated in the final hydrogel, an optimal amount of GO helped the scaffold retain its printed shape even after prolonged cell culture.

reduction in the absence of GO, indicating that GO prevents shrinkage. Unexpectedly, GO-loaded hydrogels exhibited a different trend when mesenchymal stem cells (MSC) were included in the bioprinting ink. Hydrogels with the greatest concentration of GO exhibited lattice pore closure, lattice line expansion, and loss of printing fidelity over time. Beyond increasing the printing fidelity of alginate/gelatin 3D bioprinting ink, GO inclusion was found to increase MSC cell spreading, osteogenesis, and biomineralization. Since many hydrogels are known to undergo significant shape change when exposed to biological environments, including nanomaterials, it may be prudent to ensure that 3D bioprinted materials retain their intended structures over time.

Hsieh et al. used nanoparticle dispersions to create a polyurethane-based thermoresponsive ink that gels upon physiological temperatures [15]. Interestingly, while the final poly(ε-caprolactone) diol-poly (lactide) diol polymer is only soluble in organic solvents, the synthesis procedure and resulting water-based dispersion allows for mixing with cells in an aqueous environment [15,167]. With the ability to directly mix cells in the bioink, the authors incorporated neural stem cells (NSC) into 3D-printed structures with different polymer concentrations [15]. Softer hydrogels arising from inks using (1) less concentrated dispersions and (2) poly(D,L-lactide) diol [versus enantiomer poly(L-lactide) diol)] were found to better promote cell proliferation and neurogenesis. As an interesting aside, the cell-laden bioink was then repurposed as an injectable hydrogel and used to rescue zebrafish models for central nervous system damage caused by ethanol and cerebellum puncture lesions. Careful use of nanomaterials (e.g., polymer nanoparticle dispersions) can enable further 3D bioprinting research using a wider scope of materials.

Until total printing fidelity (translating CAD to physical products without deviation) and complete biocompatibility are achieved, there will be motivation to expand printing modalities for 3D bioprinting. Nanomaterials are particularly suited for expanding printing modalities by (1) broadening the capacity of 3D printers to function with sensitive biological molecules and payloads and (2) ensuring that printed structures retain their shape despite limited biopolymer robustness. Future work in the field can focus on generating new nanomaterials with specific properties tailored for bioprinting (e.g., high thixotropy for extrusion bioprinting fidelity) and new techniques to render nanomaterials suitable for 3D printing (e.g., nanoemulsions of hydrophobic nanomaterials in aqueous media).

3.2.1.2. Optical properties. As one of the first 3D printing modalities, stereolithography retains a substantial share of scientific publication and work, despite the emergence of other printing techniques. The ability of light to penetrate through stereolithography inks remains a key concern when optimizing and integrating this technique into biological applications. Nanomaterials have been investigated to enhance and dampen the efficiency of photocrosslinking to modulate the optical properties of stereolithography inks.

Miao et al. mixed various nanomaterials (magnetic nanoparticles, carbon nanofibers, hydroxyapatite nanoparticles, and graphene) into a soybean oil epoxidized acrylate stereolithography ink [135]. The authors found that nanomaterial-supplemented inks accentuated programmed shape change in 4D printed hydrogels (Fig. 7A, B). Two potential mechanisms are proposed. (1) Since the nanomaterials attenuated the penetration of light through the ink, there is a more drastic difference in crosslinking efficiency between the top and bottom of the printed hydrogel. This difference in crosslinking efficiency translates to differences in curvature for the final printed material as the top and bottom experience different internal forces. (2) The inclusion of nanomaterials resulted in a porous and surficial structure, which may contribute to different swelling between the top and bottom of the hydrogel. Despite the inclusion of graphene and resulting changes in hydrogel curvature, human mesenchymal stem cells could be seeded onto the hydrogel and induced into a neuronal lineage. Moreover, the expression of neurogenesis-related genes was increased compared to cells seeded on similar 4D-printed structures without graphene. In this demonstration, nanomaterials acted to regulate the optical properties of the ink, which translated to functional differences in the final product.

As an alternative to photoinitiator-based crosslinking, Pawar et al. proposed the use of gold-tipped cadmium sulfide (CdS-Au) nanorods as a photocatalyst means of generating free radicals for polymerization [143]. Several advantages over conventional organic photoinitiators were mentioned, including high absorbance cross-section at visible wavelengths, high water dispersibility (when coated with PEI), and ability to generate free radicals without breaking down. Rather than undergoing homolytic breakdown as with most organic photoinitiators (e.g., Irgacure 2959), the CdS-Au nanorod undergoes electron-hole recombination to generate free radicals from water or molecular oxygen (normally considered to be a polymerization inhibitor). By employing a DLP printer, a crosslinking process was carried out on an

ink blend containing PEGDA, acrylamide, and CdS-Au nanorods. The outcome of this process was the successful formation of a C180 Buckyball hydrogel, which displayed superior efficiency when compared to Irgacure 2959. Previous studies have noted that semiconductor nanorods have exceptionally high two-photon cross-sections, which can be exploited for high-resolution two-photon photopolymerization and voxel (3D unit) printing (Fig. 8D, E). Accordingly, the PEGDA-CdS-Au printing gel was crosslinked using two-photon polymerization at a wavelength of 840 nm. Future work in this field targeting nerve regeneration would have to move away from CdS due to the potential for leaching toxic cadmium ions.

Photopolymerization is currently dominated by UV light, which presents notable problems related to limited curing depth and potential damage to biological molecules. Zhu et al. demonstrated the use of upconversion nanoparticles (UCNP, materials capable of anti-Stokes shift) to enable 3D near-infrared direct writing (NIR-DIW) with higher light penetration and lower cytotoxicity than UV [153]. The UCNP employed here is composed of $NaYF_4$:Yb,Tm for absorption at 980 nm and emission at approximately 475 nm to activate the titanocene photoinitiator. Moreover, the NIR-DIW could crosslink printed ink shortly after deposition, leading to higher printing fidelity than post-printing curing (affected by ink spreading over time) and the creation of free-standing structures with overhangs. The incident revealed that NIR crosslinking light lies outside the absorption spectra for several pigments, such as red, yellow, blue, white, and black. Consequently, advancements in this area have made it achievable to print inks in multiple colors without the necessity of making substantial modifications in crosslinking efficiency or mechanical properties. The presented work does not mention biological applications, but future work can easily expand upon UCNP-enabled NIR-DIW. NIR light presents significantly lower toxicity and mutagenicity than UV light, which is beneficial for direct printing of cellularized inks. Additionally, biological payloads may be damaged upon exposure to high-energy UV light (e.g., fluorescent tracking molecules); lower-energy NIR light would circumnavigate such concerns. Transitioning away from UV light to relatively benign NIR light would represent a significant step forward for light-based printing of biological materials.

Traditional light attenuation constraints with UV and visible light significantly limit the potential for 3D voxel-based printing. NIR light exhibits significantly lower attenuation in aqueous and biological

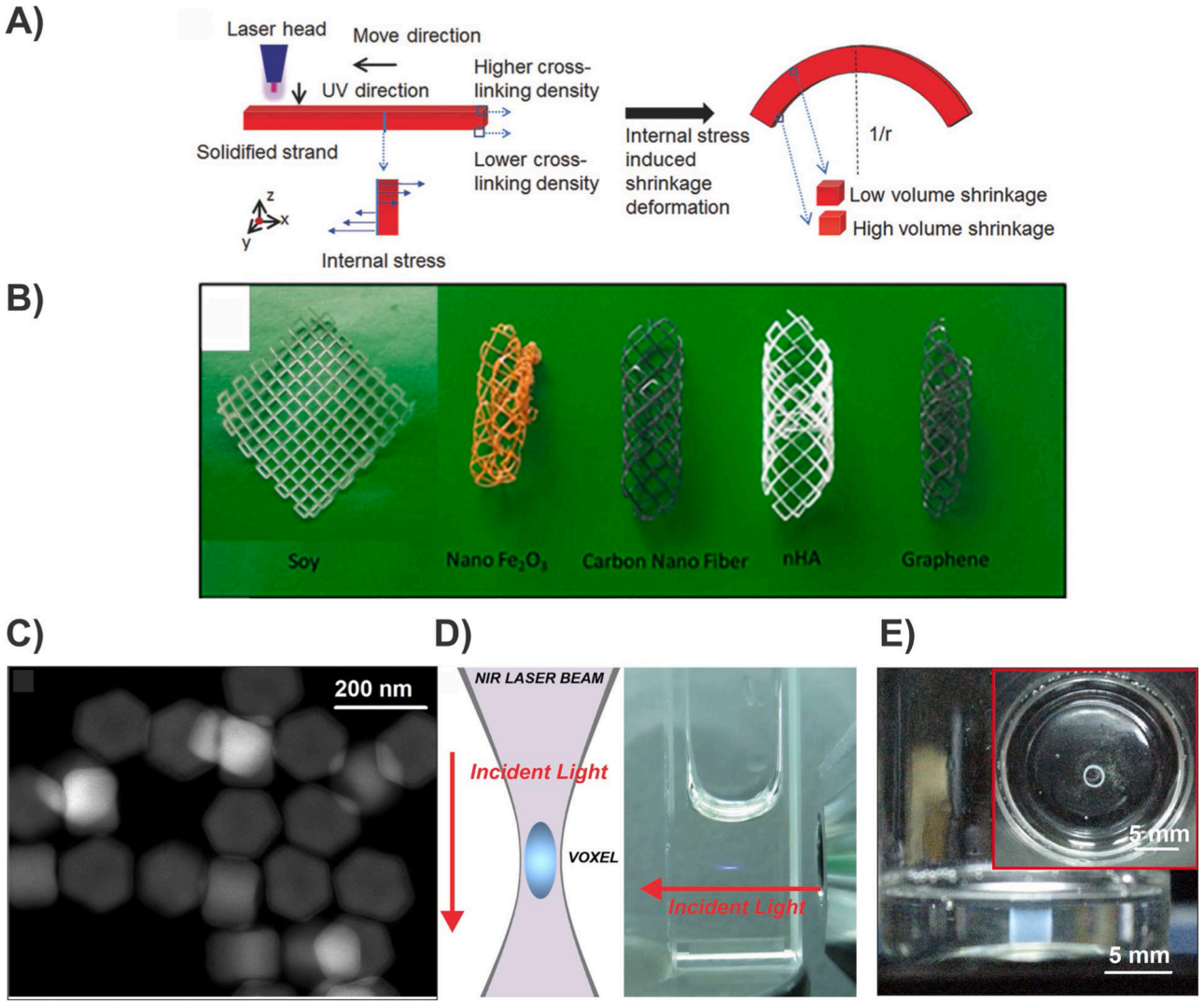

Fig. 8. Nanomaterials modulate the crosslinking efficiency of stereolithography (light-based) bioprinting. A-B) (A) Schematic diagram of how differential crosslinking efficiency in a scaffold result in internal stresses and deformation in a soft bioprinting ink (reproduced with permission from Ref. [135]). (B) Various nanomaterials were added to soybean oil epoxidized acrylate ink to yield inks with different absorbance spectra. Nanomaterials with higher absorbance resulted in greater curvature in the final construct due to greater crosslinking differences between the top and bottom layers. C-D) (C) Upconversion nanoparticles were employed for (D) voxel printing within the printing bath volume via NIR light (reproduced with permission from Ref. [154]). Incident light labels added for clarity. (E) A hollow tube structure was printed within the bioink reservoir volume. Abbreviations: nHA- nanohydroxyapatite, NIR- near infrared.

media, which enable the potential of 3D voxel printing when combined with upconversion nanoparticles as demonstrated by Rocheva et al. [154]. Their core-shell $NaYF_4$:Yb,Tm/$NaYF_4$ UCNP responds to 975 nm incident light and emits primarily 288 nm, 345 nm, and 360 nm light to activate the Irgacure 369 and Darocure TPO photoinitiators. To enable 3D printing, a NIR light was focused using a lens to form a beam caustic (focused area where light intensity is maximized) that represents the printed voxel inside a bath of synthetic acrylate oligomers. A torus with a thickness of 50 μm could be printed using this system, with the outer surface exhibiting nanoscale roughness caused by polymer growth around the UCNP. Further analysis demonstrates that a specific concentration of UCNP is required to generate a cohesive, connected, crosslinked polymer matrix (i.e., final printed product). In this demonstration, 0.4 % of the ink volume or approximately 17 mg ml^{-1} UCNP loading is required to form a printed structure. Here, the ability to use NIR light due to UCNP-based photocrosslinking enables high-resolution voxel-based printing with future potential to form freestanding constructs and encapsulate cells in biologically active matrices for nerve regeneration.

Rather than using nanomaterials to modulate 3D bioprinting ink photocrosslinking, Li et al. sought to use nanomaterials to noninvasively monitor stem cell differentiation into neurons. While numerous neurogenesis sensors exist, the authors utilized photoactive tetrapodal-shaped zinc oxide microparticles (t-ZnO) since key physicochemical properties make it amenable to 3D bioprinting ink incorporation [166]. More specifically, t-ZnO can operate under physiological conditions (i.e., serum-containing cell culture media) conditions, be incorporated into aqueous-based inks without extensive modifications to the microparticle surface or biomaterial composition, and permit continuous operation (i.e., no photobleaching). t-ZnO powder was suspended in an alginate/-Pluronic F127-based solution and extruded without apparent damage to the tetrapodal microstructure (attributed to protection from the bioink). SH-SY5Y cells cultured on the 3D printed structure exhibited normal viability and differentiation into dopaminergic neurons. Moreover, the production of dopamine (surrogate metric for extent of neurogenesis) could be noninvasively monitored throughout the hydrogel by observing t-ZnO autofluorescence quenching as dopamine polymerizes on the microparticle surface. As 3D bioprinting moves towards greater *in vivo* use, the demand for noninvasive neurogenesis tracking is likely to follow since clinicians will need a means of monitoring cell behavior after implantation.

Nanomaterial-enhanced stereolithography inks demonstrate a widened range of functionality and higher printing fidelity, though substantial room for improvement can be found. Photocrosslinking efficiency at higher wavelengths is substantially lower than reactions with lower wavelengths, particularly when processes such as upconversion or multi-photon photopolymerization are utilized. This decrease in reaction efficiency necessitates higher light intensity or longer duration, both of which can lead to deleterious effects, such as ink heating. Since numerous cell sensing technologies rely on light, the principles to ensure efficient photocrosslinking can naturally extend to augmenting cell monitoring functions. Further work in the field may, therefore, involve either continued expansion of stereolithography printing capability, adding additional optical functions, or enhancement of existing modalities.

3.2.1.3. Mechanical reinforcement. Investigations of bioprinting ink mechanical reinforcement generally seek two primary goals: increasing printability and modulating the mechanical properties of the final construct to target biological needs. This fine-tuning of bioprinting inks enhances printing fidelity (i.e., deviation of final structure from CAD) and can improve cell adhesion, survival, differentiation, etc., depending on the exact nature of the reinforcing material. Illustrative examples of mechanical reinforcement are shared herein.

While exogenous, non-native materials are commonly used to augment the printability of bioinks, native extracellular matrix materials can also be employed for this purpose with the benefit of minimizing adverse foreign body responses. Clark et al. mixed unmodified cryo-milled gelatin (denatured collagen) nanoparticles in a collagen methacrylate-thiolated hyaluronic acid bioink to enhance key rheological properties [142]. Because non-cryo-milled gelatin nanoparticles, which are approximately one order of magnitude larger, exerted a significantly smaller effect, it is important to note that the cryo-milling stage is necessary for suitable physical interactions (such as capillary action between neighboring particles). The thixotropic point (shear strain where the material transitions from an elastic solid to viscous liquid) and Young's modulus were substantially increased with addition of the cryomilled gelatin nanoparticles. Additional characterization of the thixotropic recovery reveals that the nanoparticle-supplemented bioink transitions back into an elastic solid ($G' > G''$) in less time than the native bioink. Taken together, the cryo-milled gelatin nanoparticles enhance printability since freshly extruded bioink quickly transitions from a viscous liquid back to an elastic solid, preserving the original printed structure. Additionally, the mechanical reinforcement and increased Young's modulus allow for free-standing, hollow structures to be printed without additional support materials. This system was verified to be biocompatible as HepG2 organoids were included in the bioink for 3D printing. Cells maintained proliferation and responded to various drugs (acetaminophen and troglitazone) at concentrations reported elsewhere. Here, rheological improvement was achieved using nanoparticles composed of benign, naturally occurring ECM biomaterials.

Numerous bioinks have interesting biological properties but lack the mechanical properties necessary for high printing fidelity due to frequent structural collapse, swelling, and low mechanical strength. To augment these deficits, Lee et al. incorporated cationic silica nanoparticles to an anionic bioink (composed of alginate and gellan gum) [136]. The resulting electrostatic interactions reduced the net charge of the bioprinting solution, which resulted in less swelling and higher printing fidelity once placed in cell culture. While the inclusion of cationic nanoparticles caused the viscosity to increase across all shear rates tested, the effect was most pronounced at lower shear rates compared to higher shear rates (Fig. 9A). This allows for the nanoparticle-supplemented ink to easily pass through a needle (high shear rate) due to similar viscosity as the native bioink while simultaneously forming a robust droplet once deposited on a surface (low shear rate) due to higher viscosity. Interestingly, the storage modulus of the final nanoparticle-supplemented hydrogel was size-dependent, with large nanoparticles (over 100 nm) showing no increase while smaller nanoparticles (20–40 nm) showed substantial increases compared to the native bioink. As expected from the improved rheological properties, printing fidelity was increased while printing (lower incidence of collapse), immediately after printing (less error from the 3D design used), after ionically crosslinking the alginate with calcium ions (less shrinkage), and after incubation in isotonic saline (less swelling) (Fig. 9B–D). Cell viability and matrix secretion from encapsulated chondrocytes were found to not be affected by cationic nanoparticle presence. With this demonstration, the mechanical deficiencies of common bioprinting inks were remedied by adding functionalized nanoparticles.

While nanomaterials are most commonly employed to reinforce and increase mechanical strength, Huang et al. incorporated multilayered GO and Pluronic P123-coated graphene (G-P) into a polyurethane (PU)-dispersion printing ink to decrease the storage modulus of the final structure [147]. The G-P-containing ink was found to have the lowest shear modulus, followed by PU/GO and native PU with the highest shear modulus. Neural stem cells were printed with these inks and assayed for metabolic activity and astrogenesis/neurogenesis. Interestingly, the cells embedded in the softest ink (i.e., PU/G-P) were found to have the highest metabolic activity and differentiation into both astrocytes and neurons. The authors attribute these results to the modulation of the composite hydrogel rheological behavior, specifically the ability of the

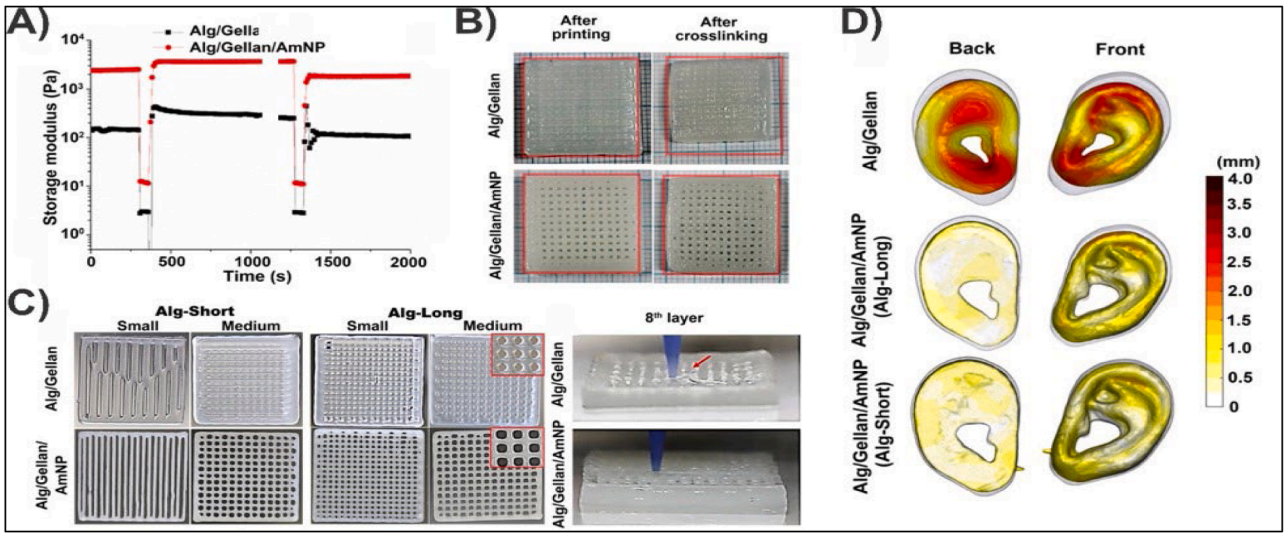

Fig. 9. Nanomaterials improve the printability and mechanical integrity of bioprinting inks. (A) Cationic silica nanoparticles (AmNP) neutralize the negative charge from alginate (Alg)/gellan gum bioink, which results in increased stiffness while retaining shear thinning when extruded through syringes (reproduced with permission from Ref. [136]). The AmNP-supplemented bioink retains higher printing fidelity compared to the bare bioink both in the (B) X-Y plane and (C) along the Z-axis due to higher stiffness. (D) The alginate/gellan gum/AmNP also retains their original printing design after crosslinking.

GO and G-P to disrupt the gelation of the PU dispersion. This study, in addition to reporting a bioink that supports neural stem cell growth and differentiation, illustrates the potential for nanomaterials to alter printed hydrogels in unorthodox ways.

Despite its relative conceptual simplicity, there is still significant room for nanomaterial-mediated mechanical reinforcement investigation. The field of surface chemistry modification and repertoire of available nanomaterials is constantly expanding, which can lead to novel mixtures with drastically divergent properties. As seen with Huang et al., the addition of GO and Pluronic P123-coated graphene resulted in a net reduction in shear modulus despite the nanomaterials' high theoretical shear modulus [147]. There is significant potential in conducting further work in the area of bioprinting, as it serves a dual purpose of advancing the development of innovative materials and shedding light on unforeseen interactions, which can inform future research endeavors.

Another avenue for exploration is the development of anisotropic reinforcement materials. At the present, most mechanical reinforcement work appears to focus on achieving a homogenous distribution of nanomaterials (e.g., nanoparticles) (Table 2). Further advances in the field may seek to mimic the natural anisotropy of neuronal tissues as opposed to the predominantly isotropic inks currently reported. This may be reasonably achieved by either using printing stress to align nanomaterials or using self-assembled materials that form anisotropic features post-printing [168].

3.2.1.4. Electrical conductivity. Neurological tissue is naturally conductive and depends on electrical signaling for *in vivo* function. Treatments seeking to replace or regenerate neurological tissue must therefore replicate its electrical conductivity to achieve functional recovery. Numerous nanomaterials are naturally conductive due to their metallic constituents (e.g., gold nanoparticles) or feature highly conjugated π-bond systems (e.g., graphene), making them ideal candidates to bolster bioprinting ink conductivity.

While the inclusion of graphene to bolster electrical conductivity is reasonably commonplace, the hydrophobicity of graphene presents significant problems for aqueous-based 3D bioprinting inks. To circumvent this limitation, Fang et al. incorporated GO (aqueous stable but lower electrical conductivity than graphene) into a PCL-based melt electrowiring (MEW) 3D printing ink [146]. After the 3D structure was generated, the resulting GO/PCL construct was heated to 150 °C to produce reduced GO (rGO). The resulting rGO/PCL mesh exhibited higher electrical conductivity and lower impedance than native PCL meshes. rGO/PCL microfiber meshes were then combined with electrospun PCL/collagen nanofibers and MEW PCL meshes to form hierarchal multiscale, hollow and filled nerve guidance conduits (NGC). When implanted into a rat sciatic nerve injury model, the filled NGC outperformed hollow NGC at promoting histological recovery, attenuating inflammation, and nerve remyelination. While these results are encouraging for regenerating nerves after injury, it should be noted that both the filled and hollow NGC contained rGO. Thus, the presumed benefit of rGO incorporation (i.e., better electrical conductivity promoting nerve generation) cannot be properly verified. Future work looking to exploit the electrical conductivity of graphene for 3D bioprinting can utilize a similar approach- GO is incorporated into the bioprinting ink before a benign reducing agent converts printed GO-containing structures into rGO with recovered mechanical and electrical function.

Titanium carbide (Ti_3C_2) boasts both high mechanical strength and electrical conductivity. Nanosheets of this material can be readily generated via selective etching of bulk Ti_3AlC_2. Rastin et al. reported a 3D bioprinting, nanocomposite ink using a hyaluronic acid-alginate blend (HA/Alg) and Ti_3C_2 nanosheets at varying concentrations [165]. When 5 mg ml^{-1} of the nanomaterial was used, both mechanical strength and electrical conductivity were greatly increased compared to bare HA/Alg ink. Decreasing the concentration of Ti_3C_2 to 1 mg ml^{-1} still yielded a substantial increase in conductivity, but the mechanical properties (specifically compressive modulus) underwent no significant changes. HEK-293 cells were found to have similar viabilities, whether 3D bioprinted or bulk crosslinked in 1 mg ml^{-1} Ti_3C_2-reinforced HA/Alg. While no experiments were reported with neural cells, this bioink presents interesting opportunities for nerve regeneration due to its electrical conductivity and modular effects on mechanical properties.

One approach to incorporating large hydrophobic, electrically conductive polymers in bioprinting inks is to generate an aqueous dispersion. One such commercially available poly(3,4-ethylenedioxythiophene):poly(styrenesulfonate) (PEDOT:PSS) dispersion was mixed with gelatin methacrylate (GelMA) to print a conductive hydrogel [157]. The process required two crosslinking steps: (1) temporary ionic and thermal crosslinking of PSS and gelatin with a cold calcium solution and (2) permanent light-mediated covalent crosslinking between methacrylate groups. The inclusion of PEDOT:PSS into

the GelMA increased electrical conductivity while not appreciably altering cell viability for embedded C2C12 myoblasts. Moreover, the hydrogel was implanted into rats without significant immunological (e.g., lymphocyte and macrophage infiltration) response and underwent biodegradation without substantial damage to nearby tissue. Here, the electrical conductivity of a 3D bioprinted scaffold is substantially increased without exogenous metals or noticeable tissue damage from graphene-derivatives.

An alternative approach used by Heo et al. for 3D printing with (PEDOT:PSS) dispersions is to lyophilize the dispersion to yield a solid polymer (thus destroying the dispersion) and resuspending it in a compatible bioink [158]. Polyethylene glycol diacrylate (PEGDA) was found to be suitable to resuspend PEDOT:PSS for 3D printing. The characteristic conductivity of PEDOT:PSS was retained in the final hydrogel, along with increased neural cell attachment on the hydrogel surface when compared to native PEDGA hydrogels. While cells were not directly 3D printed along with the PEDOT:PSS/PEGDA solution, the authors were able to coat the printed hydrogel in a cell-laden GelMA solution. The PEDOT:PSS/PEGDA/GelMA hydrogel was then cross-linked to form a single hydrogel with cells within the pores of the original PEDOT:PSS/PEGDA hydrogel. The presence of PEDOT:PSS in the hydrogel matrix was utilized to enable electrical stimulation of embedded cells. While cells in PEGDA/GelMA remained unresponsive to 1 V electrical stimulation, cells in PEDOT:PSS/PEGDA/GelMA increased expression of neuronal genes TUBB3 and neurofilament (Fig. 10B). Even though the original nanomaterial dispersion structure was lost during processing, the material significantly influenced the electrical properties of the final hydrogel.

While PEDOT:PSS is well-characterized in literature, several reports have noted the potential for cytotoxicity arising from the PSS carrier. Gao et al. utilized a similar material- PEDOT: sulfonated lignin (PEDOT:LS) that is reported to exhibit greater biocompatibility and electrical conductivity compared to PEDOT:PSS [156]. When combined with a GelMA and hyaluronic acid methacrylate (HAMA)-based 3D bioprinting ink (Gel/HA/PL), the PEDOT:LS imparted increased conductivity and decreased impedance without appreciably affecting porosity, swelling

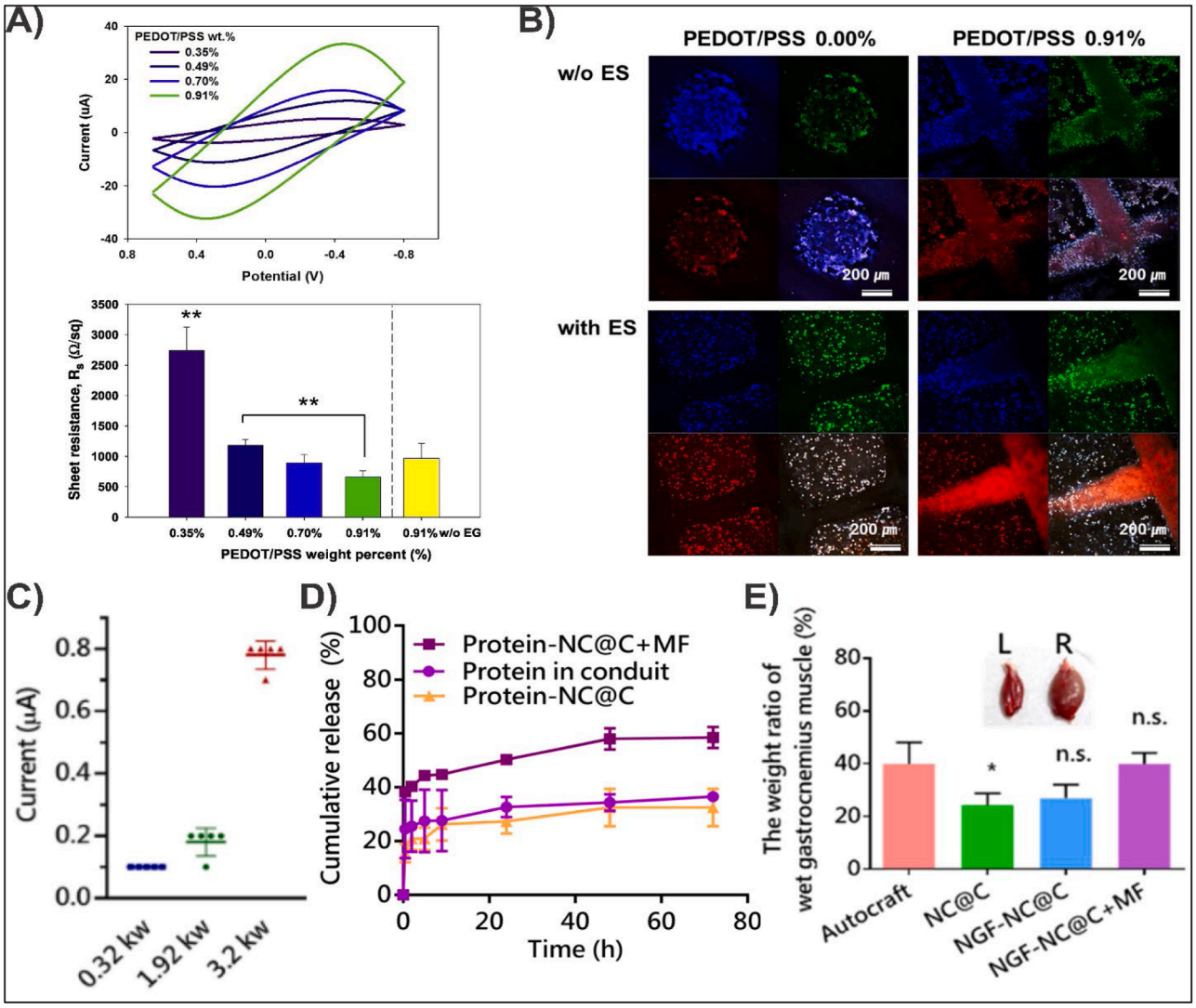

Fig. 10. Nanomaterials improve electrical conductivity of bioprinting inks for electrical stimulation. A-B) (A) Poly(3,4-ethylenedioxythiophene) polystyrene sulfonate (PEDOT:PSS) nanoparticle dispersion was disrupted before incorporation into a polyethylene glycol diacrylate (PEGDA)-based printing ink to improve cyclic voltammetry and reduce resistance (reproduced with permission from Ref. [158]). (B) This produces a scaffold that enables greater neurogenesis (green: neurofilament, red: TUBB3, blue: DAPI) in response to electrical stimulation (ES). C-E) A "sandwich nanocookie" (NC) composed of porous carbon, silica, and reduced GO was supplemented into a polyurethane-based printing ink to fabricate a conduit (NC@C) which (C) produces an electrical current in response to a magnetic field (MF) (reproduced with permission from Ref. [148]). (D) This electromagnetic response accelerates drug release from the NC@C. (E) Conduits with the nanocookie and nerve growth factor (NGF) promoted greater muscle recovery after simulated nerve damage.

ratio, mechanical strength, or degradation kinetics. NSCs suspended in the Gel/HA/PL ink exhibited good survival and underwent neurogenesis, with PEDOT:PL enhancing expression of early neurogenesis markers. Upon implantation into rat model of SCI (T7–8 transection) the NSC-loaded Gel/HA/PL constructs produced greater recovery of motor function (BBB score, incline plate, hindlimb spreading tests) and histological recovery (reduced astrocyte scar, increased neurogenesis, and greater myelination) than the Gel/HA with only PEDOT:LS or NSC individually. Here, the authors demonstrate that PEDOT:LS is a viable alternative to the more popular PEDOT:PSS.

An alternative approach to incorporating conductive, hydrophobic polymers in aqueous-based inks is to crosslink the constituent water-soluble monomers after 3D printing. Depending on the exact nature of the monomer species and crosslinking reaction, problems may arise with cell viability and side reactions with other biopolymers in the 3D printing ink (e.g., conventional redox crosslinking to form PEDOT can be cytotoxic). Li et al. developed a relatively benign conductive 3D bioprinting ink system with a modified 3,4-ethylenedioxythiophene sulfate salt (ETE-S) monomer dissolved in an aqueous hyaluronic acid/PEG-based ink with horseradish peroxidase acting as an enzymatic *in situ* crosslinker [161]. With this scheme, the authors claimed to generate poly-ETE-S (PETE-S) "nanoscale conductive networks" within the finished 3D printed scaffold by adding moderate amounts of hydrogen peroxide. The formation of PETE-S causes the scaffold to increase in opacity (turns dark blue), stiffness, and electrical conductivity. Moreover, both the ETE-S monomer and hydrogen peroxide-induced crosslinking reaction were found to be biocompatible with PC12 cells. Cell proliferation was also enhanced in 3D printed scaffolds with moderate (1–10 mg ml^{-1}) PETE-S content. Thus, several approaches may be undertaken to generate electrically conductive biopolymer printing inks, depending on the exact specifications and needs of the user.

Fang et al. combined a multitude of nanomaterials to create a "nanocookie" (NC) material capable of imparting magnetic responsiveness in a 3D bioprinted matrix [148]. The NC consists of GO nanosheets with adsorbed cetrimonium bromide to act as a template for mesoporous silica deposition and styrene polymerization. Once the GO-SiO_2-polystyrene nanocomposite was assembled, it was calcinated to yield the final NC. As a result of the mesoporous carbonized silica surface, the NC drug adsorption capacity is greater than the starting graphite. Assembled NC were also found to display weak magnetic properties. When exposed to a magnetic field, (1) the release of adsorbed small molecules and proteins was accelerated, which the authors attribute to electrostatic repulsive forces and (2) eddy currents were produced (Fig. 10C, D). Incorporation of the NC into a polyurethane-based bioink would increase the Young's modulus (up to a certain point) and impart a rough nanoscale surface to the final printed structure. Since the scaffold could load neurogenic drugs (e.g., NGF) and electrically stimulating seeded cells (important for neuronal maturation), the authors sought to use NC-loaded, 3D printed conduits to differentiate PC12 into neurons. While NGF-NC@conduits were able to moderately increase the% of cells displaying neurites and axonal lengths, the use of a magnetic field (15 min stimulation) significantly compounded the effect of NGF-NC@conduit culture due to accelerated NGF release and magnetically-induced electrical stimulation. To conclude the study, the authors performed an experiment where they implanted devices into rats with injured sciatic nerves (Fig. 10E). Key recovery metrics included the ratio of injured: uninjured gastrocnemius muscle mass, gastrocnemius muscle fiber size, sciatic functional index, and number of myelin sheath layers found the NGF-NC@conduit scaffold to be comparable or exceed the performance of autografts. The multi-component (carbon, GO, mesoporous silica) NC material imparted multiple new functionalities to the 3D-printed bioink for enhanced neurogenesis.

The abundant electrical conductivity in current nanomaterials is due to their metallic and highly conjugated characteristics, but these systems also face significant drawbacks. Such large quantities of metals as discrete nanoparticles are highly foreign to human bodies, while highly conjugated polymers tend to be hydrophobic (or amphiphilic), lack biodegradation mechanisms, and sensitivity to oxidative biomolecules (e.g., hemoglobin) [169]. Future work can focus on either generation and incorporation of novel biomaterials, refining scaffold preparation workflows, or optimizing bioink composition to maximize the utility of limited nanomaterial loading.

3.2.1.5. Tunable porosity. All biological tissues are subjected to nutrient diffusion constraints when placed *in vivo*. While vasculature can assist with nutrient exchange, matrix porosity remains a predominant factor mediating diffusion between capillaries and target cells. The ability to ensure proper porosity (i.e., high enough to allow nutrient exchange, low enough to ensure tissue integrity) remains of vital importance to translating 3D bioprinting to *in vivo* neurological recovery. To this end, nanomaterials can be employed to tune scaffold porosity.

Incorporating sacrificial porogens into 3D printing inks is a relatively simple use for nanomaterials. In this technique, a nanomaterial is selected to have vastly different solubilities than the printing matrix, so a post-fabrication washing step can specifically leach the nanomaterial, leaving behind a pore. A simple, illustrative example can be found in Dang et al.'s work whereby disodium hydrogel phosphate and sodium chloride salts with diameters less than 38 μm were suspended in PCL in chloroform [140]. PCL with suspended salts was recovered via solvent evaporation before loading into a fused deposition modeling machine for 3D printing. The water-soluble salts were leached out of the printed hydrophobic matrix to yield a microporous scaffold that can be loaded with drugs. Notably, a critical ratio of porogen is required to allow sufficient water diffusion throughout all pores of the entire matrix (i.e., percolation threshold), while excessive porogen concentration failed to print (Fig. 11A). As a result of increased porosity, various physicochemical features were altered including lower compressive modulus, increased drug loading, and reduced burst release (Fig. 11B, C). The broad applicability of this technique and plentiful supply of potential porogens allows for ready integration with 3D printed neurogenesis scaffolds.

The core principles of enhancing scaffold physicochemical properties via nanomaterial porogens were put into practice by Shahriari et al. for neural engineering [141]. Here, NaCl was ground and size separated via sieving for addition into PCL in a similar scheme to Dang et al.'s work [140]. The NaCl-loaded PCL was further modified by wrapping around a sacrificial polystyrene (PS) rod to form a core-shell 3D printing filament [141]. This resulting filament was fuse-printed and leached to produce hollow (PS removal) 3D printed scaffolds with adjustable porosity (NaCl removal). To test neural tissue engineering potential, the authors harvested primary rat dorsal root ganglia (DRGs) for placement at the edge of porous and non-porous 3D printed scaffolds. After 12 days of seeding, DRGs on porous 3D scaffolds exhibited longer neurofilament-positive processes and greater Schwann cell migration compared to non-porous scaffolds. This work provides exemplary evidence that tuning porosity is vital to advancing neural tissue engineering since improved microscale porosity (i.e., NaCl microparticle porogen) imparts greater performance to 3D printed scaffolds, even if the scaffolds already contain macroscale porosity (i.e., hollow cores from PS removal).

Conventional porogen techniques will generally involve organic solvents to either dissolve the matrix material or leach the sacrificial porogen. To minimize the requirement for toxic organic solvents, Ying et al. used high-molecular-weight poly(ethylene oxide) (PEO) in GelMA to form a bi-phasic, dual aqueous emulsion [159]. The PEO could be leached via immersion in saline after GelMA is crosslinked via free-radical polymerization. After determining the optimal concentration range of PEO to form stable emulsions, the hydrogel pore sizes could be varied from 20 to 60 μm by varying the ratio of PEO to GelMA (Fig. 11D). The inclusion of PEO into the GelMA-based printing ink also resulted in a decrease in viscosity, which can alter printability, particularly when dealing with extrusion-style printers. To test cell

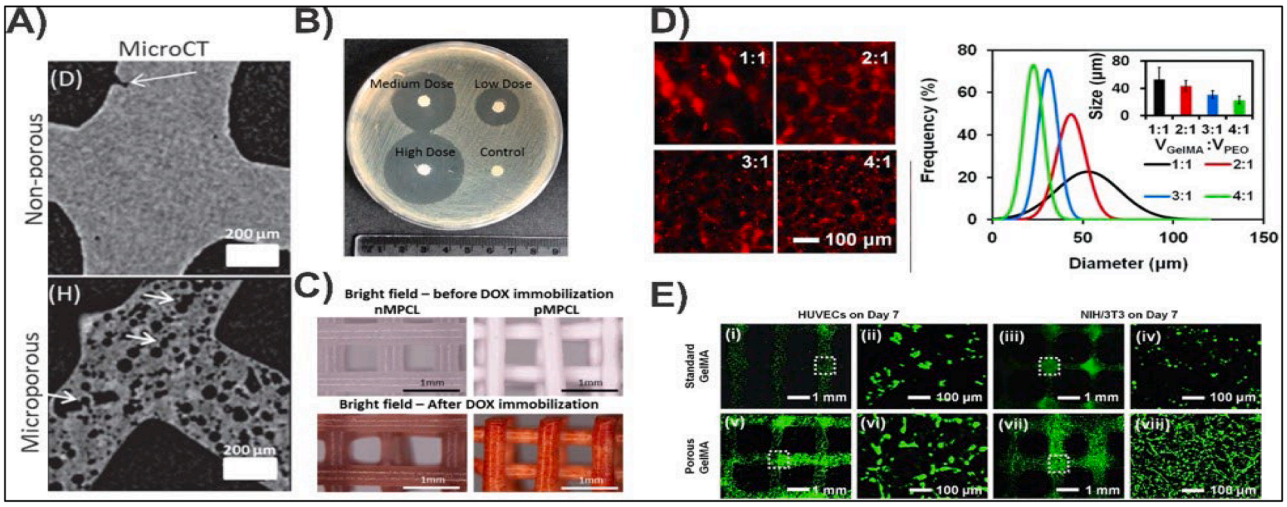

Fig. 11. Nanomaterials for defined bioprinted scaffold porosity. A-C) (A) Without NaCl and Na_2HPO_4 nanocrystals, the printed medical grade polycaprolactone (MPCL) scaffolds remain non-porous (nMPCL) (reproduced with permission from Ref. [140]). In contrast, MPCL with nanocrystal porogens display significantly increased porosity (pMPCL) which was used to adsorb a high concentration of (B) cefazolin to prevent *S. aureus* colonization and (C) doxorubicin (red, DOX). D-E) (D) Rather than incorporate a solid porogen, high molecular weight polyethyelene oxide (PEO) can form a nanoemulsion in gelatin methacrylate (GelMA) bioprinting ink which results in defined pores (reproduced with permission from Ref. [159]). (E) These pores support encapsulated cell growth and spreading in the matrix for human umbilical vein endothelial cells (HUVEC) and NIH/3T3 cell lines.

encapsulation, HepG2 (human hepatocellular carcinoma cells), HUVEC (human umbilical vein endothelial cells), and NIH/3T3 (mouse embryonic fibroblasts) were directly incorporated into the bi-phasic printing ink. While the PEO emulsion resulted in a modest reduction in cell viability, this was largely ablated when residual PEO was leached out with phosphate-buffered saline. The leftover pores allowed for significantly more proliferation and spreading compared to the non-emulsion GelMA hydrogels. To demonstrate the versatility and printing fidelity of the PEO/GelMA ink, the authors were able to create complex designs using both extrusion and stereolithography printers. Even after a week of cell culture, the scaffolds were largely able to retain their original printing shape. Here, the controlled development of hydrogel pores could be induced with an aqueous bi-phasic emulsion without the use of organic solvents.

Porosity-tuning technology is rather well developed due to its broad applicability and interest in the field of biomedical research. Existing porogen methodologies, such as solvent leaching, are well-suited for fabrication processes that do not involve the encapsulation of living cells, due to their harsh conditions that can compromise cell viability. Looking forward, there is a compelling opportunity to concentrate research efforts on the development of biocompatible porogen techniques that employ biodegradable nanomaterials. This innovative approach promises to revolutionize the field by facilitating the integration of biocompatible bioprinting processes with the creation and adjustment of pores using nanomaterial templates. Such advancements would be instrumental in refining scaffold architectures to mimic natural tissue structures more closely, thereby enhancing cell integration and function within engineered tissues. This direction not only holds the potential to significantly improve the fidelity and functionality of tissue-engineered constructs but also opens new avenues for creating more effective and personalized regenerative medicine solutions.

3.2.2. *Inducing neurogenesis pathways*

3.2.2.1. Passive nanomaterial drug carriers. Among established means of inducing stem cell differentiation, differentiation factors, drugs, and assorted peptides/proteins remain paramount in scientific research. Unfortunately, many differentiation factors are labile and subject to rapid degradation in suboptimal conditions. Likewise, small molecules may be subjected to premature clearance. Nanomaterials can provide a means of extending the bioactivity of differentiation factors and drugs and, by extension, increase the efficacy of stem cell-based biomedical interventions. The most developed application of nanomaterial-drug conjugates are as passive drug carriers, as discussed here.

The basic premise of passive nanomaterial drug carriers can be seen in Lee et al.'s work, whereby nerve growth factor (NGF) and bovine serum albumin (BSA) were encapsulated in poly lactic-co-glycolic acid (PLGA) nanoparticles for embedding in a 3D printed PEGDA hydrogel [163]. Without nanoparticle encapsulation, the proteins underwent severe burst release within 10 h. The encapsulation of proteins in nanoparticles allowed for more sustained release, which is advantageous for long-term treatments and regeneration. Beyond modulating payload release from the scaffold, the PLGA nanoparticles were able to increase the Young's modulus of the scaffold and decrease contact angle at higher concentrations, allowing for better wettability and cell adhesion. *In vitro* experiments involving PC-12 and primary rat cortical neuron cultures showed that scaffolds with NGF-loaded nanoparticles outperformed non-encapsulated NGF at inducing neurite growth. While relatively simple, the idea of using nanomaterials as passive drug carriers can significantly increase the effectiveness of neurogenic payloads, presumably by altering pharmacokinetics.

While neurogenesis is undoubtedly an important aspect of nerve regeneration, optimal functional recovery requires axonal remyelination. RGFP966 is a hydrophobic small molecule under investigation for its ability to induce Schwann cells to remyelinate nearby neurons. To promote sustained, local release of RGFP966 at the site of nerve repair, Xu et al. encapsulated the molecule in monomethoxy poly(ethylene glycol)–poly(ε-caprolactone) (MPEG-PCL) nanoparticles for 3D printing in a GelMA matrix (Fig. 12A) [152]. After an initial burst release, approximately 70 % of the drug remained available for sustained release (Fig. 12B). Although cells were not directly 3D printed in the material, proof of biological activity was demonstrated during *in vitro* and *in vivo* experiments. Co-cultures of PC12 and Schwann cells show enhanced neurite growth (PC12) along with enhanced release of myelin-related proteins (Schwann cells) in a RGFP966 dose-dependent manner. 3D printed conduits were printed for *in vivo* remyelination of transected sciatic nerves (Fig. 12C). Notable results include increased post-injury nerve conduction velocity, thickness of myelin sheath, and innervated muscle fiber diameter that showed no significant difference compared to autografts (Fig. 12D–F). The inclusion of RGP966 encapsulated in

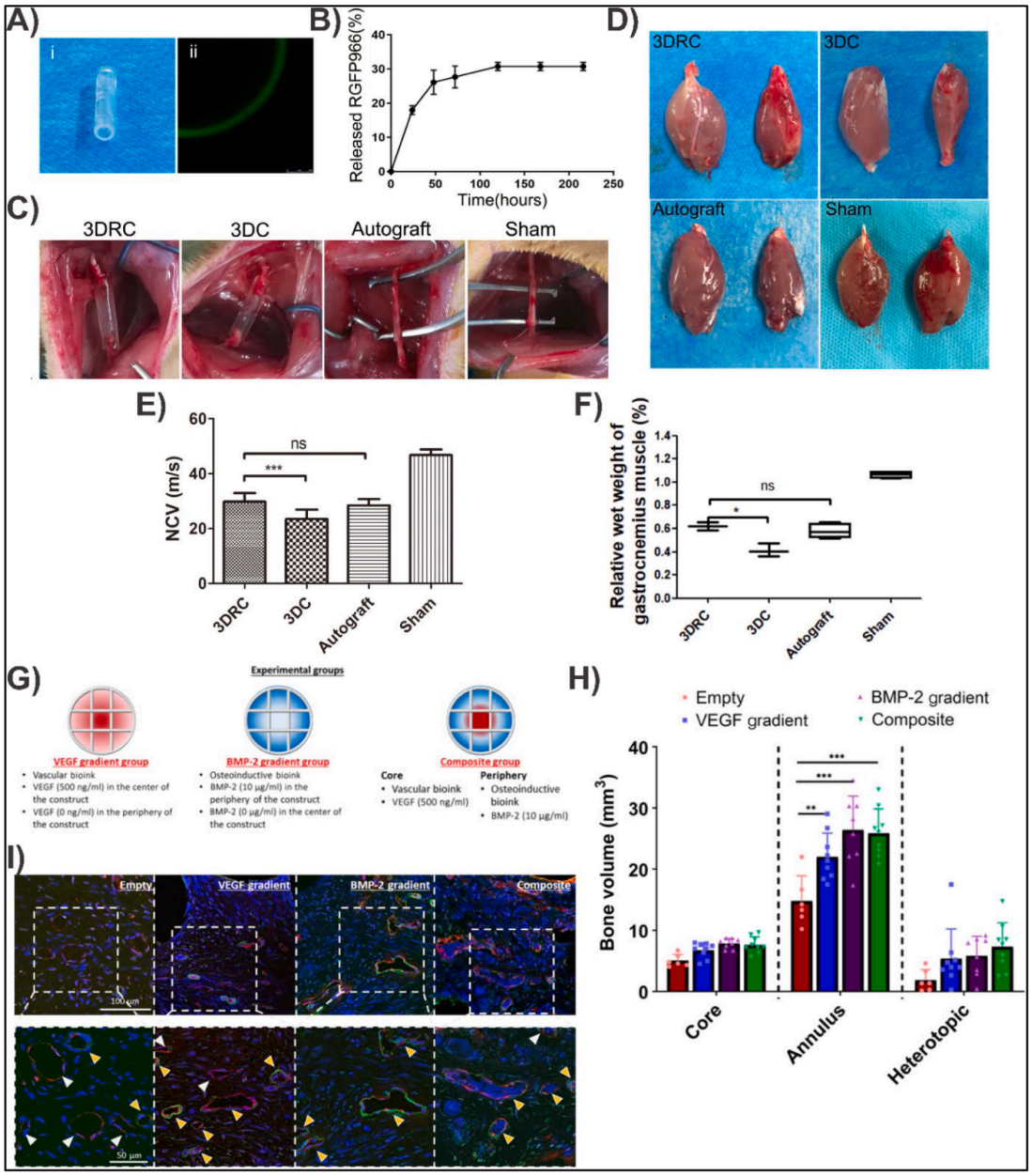

Fig. 12. Nanomaterials increase the pharmacokinetics and efficacy of encapsulated payloads. A-F) Monomethoxy polyethylene glycol–polycaprolactone was loaded with RGFP966 to supplement a gelatin methacrylate-based bioink that can induce Schwann cell remyelination (reproduced with permission from Ref. [152]). (A) To verify homogenous distribution of drug-nanoparticles within the printed structure, coumarin-6 was loaded as a fluorescent model drug with similar hydrophobicity. (B) After a short burst release period, a significant portion of coumarin-6 remained encapsulated within the hydrogel to enable sustained release. (C) Conduits with RGFP966 (3DRC) were implanted into a sciatic nerve injury model and compared to conduits without the drug (3DC) and autografts. 3DRC performed on par with autografts for (D,F) post-injury gastrocnemius muscle mass and (E) restoring nerve conduction velocity (NCV). (G-I) (G) Vascular (VEGF [vascular endothelial growth factor] and nanohydroxyapatite) and osteoinductive (BMP2 [bone morphogenetic protein 2] and Laponite) alginate-methylcellulose bioinks were co-printed to create a vascular core surrounded by ossified tissue on the periphery (reproduced with permission from Ref. [150]). (H) A significant portion of *in vivo* bone formation (femoral implantation) was restricted to the intended annulus periphery as opposed to the vascular core or formation of heterotropic bone outside of the scaffold. (I) Bioprinted scaffolds displayed mature (yellow arrowheads) and immature (white arrowheads) blood vessels within the core of the scaffold.

MPEG-PCL nanoparticles elevated the performance of these scaffolds to autologous autografts, which are the gold standard of nerve repair.

Another paper by the same group investigated the use of another hydrophobic molecule, XMU-MP-1, to promote nerve regeneration [170]. This drug was also encapsulated in MPEG-PCL nanoparticles for 3D printing in a GelMA matrix. While they reported *in vitro* experiments did not directly investigate its effects on neurons, Schwann cells were found to increase secretion of neurotrophic factors along with promoting Schwann cell proliferation. *In vivo* experiments were conducted by transplanting conduits into the site of nerve injury. Nerve conduction velocity, myelin sheath thickness, and innervated muscle fiber diameter were found to show no significant difference compared to autografts. The MPEG-PCL nanoparticle/GelMA 3D bioprinting ink system has been shown to be modular and easily adapted to accommodate various hydrophobic payloads that would otherwise necessitate organic solvents.

Differing physicochemical properties of different nanomaterials can result in drastically altered drug release profiles. Freeman et al. examined the release of two different payloads, vascular endothelial growth factor (VEGF) and bone morphogenic protein-2 (BMP2), that have been adsorbed onto hydroxyapatite (nHA) and Laponite® clay nanoparticles

in an alginate-methylcellulose bioink (Fig. 12G) [150]. Preliminary experiments found that Laponite® was more effective at modulating the release of VEGF compared to nHA, which the authors attribute to the more negative electrostatic charge of the Laponite®. Since the VEGF-nHA release profile mimicked the angiogenesis patterns found in bone fracture healing, this nanoparticle-payload combination was used to form a vascular bioink. 3D printing VEGF-nHA gradients (compared to homogenous VEGF-nHA printing) allowed for more blood vessel formation throughout the entirety of the scaffold when transplanted into a mouse. Meanwhile, the slower release profile of Laponite® was used with BMP-2 for osteogenesis. After an initial burst release, a sustained release profile persisted from day 7 to 35. The BMP2-Laponite® bioink was combined with bone marrow-derived mesenchymal stem cells and subcutaneously implanted into mice. BMP2-Laponite® slow release bioinks resulted in a spatially defined mineral deposition increase. The final demonstration combined a vascular core with an osteogenic periphery for a rat femoral defect model (Fig. 12H–I). The promotion of both angiogenesis and osteogenesis was achieved by incorporating their respective payload-nanoparticle bioinks. Furthermore, the 3D bioprinting digital model indicated that bone formation predominantly occurred in the osteogenic areas situated at the periphery of the scaffold. This finding provides valuable insights into the process. This fast-/slow-drug release platform can be adapted to promote nerve regeneration with slight modifications to payloads and nanoparticle composition.

Nanomaterials as passive drug carriers are a well-established paradigm in 3D bioprinting and the broader field of biomedical engineering. Novel, impactful work in this field is now directed toward passive nanocarriers with additional bioactive moieties and uses. Auxiliary functions, such as modulating bioink mechanical properties, controlling drug release, and nanomaterials themselves, acting as differentiation factors, may soon become as important as the ability of nanocarriers to protect sensitive payloads from degradation (Table 2). The volume and maturity of publications using nanomaterials as passive drug carriers testifies to their importance in bioengineering.

3.2.2.2. Biophysical cues for stem cell differentiation. A growing body of evidence has suggested biophysical cues act as important cues for stem cell differentiation. Naturally, this has spurred growth in the 3D bioprinting of various nanomaterials to activate biomechanical signaling pathways in cells. Several advantages can be seen in utilizing biophysical cues compared to soluble differentiation factors, including resistance to premature clearance and persistence in the extracellular matrix (if the matrix remains intact). Nanomaterials are well-suited to providing these biophysical cues due to their appropriate size and scale.

Lee et al. sought to integrate PCL and PCL-gelatin electrospinning with PEGDA 3D printing [162]. More specifically, PEGDA stereolithography printing was performed on top of the aligned PCL and PCL-gelatin fibers to form a composite scaffold for neural stem cell (NSC) culture. Mechanical measurements found that both variants of electrospun fibers augmented the printed scaffold's Young's modulus and ultimate tensile strength. Remarkably, PCL fiber-reinforced scaffolds reduced TUBB3-positive staining after seeded NSC were induced to differentiate into neurons; meanwhile, PCL-gelatin fiber-reinforced scaffolds showed no significant difference to the base PEGDA scaffold. The incorporation of both PCL and PCL-gelatin fibers caused NSCs to align within the direction of the fibers, indicating that the electrospun fibers provide biophysical cues to influence cell behavior. Finally, PCL-gelatin fiber-reinforced scaffolds induced cells to develop longer neurites than PCL-reinforced and bare scaffolds. The differences between PCL and PCL-gelatin fibers may be at least partially attributed to significant differences in hydrophilicity. While PCL fibers were found to be highly hydrophobic and increase the contact angle of the final reinforced scaffold, PCL-gelatin fibers are noticeably more hydrophilic and resulted in a decrease in contact angle when used to form a composite scaffold. Taken together, electrospun fibers were used to impart key biophysical cues onto 3D-printed scaffolds to promote neurite growth.

Electrohydrodynamic jet (EHD jet) printing is a relatively new approach to simultaneously generate nanofibers as the building blocks for 3D printing. Much like electrospinning, EHD jet printing uses electrostatic forces to form a Taylor cone that produces a nanoscale jet for nanofiber collection. When combined with a mechanical stage, the collected nanofibers can be used to form a desired 3D structure. Liashenko et al. combined jet-deflecting electrodes with EHD jet printing to generate 3D structures composed of PEO nanofibers (Fig. 13A) [160]. Additionally, the authors demonstrated that this technology can be combined with conductive polymers and nanoparticles without significantly altering the printability of the PEO ink. Nanofibers in this paper were reported to range from 100 to 350 nm in diameter, while the printed track resolution (i.e., the CAD patterns that nanofibers are deposited in the shape of) is approximately 40 μm (Fig. 13B). With this technology, it is possible to seamlessly incorporate biophysical signaling from nanofibers with 3D printed structures for tissue reconstruction.

Wang et al. combined microfiber EHD jet printing with nanomaterials, specifically graphene, to target nerve regeneration [149]. PCL with embedded graphene was used as the core of the EHD microfiber, while PEO comprised the sacrificial, gelatin- and dopamine hydrochloride-loaded drug release core. EHD jet printing fidelity was preserved despite the inclusion of graphene, up to a concentration of 0.3% w/w. Moreover, the individual layers would be seen under scanning electron microscopy, indicating that biophysical cues from microfibers are well-preserved in the final product. The tensile strength and elastic modulus were found to decrease with increasing graphene content, potentially assisting with replicating the natural mechanical properties of nerves. In contrast, drug release appeared to be largely unaffected by graphene content. When PC12 cells were seeded on scaffolds of varying graphene content, the authors noted that graphene promoted cell extensions and biocompatibility compared to scaffolds without graphene. Additionally, cell migration was found to be optimal when a moderate amount of graphene (0.05 %) was incorporated into the scaffold. The promise of EHD jet printing of nanofibers combined with compatibility with nanomaterials opens the possibility of targeting neurogenesis via multiple biophysical pathways.

While Chen et al.'s work incorporating cellulose nanofibers (CNF) into 3D bioprinting inks did not explicitly examine biophysical cues to induce neurogenesis, the possibility of using this concept in future neurogenesis studies bears merit and relevancy that is appropriate for this section [138]. CNF was introduced to their waterborne polyurethane suspension ink (PU, discussed in Section 3.2.1.1) to increase the viscosity of printing. Interestingly, the step where CNF is introduced to the suspension synthesis had a significant effect on the nature of the final nanocomposite printing ink. Nanocomposite inks that saw increased viscosities were found to have "skewer-like structures," where PU suspension nanoparticles were wrapped around CNF (Fig. 13C). The authors proposed that the enhanced contact between PU nanoparticles and CNF indicate increased intermolecular interactions (e.g., hydrogen bonds). These intermolecular interactions can be further modulated with small molecules (e.g., triethylamine to neutralize negative charges on PU nanoparticles and CNF). When compared to PU printing inks reinforced with high molecular weight PEO (900 kDa), the PU/CNF scaffold was more resistant to fracturing, displayed higher adhesion strength between layers, and retained higher printing fidelity after immersion in saline solutions while still retaining microscale pores for diffusion. Fibroblasts seeded on PU/CNF were less prone to aggregation, displayed greater attachment onto the scaffold surface, and exhibited greater proliferation compared to cells seeded on the PU/PEO scaffold [Fig. 13D]. Subsequent work could investigate the dual role of reinforcing fibers in modulating printability and influencing biophysical pathways in seeded cells.

Including novel biophysical cues in 3D bioprinted scaffolds can complement traditional differentiation factor-mediated neurogenesis. While direct-writing, nanoscale bioprinting is still limited by substantial

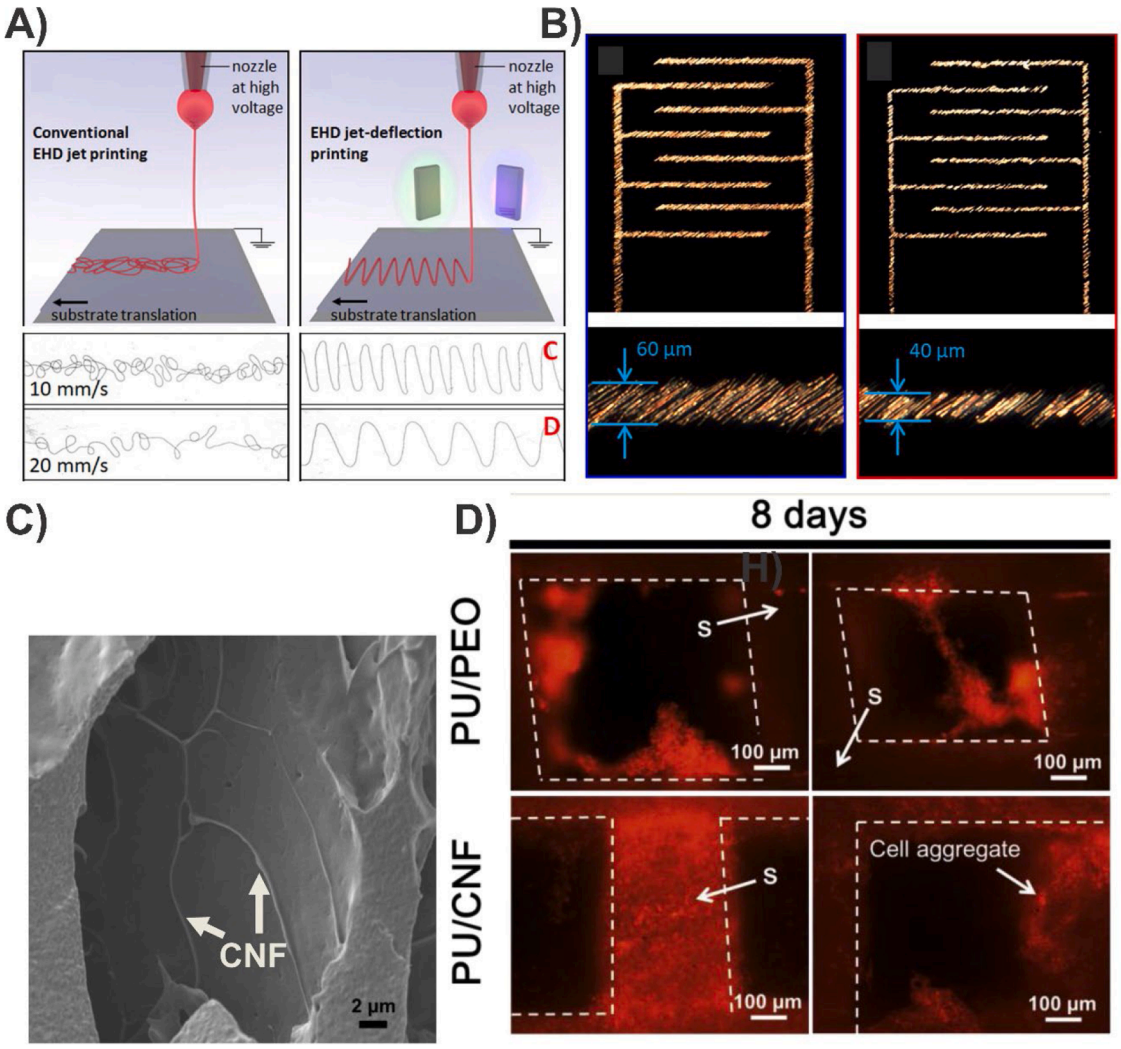

Fig. 13. Biophysical cues (e.g., nanofibers) can be included onto 3D printed scaffolds as a post-fabrication modification or as a printing building block. A-B) (A) Electrohydrodynamic (EHD) 3D printing uses an electrostatic jet (similar to electrospinning) to deposit nanofibers in a defined pattern (reproduced with permission from Ref. [160]). (B) Electrodes can be positioned and tuned (e.g., deflection frequency) to precisely control bioink deposition and create defined nano-scale patterns. C-D) (C) Nanofibers can be integrated directly into various bioprinting inks for reasons beyond biophysical cues. Cellulose nanofibers (CNF) in polyurethane nanoparticle-based bioinks form "skewers" to increase solution viscosity and printability (reproduced with permission from Ref. [138]). (D) Nanofibers are retained after printing in polyurethane (PU/CNF) bioink and can function as biophysical cues to enhance cell attachment and growth compared to polyurethane with polyethylene oxide (PU/PEO).

technical constraints, anisotropic nanomaterial building blocks, and payloads represent one of the most promising methods of incorporating nanoscale biophysical cues into 3D scaffolds. To further improve the impact of biophysical cues, future work can be directed to ensure greater control of nanomaterial arrangement in 3D space. Most notably, nano- and microfibers are known to be most impactful for neurogenesis when aligned in a single direction. Recently developed techniques have allowed researchers to exert significant spatial control over nanomaterial alignment directly during 3D bioprinting processes, leaving substantial room for investigation into scaffolds with integrated biophysical cues.

3.3. Looking forward with 4D and post-fabrication printing technologies

3D bioprinting has great utility and control over generating detailed structures for transplantation into defined injury sites. However, the process of injury regeneration is dynamic, and there is often little direct control over transplanted tissue once placed in a patient. The inability for clinicians to control conventional 3D bioprinted structures after fabrication is a major driving force behind interest in 4D printing (3D printing of structures with the ability to trigger a rearrangement after fabrication) and post-fabrication printing. Nanomaterials are well-suited for 4D and post-fabrication bioprinting since their varied physicochemical properties allow for a wide library of triggers (e.g., light) and responses (e.g., heat) after printing.

In situations where direct incorporation of nanomaterials into a bioprinting ink is infeasible, post fabrication modification of finished scaffolds may represent an alternative means of integrating nanomaterials into 3D bioprinting. Among the most versatile techniques of post-fabrication modification are surface coatings, such as drop casting or dip coating. Li et al. utilized drop casting as a means of surface coating 3D printed PCL scaffolds (hydrophobic) with titanium carbide nanosheets ($Ti_3C_2T_x$, hydrophilic) [164]. More specifically, PCL scaffolds were generated via melt electrospinning writing (MEW), which were then subjected to drop casting with $Ti_3C_2T_x$ in 70 % ethanol. This nanomaterial coating improved scaffold material characteristics for both electrical conductivity and hydrophilicity compared to pristine PCL. Additionally, the original morphology of the printed PCL scaffolds could be preserved by optimizing the $Ti_3C_2T_x$ coating concentration and number of applied coatings. The modified scaffolds were then seeded

with SH-SY5Y cells and monitored for proliferation and neurogenesis. Cells on $Ti_3C_2T_x$-coated scaffolds exhibited more robust cell adhesion, process extension, proliferation, and neuronal differentiation (TUBB3 expression), and cell-cell interactions compared to SH-SY5Y on pristine PCL scaffold. To further corroborate the role of $Ti_3C_2T_x$ in promoting functional neurogenesis, cells on $Ti_3C_2T_x$-coated PCL scaffolds showed oscillatory calcium movement, indicating electrical and synaptic activity. As an added functionality, $Ti_3C_2T_x$ produces a photothermal effect that can be used to trigger a capacitive current in neurons. The authors exploited this nanomaterial feature to induce neural activity on $Ti_3C_2T_x$-coated scaffolds with high spatial and temporal control via 640 nm light. Due to the modularity of the post-fabrication coating technique, future work in the field can utilize other functional nanomaterials to tailor other scaffold surface properties.

Nanomaterials may be used to accentuate pre-existing 4D printing mechanisms. Miao et al. incorporated graphene into a soybean oil epoxidized acrylate (SOEA) stereolithography ink with innate shape memory effect (Fig. 14A) [135]. Greater concentrations of graphene in the ink allowed the material to undergo increased deformation upon heating, presumably due to the creation of different internal forces during bioprinting (see Section 3.2.1.2 Optical Properties for greater discussion) (Fig. 14B). The authors theorized this can be utilized to repair nerve damage by allowing a sheet of graphene-SOEA to naturally wrap around torn nerve endings once exposed to physiological temperatures (Fig. 14C). SOEA and graphene-SOEA were both found to support hMSC growth and neurogenesis, though graphene enabled greater expression of neurogenin 2, neuron specific enolase, and Tau proteins (Fig. 14D). Additionally, the process of 4D bioprinting conduits imparts micron-scale biophysical features, which also assist with hMSC neurogenesis and alignment. Since the mechanism of internal stresses is not specific to SOEA ink, this approach of nanomaterial-augmented shape memory effect may be extended to other bioprinting inks.

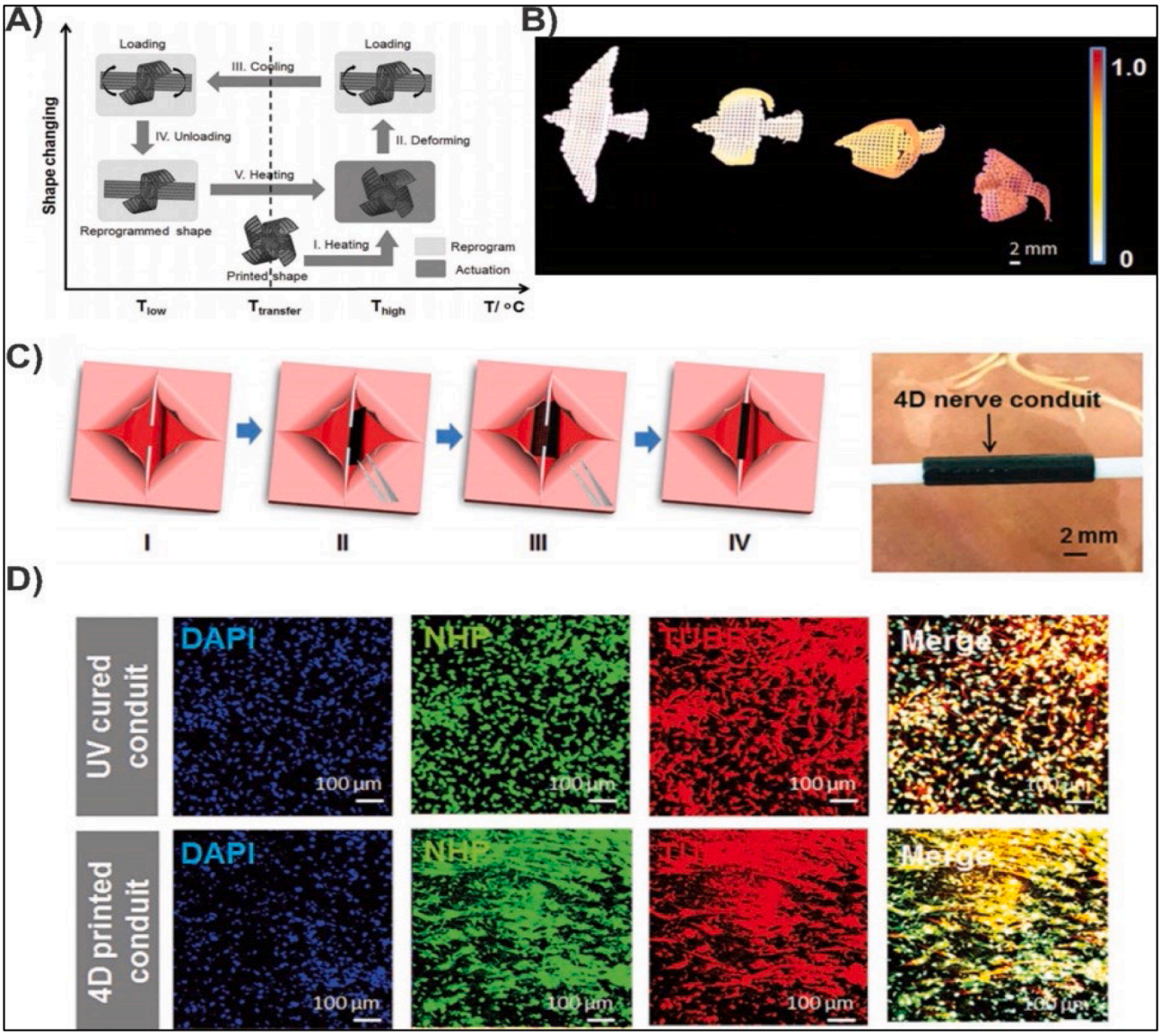

Fig. 14. Nanomaterials can be used to actuate 4D printing mechanisms. (A) Shape memory effect allows for printed materials to regain a pre-configured shape after the introduction of a particular stimulus (e.g., heat) (reproduced with permission from Ref. [135]). (B) Incorporating increasing quantities of graphene into the epoxidized acrylate soybean oil ink (left to right) allowed the printed materials to undergo greater deformation due to the laser-induced internal stresses (see 4.3.1.2 Optical Properties). (C) To adapt this system for nerve repair, the graphene-ink would be temporarily fixed as a flat sheet to facilitate surgical implantation before the elevated patient temperature causes the conduit to envelope detached nerve endings. (D) Human MSC cultured and induced to neurogenesis on the 4D printed conduits showed increased expression of neurofilament heavy peptide (NHP) and tubulin β−3 (TUBB3) compared to the conventional UV-cured conduit (which lacks microfeatures imparted during printing).

Normally, shape memory polymers are placed in an incubator to enable transformations after 3D printing, but this approach may not be unsuitable for *in vivo* and cell applications if the temperatures required are physiologically intolerable. Instead, graphene can be used to capture and convert NIR light to heat. Cui et al. exploited the unique photothermal effects of graphene to create a remotely triggered 4D printed nanocomposite ink [144]. The incorporation of graphene into the ink resulted in greater viscosity and heat flow until the extrusion head of the 3D printer was no longer capable of reliably printing the material. Interestingly, small quantities of graphene resulted in scaffolds with lower tensile moduli than the unmodified ink, whereas higher concentrations resulted in higher tensile modulus. More importantly, deformed graphene-nanocomposite scaffolds could revert to their original shape in response to NIR light. This property was exploited to create a variety of different conformations from a single 3D model by selectively illuminating certain areas of the scaffold. As a biological demonstration, the authors seeded neural stem cells (NSC) on printed, deformed scaffolds. While excessive light exposure caused thermally induced cell death, careful modulation of light intensity can balance the need for acceptable cell viability with sufficient temperature to enable the shape memory effect. Neurogenesis was even found to be enhanced on graphene-nanocomposite scaffolds, which the authors attributed to optoelectrical stimulation during NIR light exposure. In this demonstration, the numerous unique interactions between light and graphene were used to create a neurogenic scaffold that can be remotely controlled to undergo shape changes.

While cellulose is useful for scaffold mechanical reinforcement before and after printing, it lacks biological activity. Le et al. describe a relatively simple and flexible means of converting cellulose into graphene using ultrafast laser pulses with femtosecond pulse durations [139]. This allows for the conversion of cellulose into graphene under ambient conditions. The laser-induced graphene (LIG) displays good electrical properties and can be printed at micron-scale resolutions under ambient conditions. While biological applications were not explored in this study, the LIG exhibits characteristic Raman, XRD, and XPS spectra which suggest that key physicochemical properties such as high π-electron conjugation and oxygen-containing functional groups are present to interact with biological molecules. The potential for cellulose to be converted into LIG via post-fabrication protocols is advantageous since graphene-related printing complications, such as excessive light adsorption (for stereolithography), and poor solubility in aqueous solutions are avoided. Examples of applications of this technology include guiding electrical signals and selective cell seeding via direct writing of conductive LIG channels in cellulose-reinforced scaffolds.

The emerging field of 4D printing holds exceptional promise for neural regeneration, given the inherent sensitivity and complexity of neural tissues. The clinical landscape often discourages repeated interventions and surgeries on such tissues due to the potential for damage and the complexities involved in recovery, thus highlighting the significance of creating structures that can adapt or transform after being printed and implanted. For instance, a scaffold engineered through 4D printing technology can be designed to be more compact during transplantation, facilitating a less invasive procedure. Subsequently, this scaffold can then expand or morph into its pre-designed, more complex structure to better support neural regeneration and integration within the body. Given that 4D printing is in its nascent stages—especially when compared to the more established field of 3D printing—examples of 4D-printed neural tissues are currently limited. However, the anticipation for future advancements is high. As the technology progresses, and as novel materials and methodologies are developed, the adaptation of 4D printing techniques for biological applications is expected to expand. This evolution will likely unveil new possibilities for regenerative medicine, particularly in the creation of dynamic and responsive neural tissue scaffolds.

4. Concluding remarks and future perspectives

In conclusion, 3D bioprinting sits at the intersection of technological innovation, material science, and tissue regeneration biology. This review highlights significant progress in regenerative medicine, particularly in neural tissue engineering, while recognizing the unique challenges and opportunities in this field. Due to the limited capacity for endogenous neural regeneration, there is a critical need for advanced therapeutic strategies. This review demonstrates how bioink compositions, crosslinking methods, and printing techniques can influence the therapeutic efficacy of bioprinted scaffolds and hydrogels, particularly in promoting neuronal differentiation.

However, 3D bioprinting for neural applications remains in its infancy, with several areas requiring focused research. Future efforts should prioritize improving cell viability post-printing, enhancing resolution, and refining crosslinking methods to better support complex neural architectures. Additionally, the field must address challenges such as long-term stability of printed constructs, spatiotemporal control of therapeutic agent delivery, and functional integration of transplanted cells with host tissues. Innovations in bioink formulations—particularly those capable of modulating biophysical and biochemical cues—will be crucial in advancing neural regeneration.

Moving forward, research should focus on developing bioinks that mimic the intricate microenvironment of neural tissues, as well as on exploring multimaterial bioprinting approaches to combine different functional properties in a single construct. There is also a need for more robust *in vivo* models to evaluate the long-term efficacy of bioprinted neural constructs in clinical settings. By addressing these specific challenges, 3D bioprinting can make transformative advances in treating spinal cord injuries, peripheral nerve damage, and other neural disorders. Expanding interdisciplinary collaborations will be key to unlocking the full therapeutic potential of 3D bioprinting for neural regeneration, paving the way for innovative, patient-centered therapies.

CRediT authorship contribution statement

Cemile Kilic Bektas: Writing – review & editing, Writing – original draft, Visualization, Methodology, Conceptualization. **Jeffrey Luo:** Writing – original draft, Methodology, Conceptualization. **Brian Conley:** Writing – original draft, Methodology. **Kim-Phuong N. Le:** Writing – review & editing, Writing – original draft, Conceptualization. **Ki-Bum Lee:** Writing – review & editing, Supervision, Conceptualization.

Declaration of competing interest

The authors declare that they have no known competing financial interests or personal relationships that could have appeared to influence the work reported in this paper.

Acknowledgments

C.B. and J.L. appreciate the fellowship of the NIH T32 Postdoctoral Training Program in Translational Research in Regenerative Medicine under Award Number T32EB005583. Ki-Bum Lee acknowledges the partial financial support from the NSF (CBET-1803517), the New Jersey Commission on Spinal Cord (CSCR17IRG010; CSCR16ERG019), NIH R01 (1R01DC016612, 1R01NS130836-01A1, 3R01DC016612-01S1, and 5R01DC016612-02S1), NIH RM1 (RM1 NS133003-01), NIH R21 (R21 NS132556-01), Alzheimer's Association (AARG-NTF-21-847862), CDMRP (OCRP, OC220235P1), N.J. Commission on Cancer Research (COCR23PPR007), and HealthAdvance (NHLBI, U01HL150852).

References

[1] X. Bichat, G. Hayward, Joseph Meredith Toner Collection (Library of Congress), General anatomy, Applied to Physiology and Medicine, Richardson and Lord, Boston, 1822.
[2] R. Virchow, F. Chance, Cellular pathology, As Based Upon Physiological and Pathological histology. Twenty lectures Delivered in the Pathological institute of Berlin during the Months of February, March and April, R. M. De Witt, New York, 1858, p. 1860.
[3] P. Zhuang, A.X. Sun, J. An, C.K. Chua, S.Y. Chew, 3D neural tissue models: from spheroids to bioprinting, Biomaterials 154 (2018) 113–133.
[4] E.R. Shamir, A.J. Ewald, Three-dimensional organotypic culture: experimental models of mammalian biology and disease, Nat. Rev. Mol. Cell Biol. 15 (10) (2014) 647–664.
[5] O. Habanjar, M. Diab-Assaf, F. Caldefie-Chezet, L. Delort, 3D cell culture systems: tumor application, advantages, and disadvantages, Int. J. Mol. Sci. 22 (22) (2021).
[6] C. Jensen, Y. Teng, Is it time to start transitioning from 2D to 3D cell culture? Front. Mol. Biosci. 7 (2020).
[7] S.K. Doke, S.C. Dhawale, Alternatives to animal testing: a review, Saudi Pharm. J. 23 (3) (2015) 223–229.
[8] E. Knight, S. Przyborski, Advances in 3D cell culture technologies enabling tissue-like structures to be created *in vitro*, J. Anat. 227 (6) (2015) 746–756.
[9] J.J. Campbell, C.J. Watson, Three-dimensional culture models of mammary gland, Organogenesis 5 (2) (2009) 43–49.
[10] S.V. Murphy, A. Atala, 3D bioprinting of tissues and organs, Nat. Biotechnol. 32 (8) (2014) 773–785.
[11] Y.M. Peng, C. Unluer, Development of alternative cementitious binders for 3D printing applications: a critical review of progress, advantages and challenges, Compos. Part B Eng. 252 (2023).
[12] T. Kornfeld, P.M. Vogt, C. Radtke, Nerve grafting for peripheral nerve injuries with extended defect sizes, Wien. Med. Wochenschr. 169 (9–10) (2019) 240–251.
[13] X. Dai, C. Ma, Q. Lan, T. Xu, 3D bioprinted glioma stem cells for brain tumor model and applications of drug susceptibility, Biofabrication 8 (4) (2016) 045005.
[14] H.W. Han, S.H. Hsu, Using 3D bioprinting to produce mini-brain, Neural Regen. Res. 12 (10) (2017) 1595–1596.
[15] F.Y. Hsieh, H.H. Lin, S.H. Hsu, 3D bioprinting of neural stem cell-laden thermoresponsive biodegradable polyurethane hydrogel and potential in central nervous system repair, Biomaterials 71 (2015) 48–57.
[16] K.C. Cheng, Y.M. Sun, S.H. Hsu, Development of double network polyurethane-chitosan composite bioinks for soft neural tissue engineering, J. Mater. Chem. B 11 (16) (2023) 3592–3606.
[17] W.J. Huang, J. Wang, Development of 3D-printed, biodegradable, conductive PGSA composites for nerve tissue regeneration, Macromol. Biosci. 23 (3) (2023) e2200470.
[18] L. Zhang, H. Zhang, H. Wang, K. Guo, H. Zhu, S. Li, F. Gao, S. Li, Z. Yang, X. Liu, X. Zheng, Fabrication of multi-channel nerve guidance conduits containing schwann cells based on multi-material 3D bioprinting, 3D Print. Addit. Manuf. 10 (5) (2023) 1046–1054.
[19] S. Das, J. Thimukonda Jegadeesan, B. Basu, Advancing peripheral nerve regeneration: 3D bioprinting of GelMA-based cell-laden electroactive bioinks for nerve conduits, ACS Biomater. Sci. Eng. (2024).
[20] T. Boland, W.C. Wilson, T. Xu, Ink-jet printing of viable cells, 2006.
[21] K. Holzl, S. Lin, L. Tytgat, S. Van Vlierberghe, L. Gu, A. Ovsianikov, Bioink properties before, during and after 3D bioprinting, Biofabrication 8 (3) (2016) 032002.
[22] M. Dey, I.T. Ozbolat, 3D bioprinting of cells, tissues and organs, Sci. Rep. 10 (1) (2020) 14023.
[23] H. Cui, M. Nowicki, J.P. Fisher, L.G. Zhang, 3D bioprinting for organ regeneration, Adv. Healthc. Mater. 6 (1) (2017).
[24] M. Askari, M. Afzali Naniz, M. Kouhi, A. Saberi, A. Zolfagharian, M. Bodaghi, Recent progress in extrusion 3D bioprinting of hydrogel biomaterials for tissue regeneration: a comprehensive review with focus on advanced fabrication techniques, Biomater. Sci. 9 (3) (2021) 535–573.
[25] C.S. Ong, P. Yesantharao, C.Y. Huang, G. Mattson, J. Boktor, T. Fukunishi, H. Zhang, N. Hibino, 3D bioprinting using stem cells, Pediatr. Res. 83 (1–2) (2018) 223–231.
[26] T. Bedir, S. Ulag, C.B. Ustundag, O. Gunduz, 3D bioprinting applications in neural tissue engineering for spinal cord injury repair, Mater. Sci. Eng. C Mater. 110 (2020).
[27] M. Cadena, L.Q. Ning, A. King, B. Hwang, L.Q. Jin, V. Serpooshan, S.A. Sloan, 3D bioprinting of neural tissues, Adv. Healthc. Mater. 10 (15) (2021).
[28] J. Zhang, A.Q. Vo, X. Feng, S. Bandari, M.A. Repka, Pharmaceutical additive manufacturing: a novel tool for complex and personalized drug delivery systems, AAPS. PharmSciTech 19 (8) (2018) 3388–3402.
[29] A.K. Miri, I. Mirzaee, S. Hassan, S. Mesbah Oskui, D. Nieto, A. Khademhosseini, Y. S. Zhang, Effective bioprinting resolution in tissue model fabrication, Lab Chip 19 (11) (2019) 2019–2037.
[30] V. Yusupov, S. Churbanov, E. Churbanova, K. Bardakova, A. Antoshin, S. Evlashin, P. Timashev, N. Minaev, Laser-induced forward transfer hydrogel printing: a defined route for highly controlled process, Int. J. Bioprint. 6 (3) (2020).
[31] S. Jentsch, R. Nasehi, C. Kuckelkorn, B. Gundert, S. Aveic, H. Fischer, Multiscale 3D bioprinting by nozzle-free acoustic droplet ejection, Small Methods 5 (6) (2021).
[32] Poietis, Next-generation bioprinting, 2024. https://poietis.com/ngb/. (Accessed March 9 2024).
[33] R. Boni, A. Ali, A. Shavandi, A.N. Clarkson, Current and novel polymeric biomaterials for neural tissue engineering, J. Biomed. Sci. 25 (1) (2018) 90.
[34] P. Madhusudanan, G. Raju, S. Shankarappa, Hydrogel systems and their role in neural tissue engineering, J. R. Soc. Interface 17 (162) (2020) 20190505.
[35] T.J. Hinton, Q. Jallerat, R.N. Palchesko, J.H. Park, M.S. Grodzicki, H.J. Shue, M. H. Ramadan, A.R. Hudson, A.W. Feinberg, Three-dimensional printing of complex biological structures by freeform reversible embedding of suspended hydrogels, Sci. Adv. 1 (9) (2015) e1500758.
[36] E. Abelseth, L. Abelseth, L. De la Vega, S.T. Beyer, S.J. Wadsworth, S.M. Willerth, 3D printing of neural tissues derived from human induced pluripotent stem cells using a fibrin-based bioink, ACS Biomater. Sci. Eng. 5 (1) (2019) 234–243.
[37] M.R. Perez, R. Sharma, N.Z. Masri, S.M. Willerth, 3D bioprinting mesenchymal stem cell-derived neural tissues using a fibrin-based bioink, Biomolecules 11 (8) (2021).
[38] M. Pagac, J. Hajnys, Q.P. Ma, L. Jancar, J. Jansa, P. Stefek, J. Mesicek, A review of vat photopolymerization technology: materials, applications, challenges, and future trends of 3D printing, Polymers 13 (4) (2021) (Basel).
[39] P. Somers, Z. Liang, J.E. Johnson, B.W. Boudouris, L. Pan, X. Xu, Rapid, continuous projection multi-photon 3D printing enabled by spatiotemporal focusing of femtosecond pulses, Light Sci. Appl. 10 (1) (2021) 199.
[40] F. Guillemot, L. Hutter, B. Brisson, D. Fayol, B. Viellerobe, Tissue manufacturing by bioprinting: challenges & opportunities, Cell Gene Ther. Insights 4 (8) (2018) 781–789.
[41] P.N. Bernal, P. Delrot, D. Loterie, Y. Li, J. Malda, C. Moser, R. Levato, Volumetric bioprinting of complex living-tissue constructs within seconds, Adv. Mater. 31 (42) (2019) e1904209.
[42] G. Lepousez, A. Nissant, P.M. Lledo, Adult neurogenesis and the future of the rejuvenating brain circuits, Neuron 86 (2) (2015) 387–401.
[43] D.M. Arzate, L. Covarrubias, Adult neurogenesis in the context of brain repair and functional relevance, Stem Cells Dev. 29 (9) (2020) 544–554.
[44] Y. Tang, P. Yu, L. Cheng, Current progress in the derivation and therapeutic application of neural stem cells, Cell Death Dis. 8 (10) (2017) e3108.
[45] T.Y. Cheng, M.H. Chen, W.H. Chang, M.Y. Huang, T.W. Wang, Neural stem cells encapsulated in a functionalized self-assembling peptide hydrogel for brain tissue engineering, Biomaterials 34 (8) (2013) 2005–2016.
[46] J.P. Jiang, X.Y. Liu, F. Zhao, X. Zhu, X.Y. Li, X.G. Niu, Z.T. Yao, C. Dai, H.Y. Xu, K. Ma, X.Y. Chen, S. Zhang, Three-dimensional bioprinting collagen/silk fibroin scaffold combined with neural stem cells promotes nerve regeneration after spinal cord injury, Neural Regen. Res. 15 (5) (2020) 959–968.
[47] R. Sharma, I.P.M. Smits, L. De La Vega, C. Lee, S.M. Willerth, 3D bioprinting pluripotent stem cell derived neural tissues using a novel fibrin bioink containing drug releasing microspheres, Front. Bioeng. Biotechnol. 8 (2020) 57.
[48] C. Li, M. Kuss, Y. Kong, F. Nie, X. Liu, B. Liu, A. Dunaevsky, P. Fayad, B. Duan, X. Li, 3D printed hydrogels with aligned microchannels to guide neural stem cell migration, ACS Biomater. Sci. Eng. 7 (2) (2021) 690–700.
[49] D. Joung, V. Truong, C.C. Neitzke, S.Z. Guo, P.J. Walsh, J.R. Monat, F. Meng, S. H. Park, J.R. Dutton, A.M. Parr, M.C. McAlpine, 3D printed stem-cell derived neural progenitors generate spinal cord scaffolds, Adv. Funct. Mater. 28 (39) (2018).
[50] J. Wang, X. Kong, Q. Li, C. Li, H. Yu, G. Ning, Z. Xiang, Y. Lui, S. Feng, The spatial arrangment of cells in a 3D-printed biomimetic spinal cord promotes directional differentiation and repairs the motor function after spinal cord injury, Biofabrication 13 (13) (2021).
[51] C. Nombela-Arrieta, J. Ritz, L.E. Silberstein, The elusive nature and function of mesenchymal stem cells, Nat. Rev. Mol. Cell Biol. 12 (2) (2011) 126–131.
[52] S.W. Kemp, A.A. Webb, S. Dhaliwal, S. Syed, S.K. Walsh, R. Midha, Dose and duration of nerve growth factor (NGF) administration determine the extent of behavioral recovery following peripheral nerve injury in the rat, Exp. Neurol. 229 (2) (2011) 460–470.
[53] U. Metin, M. Dededovic, D.S. Sakaguchi, S.K. Mallapragada, Development of gelatin and graphene-based nerve regeneration conduits using three-dimensional printing strategies for electrical transdifferentiation of mesenchymal stem cells, Ind. Eng. Chem. Res. 58 (18) (2019) 7421–7427.
[54] D.N. Rodriguez-Sanchez, G.B.A. Pinto, L.P. Cartarozzi, A.L.R. de Oliveira, A.L. C. Bovolato, M. de Carvalho, J.V.L. da Silva, J.A. Dernowsek, M. Golim, B. Barraviera, R.S. Ferreira, E. Deffune, M. Bertanha, R.M. Amorim, 3D-printed nerve guidance conduits multi-functionalized with canine multipotent mesenchymal stromal cells promote neuroregeneration after sciatic nerve injury in rats, Stem Cell Res. Ther. 12 (1) (2021) 303.
[55] Z.L. Lingbin Che, P. Wu, D. Song, A 3D printable and bioactive hydrogel scaffold to treat traumatic brain injury, Adv. Funct. Mater. 29 (39) (2019).
[56] Q. Zhang, P.D. Nguyen, S. Shi, J.C. Burrell, D.K. Cullen, A.D. Le, 3D bio-printed scaffold-free nerve constructs with human gingiva-derived mesenchymal stem cells promote rat facial nerve regeneration, Sci. Rep. 8 (1) (2018) 6634.
[57] A. Andrzejewska, S. Dabrowska, B. Lukomska, M. Janowski, Mesenchymal stem cells for neurological disorders, Adv. Sci. 8 (7) (2021).
[58] B. Badyra, M. Sulkowski, O. Milczarek, M. Majka, Mesenchymal stem cells as a multimodal treatment for nervous system diseases, Stem Cells Transl. Med. 9 (10) (2020) 1174–1189.
[59] M. Peljto, H. Wichterle, Programming embryonic stem cells to neuronal subtypes, Curr. Opin. Neurobiol. 21 (1) (2011) 43–51.
[60] H. Wichterle, I. Lieberam, J.A. Porter, T.M. Jessell, Directed differentiation of embryonic stem cells into motor neurons, Cell 110 (3) (2002) 385–397.

[61] A.L. Perrier, V. Tabar, T. Barberi, M.E. Rubio, J. Bruses, N. Topf, N.L. Harrison, L. Studer, Derivation of midbrain dopamine neurons from human embryonic stem cells, Proc. Natl. Acad. Sci. USA 101 (34) (2004) 12543–12548.
[62] S. Vijayavenkataraman, S. Thaharah, S. Zhang, W.F. Lu, J.Y.H. Fuh, 3D-printed PCL/rGO conductive scaffolds for peripheral nerve injury repair, Artif. Organs 43 (5) (2019) 515–523.
[63] O.A. Hamid, H.M. Eltaher, V. Sottile, J. Yang, 3D bioprinting of a stem cell-laden, multi-material tubular composite: an approach for spinal cord repair, Mater. Sci. Eng. C Mater. Biol. Appl. 120 (2021) 111707.
[64] X. Zhou, H. Cui, M. Nowicki, S. Miao, S.J. Lee, F. Masood, B.T. Harris, L.G. Zhang, Three-dimensional-bioprinted dopamine-based matrix for promoting neural regeneration, ACS Appl. Mater. Interfaces 10 (10) (2018) 8993–9001.
[65] R. Lozano, L. Stevens, B.C. Thompson, K.J. Gilmore, R. Gorkin 3rd, E.M. Stewart, M. in het Panhuis, M. Romero-Ortega, G.G. Wallace, 3D printing of layered brain-like structures using peptide modified gellan gum substrates, Biomaterials 67 (2015) 264–273.
[66] L. Ning, N. Zhu, F. Mohabatpour, M.D. Sarker, D.J. Schreyer, X. Chen, Bioprinting Schwann cell-laden scaffolds from low-viscosity hydrogel compositions, J. Mater. Chem. B 7 (29) (2019) 4538–4551.
[67] M.A. Hermida, J.D. Kumar, D. Schwarz, K.G. Laverty, A. Di Bartolo, M. Ardron, M. Bogomolnijs, A. Clavreul, P.M. Brennan, U.K. Wiegand, F.P. Melchels, W. Shu, N.R. Leslie, Three dimensional *in vitro* models of cancer: bioprinting multilineage glioblastoma models, Adv. Biol. Regul. 75 (2020) 100658.
[68] M.A. Heinrich, R. Bansal, T. Lammers, Y.S. Zhang, R. Michel Schiffelers, J. Prakash, 3D-bioprinted mini-brain: a glioblastoma model to study cellular interactions and therapeutics, Adv. Mater. 31 (14) (2019) e1806590.
[69] D.M. Kingsley, C.L. Roberge, A. Rudkouskaya, D.E. Faulkner, M. Barroso, X. Intes, D.T. Corr, Laser-based 3D bioprinting for spatial and size control of tumor spheroids and embryoid bodies, Acta Biomater. 95 (2019) 357–370.
[70] X. Wang, X. Li, X. Dai, X. Zhang, J. Zhang, T. Xu, Q. Lan, Coaxial extrusion bioprinted shell-core hydrogel microfibers mimic glioma microenvironment and enhance the drug resistance of cancer cells, Colloids Surf. B Biointerfaces 171 (2018) 291–299.
[71] P. Ramiah, L.C. du Toit, Y.E. Choonara, P.P.D. Kondiah, V. Pillay, Hydrogel-based bioinks for 3D bioprinting in tissue regeneration, Front. Mater. 7 (2020).
[72] C.S. Barros, S.J. Franco, U. Muller, Extracellular matrix: functions in the nervous system, Cold Spring Harb. Perspect. Biol. 3 (1) (2011) a005108.
[73] V. Solozobova, N. Wyvekens, J. Pruszak, Lessons from the embryonic neural stem cell niche for neural lineage differentiation of pluripotent stem cells, Stem Cell Rev. Rep. 8 (3) (2012) 813–829.
[74] N. Tasnim, L. De la Vega, S. Anil Kumar, L. Abelseth, M. Alonzo, M. Amereh, B. Joddar, S.M. Willerth, 3D bioprinting stem cell derived tissues, Cell Mol. Bioeng. 11 (4) (2018) 219–240.
[75] J. Gopinathan, I. Noh, Recent trends in bioinks for 3D printing, Biomater. Res. 22 (2018) 11.
[76] R.F. Pereira, P.J. Bártolo, 3D bioprinting of photocrosslinkable hydrogel constructs, J. Appl. Polym. Sci. 132 (48) (2015) n/a-n/a.
[77] S.M. Hull, C.D. Lindsay, L.G. Brunel, D.J. Shiwarski, J.W. Tashman, J.G. Roth, D. Myung, A.W. Feinberg, S.C. Heilshorn, 3D bioprinting using UNIversal Orthogonal Network (UNION) bioinks, Adv. Funct. Mater. 31 (7) (2021).
[78] D. Petta, A.R. Armiento, D. Grijpma, M. Alini, D. Eglin, M. D'Este, 3D bioprinting of a hyaluronan bioink through enzymatic-and visible light-crosslinking, Biofabrication 10 (4) (2018) 044104.
[79] Z. Wang, R. Abdulla, B. Parker, R. Samanipour, S. Ghosh, K. Kim, A simple and high-resolution stereolithography-based 3D bioprinting system using visible light crosslinkable bioinks, Biofabrication 7 (4) (2015) 045009.
[80] N.D. Dinh, R. Luo, M.T.A. Christine, W.N. Lin, W.C. Shih, J.C. Goh, C.H. Chen, Effective light directed assembly of building blocks with microscale control, Small 13 (24) (2017).
[81] C. Kilic Bektas, V. Hasirci, Cell loaded 3D bioprinted GelMA hydrogels for corneal stroma engineering, Biomater. Sci. 8 (1) (2019) 438–449.
[82] K. Dubbin, Y. Hori, K.K. Lewis, S.C. Heilshorn, Dual-stage crosslinking of a gel-phase bioink improves cell viability and homogeneity for 3D bioprinting, Adv. Healthc. Mater. 5 (19) (2016) 2488–2492.
[83] H. Li, Y.J. Tan, L. Li, A strategy for strong interface bonding by 3D bioprinting of oppositely charged kappa-carrageenan and gelatin hydrogels, Carbohydr. Polym. 198 (2018) 261–269.
[84] Z. Zheng, J. Wu, M. Liu, H. Wang, C. Li, M.J. Rodriguez, G. Li, X. Wang, D. L. Kaplan, 3D bioprinting of self-standing silk-based bioink, Adv. Healthc. Mater. 7 (6) (2018) e1701026.
[85] A. GhavamiNejad, N. Ashammakhi, X.Y. Wu, A. Khademhosseini, Crosslinking strategies for 3D bioprinting of polymeric hydrogels, Small 16 (35) (2020) e2002931.
[86] W. Lim, G.J. Kim, H.W. Kim, J. Lee, X. Zhang, M.G. Kang, J.W. Seo, J.M. Cha, H. J. Park, M.Y. Lee, S.R. Shin, S.Y. Shin, H. Bae, Kappa-carrageenan-based dual crosslinkable bioink for extrusion type bioprinting, Polymers 12 (10) (2020) (Basel).
[87] M. Monfared, D. Mawad, J. Rnjak-Kovacina, M.H. Stenzel, 3D bioprinting of dual-crosslinked nanocellulose hydrogels for tissue engineering applications, J. Mater. Chem. B 9 (31) (2021) 6163–6175.
[88] J.Y. Shin, Y.H. Yeo, J.E. Jeong, S.A. Park, W.H. Park, Dual-crosslinked methylcellulose hydrogels for 3D bioprinting applications, Carbohydr. Polym. 238 (2020) 116192.
[89] Z. Zhang, Y. Jin, J. Yin, C. Xu, R. Xiong, K. Christensen, B.R. Ringeisen, D. B. Chrisey, Y. Huang, Evaluation of bioink printability for bioprinting applications, Appl. Phys. Rev. 5 (4) (2018).
[90] N. Mehrban, G.Z. Teoh, M.A. Birchall, 3D bioprinting for tissue engineering: stem cells in hydrogels, Int. J. Bioprint. 2 (0) (2016) 6–19.
[91] S. Knowlton, S. Anand, T. Shah, S. Tasoglu, Bioprinting for neural tissue engineering, Trends Neurosci. 41 (1) (2018) 31–46.
[92] X. Cui, J. Li, Y. Hartanto, M. Durham, J. Tang, H. Zhang, G. Hooper, K. Lim, T. Woodfield, Advances in extrusion 3D bioprinting: a focus on multicomponent hydrogel-based bioinks, Adv. Healthc. Mater. 9 (15) (2020) e1901648.
[93] K.J. Wangensteen, L.K. Kalliainen, Collagen tube conduits in peripheral nerve repair: a retrospective analysis, Hand (N Y) 5 (3) (2010) 273–277.
[94] A. Bozkurt, K.G. Claeys, S. Schrading, J.V. Rodler, H. Altinova, J.B. Schulz, J. Weis, N. Pallua, S.G.A. van Neerven, Clinical and biometrical 12-month follow-up in patients after reconstruction of the sural nerve biopsy defect by the collagen-based nerve guide Neuromaix, Eur. J. Med. Res. 22 (1) (2017) 34.
[95] K. Elkhoury, M. Morsink, L. Sanchez-Gonzalez, C. Kahn, A. Tamayol, E. Arab-Tehrany, Biofabrication of natural hydrogels for cardiac, neural, and bone tissue engineering applications, Bioact. Mater. 6 (11) (2021) 3904–3923.
[96] H. Xu, Q. Liu, J. Casillas, M. McAnally, N. Mubtasim, L.S. Gollahon, D. Wu, C. Xu, Prediction of cell viability in dynamic optical projection stereolithography-based bioprinting using machine learning, J. Intell. Manuf. 33 (4) (2020) 995–1005.
[97] S. Knowlton, B. Yenilmez, S. Anand, S. Tasoglu, Photocrosslinking-based bioprinting: examining crosslinking schemes, Bioprinting 5 (2017) 10–18.
[98] W. Jia, P.S. Gungor-Ozkerim, Y.S. Zhang, K. Yue, K. Zhu, W. Liu, Q. Pi, B. Byambaa, M.R. Dokmeci, S.R. Shin, A. Khademhosseini, Direct 3D bioprinting of perfusable vascular constructs using a blend bioink, Biomaterials 106 (2016) 58–68.
[99] Z. Yu, H. Li, P. Xia, W. Kong, Y. Chang, C. Fu, K. Wang, X. Yang, Z. Qi, Application of fibrin-based hydrogels for nerve protection and regeneration after spinal cord injury, J. Biol. Eng. 14 (1) (2020) 22.
[100] J.C. Schense, J. Bloch, P. Aebischer, J.A. Hubbell, Enzymatic incorporation of bioactive peptides into fibrin matrices enhances neurite extension, Nat. Biotechnol. 18 (4) (2000) 415–419.
[101] S.S. Rao, J.O. Winter, Adhesion molecule-modified biomaterials for neural tissue engineering, Front. Neuroeng. 2 (2009) 6.
[102] K. Walus, S. Beyer, S.M. Willerth, Three-dimensional bioprinting healthy and diseased models of the brain tissue using stem cells, Curr. Opin. Biomed. Eng. 14 (2020) 25–33.
[103] S. Naghieh, X. Chen, Printability-a key issue in extrusion-based bioprinting, J. Pharm. Anal. 11 (5) (2021) 564–579.
[104] Y. Ding, M. Floren, W. Tan, High-throughput screening of vascular endothelium-destructive or protective microenvironments: cooperative actions of extracellular matrix composition, stiffness, and structure, Adv. Healthc. Mater. 6 (11) (2017).
[105] A. Tirella, A. Orsini, G. Vozzi, A. Ahluwalia, A phase diagram for microfabrication of geometrically controlled hydrogel scaffolds, Biofabrication 1 (4) (2009) 045002.
[106] Y.J. Lee, J.A. Park, T. Tuladhar, S.J.E. Jung, Sonochemical degradation of gelatin methacryloyl to control viscoelasticity for inkjet bioprinting, Macromol. Biosci. 23 (5) (2023).
[107] P.P. Shah, H.B. Shah, K.K. Maniar, T. Özel, Extrusion-based 3D bioprinting of alginate-based tissue constructs, Procedia CIRP 95 (2020) 143–148.
[108] B. Guillotin, A. Souquet, S. Catros, M. Duocastella, B. Pippenger, S. Bellance, R. Bareille, M. Rémy, L. Bordenave, J. Amédée, F. Guillemot, Laser assisted bioprinting of engineered tissue with high cell density and microscale organization, Biomaterials 31 (28) (2010) 7250–7256.
[109] A. GhavamiNejad, N. Ashammakhi, X.Y. Wu, A. Khademhosseini, Crosslinking strategies for 3D bioprinting of polymeric hydrogels, Small 16 (35) (2020).
[110] S. Saha, P. Datta, Characterization of bioinks for 3D bioprinting, in: A. Kumar, S. I. Voicu, V.K. Thakur (Eds.), 3D Printable Gel-Inks for Tissue Engineering, Springer Singapore, Singapore, 2021, pp. 27–77.
[111] K. Saha, A.J. Keung, E.F. Irwin, Y. Li, L. Little, D.V. Schaffer, K.E. Healy, Substrate modulus directs neural stem cell behavior, Biophys. J. 95 (9) (2008) 4426–4438.
[112] L.Y. Chan, W.R. Birch, E.K. Yim, A.B. Choo, Temporal application of topography to increase the rate of neural differentiation from human pluripotent stem cells, Biomaterials 34 (2) (2013) 382–392.
[113] A.M. Hopkins, E. DeSimone, K. Chwalek, D.L. Kaplan, 3D *in vitro* modeling of the central nervous system, Prog. Neurobiol. 125 (2015) 1–25.
[114] A. Banerjee, M. Arha, S. Choudhary, R.S. Ashton, S.R. Bhatia, D.V. Schaffer, R. S. Kane, The influence of hydrogel modulus on the proliferation and differentiation of encapsulated neural stem cells, Biomaterials 30 (27) (2009) 4695–4699.
[115] G.J. Her, H.C. Wu, M.H. Chen, M.Y. Chen, S.C. Chang, T.W. Wang, Control of three-dimensional substrate stiffness to manipulate mesenchymal stem cell fate toward neuronal or glial lineages, Acta Biomater. 9 (2) (2013) 5170–5180.
[116] M. Cadena, L. Ning, A. King, B. Hwang, L. Jin, V. Serpooshan, S.A. Sloan, 3D bioprinting of neural tissues, Adv. Healthc. Mater. 10 (15) (2021) e2001600.
[117] K. Nair, M. Gandhi, S. Khalil, K.C. Yan, M. Marcolongo, K. Barbee, W. Sun, Characterization of cell viability during bioprinting processes, Biotechnol. J. 4 (8) (2009) 1168–1177.
[118] A. Blaeser, D.F. Duarte Campos, U. Puster, W. Richtering, M.M. Stevens, H. Fischer, Controlling shear stress in 3D bioprinting is a key factor to balance printing resolution and stem cell integrity, Adv. Healthc. Mater. 5 (3) (2016) 326–333.
[119] T. Liu, C. Delavaux, Y.S. Zhang, 3D bioprinting for oncology applications, J. 3D Print. Med. 3 (2) (2019) 55–58.
[120] Y. Kang, P. Datta, S. Shanmughapriya, I.T. Ozbolat, 3D bioprinting of tumor models for cancer research, ACS Appl. Bio Mater. 3 (9) (2020) 5552–5573.

[121] S. Suryaprakash, Y.H. Lao, H.Y. Cho, M. Li, H.Y. Ji, D. Shao, H. Hu, C.H. Quek, D. Huang, R.L. Mintz, J.R. Bago, S.D. Hingtgen, K.B. Lee, K.W. Leong, Engineered mesenchymal stem cell/nanomedicine spheroid as an active drug delivery platform for combinational glioblastoma therapy, Nano Lett. 19 (3) (2019) 1701–1705.
[122] J. Ogawa, G.M. Pao, M.N. Shokhirev, I.M. Verma, Glioblastoma model using human cerebral organoids, Cell Rep. 23 (4) (2018) 1220–1229.
[123] J.S. Jeon, S. Bersini, M. Gilardi, G. Dubini, J.L. Charest, M. Moretti, R.D. Kamm, Correction for Jeon et al., Human 3D vascularized organotypic microfluidic assays to study breast cancer cell extravasation, Proc. Natl. Acad. Sci. USA 112 (7) (2015) E818.
[124] W.J. Ho, E.A. Pham, J.W. Kim, C.W. Ng, J.H. Kim, D.T. Kamei, B.M. Wu, Incorporation of multicellular spheroids into 3-D polymeric scaffolds provides an improved tumor model for screening anticancer drugs, Cancer Sci. 101 (12) (2010) 2637–2643.
[125] C.P. Beier, P. Kumar, K. Meyer, P. Leukel, V. Bruttel, I. Aschenbrenner, M. J. Riemenschneider, A. Fragoulis, P. Rummele, K. Lamszus, J.B. Schulz, J. Weis, U. Bogdahn, J. Wischhusen, P. Hau, R. Spang, D. Beier, The cancer stem cell subtype determines immune infiltration of glioblastoma, Stem Cells Dev. 21 (15) (2012) 2753–2761.
[126] L. Ma, B. Zhang, C. Zhou, Y. Li, B. Li, M. Yu, Y. Luo, L. Gao, D. Zhang, Q. Xue, Q. Qiu, B. Lin, J. Zou, H. Yang, The comparison genomics analysis with glioblastoma multiforme (GBM) cells under 3D and 2D cell culture conditions, Colloids Surf. B Biointerfaces 172 (2018) 665–673.
[127] A.D. Gitler, P. Dhillon, J. Shorter, Neurodegenerative disease: models, mechanisms, and a new hope, Dis. Model. Mech. 10 (5) (2017) 499–502.
[128] M. Jucker, The benefits and limitations of animal models for translational research in neurodegenerative diseases, Nat. Med. 16 (11) (2010) 1210–1214.
[129] S.S. Han, L.A. Williams, K.C. Eggan, Constructing and deconstructing stem cell models of neurological disease, Neuron 70 (4) (2011) 626–644.
[130] M. Bordoni, F. Rey, V. Fantini, O. Pansarasa, A.M. Di Giulio, S. Carelli, C. Cereda, From neuronal differentiation of iPSCs to 3D neuro-organoids: modelling and therapy of neurodegenerative diseases, Int. J. Mol. Sci. 19 (12) (2018).
[131] J. Penney, W.T. Ralvenius, L.H. Tsai, Modeling Alzheimer's disease with iPSC-derived brain cells, Mol. Psychiatry 25 (1) (2020) 148–167.
[132] Q. Gu, E. Tomaskovic-Crook, R. Lozano, Y. Chen, R.M. Kapsa, Q. Zhou, G. G. Wallace, J.M. Crook, Functional 3D neural mini-tissues from printed gel-based bioink and human neural stem cells, Adv. Healthc. Mater. 5 (12) (2016) 1429–1438.
[133] S. Abdelrahman, W.F. Alsanie, Z.N. Khan, H.I. Albalawi, R.I. Felimban, M. Moretti, N. Steiner, A.G. Chaudhary, C.A.E. Hauser, A Parkinson's disease model composed of 3D bioprinted dopaminergic neurons within a biomimetic peptide scaffold, Biofabrication 14 (4) (2022).
[134] Y. Zhang, H.Y. Chen, X.Y. Long, T. Xu, Three-dimensional-engineered bioprinted human neural stem cell self-assembling culture model constructs of Alzheimer's disease, Bioact. Mater. 11 (2022) 192–205.
[135] S. Miao, H. Cui, M. Nowicki, L. Xia, X. Zhou, S.J. Lee, W. Zhu, K. Sarkar, Z. Zhang, L.G. Zhang, Stereolithographic 4D bioprinting of multiresponsive architectures for neural engineering, Adv. Biosyst. 2 (9) (2018) 1800101.
[136] M. Lee, K. Bae, P. Guillon, J. Chang, O. Arlov, M. Zenobi-Wong, Exploitation of cationic silica nanoparticles for bioprinting of large-scale constructs with high printing fidelity, ACS Appl. Mater. Interfaces 10 (44) (2018) 37820–37828.
[137] S.M. Bakht, M. Gomez-Florit, T. Lamers, R.L. Reis, R.M. Domingues, M.E. Gomes, 3D bioprinting of miniaturized tissues embedded in self-assembled nanoparticle-based fibrillar platforms, Adv. Funct. Mater. (2021) 2104245.
[138] R.D. Chen, C.F. Huang, S.H. Hsu, Composites of waterborne polyurethane and cellulose nanofibers for 3D printing and bioapplications, Carbohydr. Polym. 212 (2019) 75–88.
[139] T.S.D. Le, S. Park, J. An, P.S. Lee, Y.J. Kim, Ultrafast laser pulses enable one-step graphene patterning on woods and leaves for green electronics, Adv. Funct. Mater. 29 (33) (2019) 1902771.
[140] H.P. Dang, T. Shabab, A. Shafiee, Q.C. Peiffer, K. Fox, N. Tran, T.R. Dargaville, D. W. Hutmacher, P.A. Tran, 3D printed dual macro-, microscale porous network as a tissue engineering scaffold with drug delivering function, Biofabrication 11 (3) (2019) 035014.
[141] D. Shahriari, G. Loke, I. Tafel, S. Park, P.H. Chiang, Y. Fink, P. Anikeeva, Scalable fabrication of porous microchannel nerve guidance scaffolds with complex geometries, Adv. Mater. 31 (30) (2019).
[142] C.C. Clark, J. Aleman, L. Mutkus, A. Skardal, A mechanically robust thixotropic collagen and hyaluronic acid bioink supplemented with gelatin nanoparticles, Bioprinting 16 (2019) e00058.
[143] A.A. Pawar, S. Halivni, N. Waiskopf, Y. Ben-Shahar, M. Soreni-Harari, S. Bergbreiter, U. Banin, S. Magdassi, Rapid three-dimensional printing in water using semiconductor–metal hybrid nanoparticles as photoinitiators, Nano Lett. 17 (7) (2017) 4497–4501.
[144] H. Cui, S. Miao, T. Esworthy, S.J. Lee, X. Zhou, S.Y. Hann, T.J. Webster, B. T. Harris, L.G. Zhang, A novel near-infrared light responsive 4D printed nanoarchitecture with dynamically and remotely controllable transformation, Nano Res. 12 (2019) 1381–1388.
[145] J. Zhang, H. Eyisoylu, X.H. Qin, M. Rubert, R. Muller, 3D bioprinting of graphene oxide-incorporated cell-laden bone mimicking scaffolds for promoting scaffold fidelity, osteogenic differentiation and mineralization, Acta Biomater. 121 (2021) 637–652.
[146] Y.C. Fang, C.J. Wang, Z.B. Liu, J. Ko, L. Chen, T. Zhang, Z. Xiong, L. Zhang, W. Sun, 3D printed conductive multiscale nerve guidance conduit with hierarchical fibers for peripheral nerve regeneration, Adv. Sci. 10 (12) (2023).
[147] C.T. Huang, L.K. Shrestha, K. Ariga, S.H. Hsu, A graphene–polyurethane composite hydrogel as a potential bioink for 3D bioprinting and differentiation of neural stem cells, J. Mater. Chem. B 5 (44) (2017) 8854–8864.
[148] J.H. Fang, H.H. Hsu, R.S. Hsu, C.K. Peng, Y.J. Lu, Y.Y. Chen, S.Y. Chen, S.H. Hu, 4D printing of stretchable nanocookie@conduit material hosting biocues and magnetoelectric stimulation for neurite sprouting, NPG Asia Mater. 12 (1) (2020) 1–16.
[149] B. Wang, X. Chen, Z. Ahmad, J. Huang, M.W. Chang, 3D electrohydrodynamic printing of highly aligned dual-core graphene composite matrices, Carbon 153 (2019) 285–297.
[150] F.E. Freeman, P. Pitacco, L.H.A. van Dommelen, J. Nulty, D.C. Browe, J.Y. Shin, E. Alsberg, D.J. Kelly, 3D bioprinting spatiotemporally defined patterns of growth factors to tightly control tissue regeneration, Sci. Adv. 6 (33) (2020) eabb5093.
[151] F. Afghah, M. Altunbek, C. Dikyol, B. Koc, Preparation and characterization of nanoclay-hydrogel composite support-bath for bioprinting of complex structures, Sci. Rep. 10 (1) (2020) 5257.
[152] X. Xu, J. Tao, S. Wang, L. Yang, J. Zhang, J. Zhang, H. Liu, H. Cheng, J. Xu, M. Gou, Y. Wei, 3D printing of nerve conduits with nanoparticle-encapsulated RGFP966, Appl. Mater. Today 16 (2019) 247–256.
[153] J. Zhu, Q. Zhang, T. Yang, Y. Liu, R. Liu, 3D printing of multi-scalable structures via high penetration near-infrared photopolymerization, Nat. Commun. 11 (1) (2020) 3462.
[154] V.V. Rocheva, A.V. Koroleva, A.G. Savelyev, K.V. Khaydukov, A.N. Generalova, A. V. Nechaev, A.E. Guller, V.A. Semchishen, B.N. Chichkov, E.V. Khaydukov, High-resolution 3D photopolymerization assisted by upconversion nanoparticles for rapid prototyping applications, Sci. Rep. 8 (1) (2018) 3663.
[155] A.A. Pawar, G. Saada, I. Cooperstein, L. Larush, J.A. Jackman, S.R. Tabaei, N. J. Cho, S. Magdassi, High-performance 3D printing of hydrogels by water-dispersible photoinitiator nanoparticles, Sci. Adv. 2 (4) (2016) e1501381.
[156] C. Gao, Y.X. Li, X.Y. Liu, J. Huang, Z.J. Zhang, 3D bioprinted conductive spinal cord biomimetic scaffolds for promoting neuronal differentiation of neural stem cells and repairing of spinal cord injury, Chem. Eng. J. 451 (2023).
[157] A.R. Spencer, E. Shirzaei Sani, J.R. Soucy, C.C. Corbet, A. Primbetova, R. A. Koppes, N. Annabi, Bioprinting of a cell-laden conductive hydrogel composite, ACS Appl. Mater. Interfaces 11 (34) (2019) 30518–30533.
[158] D.N. Heo, S.J. Lee, R. Timsina, X. Qiu, N.J. Castro, L.G. Zhang, Development of 3D printable conductive hydrogel with crystallized PEDOT:PSS for neural tissue engineering, Mater. Sci. Eng. C Mater. Biol. Appl. 99 (2019) 582–590.
[159] G.L. Ying, N. Jiang, S. Maharjan, Y.X. Yin, R.R. Chai, X. Cao, J.Z. Yang, A.K. Miri, S. Hassan, Y.S. Zhang, Aqueous two-phase emulsion bioink-enabled 3D bioprinting of porous hydrogels, Adv. Mater. 30 (50) (2018) e1805460.
[160] I. Liashenko, A. Ramon, A. Cabot, J. Rosell-Llompart, Ultrafast electrohydrodynamic 3D printing with *in situ* jet speed monitoring, Mater. Des. 206 (2021) 109791.
[161] C.B. Li, S. Naeimipour, F.R. Boroojeni, T. Abrahamsson, X. Strakosas, Y.P.Q. Yi, R. Rilemark, C. Lindholm, V.K. Perla, C. Musumeci, Y.Y. Li, H. Biesmans, M. Savvakis, E. Olsson, K. Tybrandt, M.J. Donahue, J.Y. Gerasimov, R. Selegård, M. Berggren, D. Aili, D.T. Simon, Engineering conductive hydrogels with tissue-like properties: a 3D bioprinting and enzymatic polymerization approach, Small Sci. (2024).
[162] S.J. Lee, M. Nowicki, B. Harris, L.G. Zhang, Fabrication of a highly aligned neural scaffold via a table top stereolithography 3D printing and electrospinning, Tissue Eng. Part A 23 (11–12) (2017) 491–502.
[163] S.J. Lee, W. Zhu, L. Heyburn, M. Nowicki, B. Harris, L.G. Zhang, Development of novel 3-D printed scaffolds with core-shell nanoparticles for nerve regeneration, IEEE Trans. Biomed. Eng. 64 (2) (2016) 408–418.
[164] J.F. Li, P. Hashemi, T.Y. Liu, K.M. Dang, M.G.K. Brunk, X. Mu, A.S. Nia, W. D. Sacher, X.L. Feng, J.K.S. Poon, 3D printed titanium carbide MXene-coated polycaprolactone scaffolds for guided neuronal growth and photothermal stimulation, Commun. Mater. 5 (1) (2024).
[165] H. Rastin, B. Zhang, A. Mazinani, K. Hassan, J. Bi, T.T. Tung, D. Losic, 3D bioprinting of cell-laden electroconductive MXene nanocomposite bioinks, Nanoscale 12 (30) (2020) 16069–16080.
[166] J.F. Li, A. Reimers, K.M. Dang, M.G.K. Brunk, J. Drewes, U.M. Hirsch, C. Willems, C.E.H. Schmelzer, T. Groth, A.S. Nia, X.L. Feng, R. Adelung, W.D. Sacher, F. Schütt, J.K.S. Poon, 3D printed neural tissues with optical dopamine sensors, Biosens. Bioelectron. 222 (2023).
[167] S.H. Hsu, K.C. Hung, Y.Y. Lin, C.H. Su, H.Y. Yeh, U.S. Jeng, C.Y. Lu, S.A. Dai, W. E. Fu, J.C. Lin, Water-based synthesis and processing of novel biodegradable elastomers for medical applications, J. Mater. Chem. B 2 (31) (2014) 5083–5092.
[168] J.J. Martin, B.E. Fiore, R.M. Erb, Designing bioinspired composite reinforcement architectures via 3D magnetic printing, Nat. Commun. 6 (1) (2015) 8641.
[169] Y. Park, J. Jung, M. Chang, Research progress on conducting polymer-based biomedical applications, Appl. Sci. 9 (6) (2019) 1070.
[170] J. Tao, J. Zhang, T. Du, X. Xu, X. Deng, S. Chen, J. Liu, Y. Chen, X. Liu, M. Xiong, Y. Luo, H. Cheng, J. Mao, L. Cardon, M. Gou, Y. Wei, Rapid 3D printing of functional nanoparticle-enhanced conduits for effective nerve repair, Acta Biomater. 90 (2019) 49–59.